PROTECTION SYSTEM REPRESENTATION IN THE

ELECTROMAGNETIC TRANSIENTS
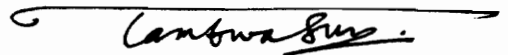
PROGRAM

by

Arvind K.S. Chaudhary

Dissertation submitted to the Faculty of the

Virginia Polytechnic Institute and State University

in partial fulfillment of the requirements for the degree of

Doctor of Philosophy

in

the Bradley Department of Electrical Engineering
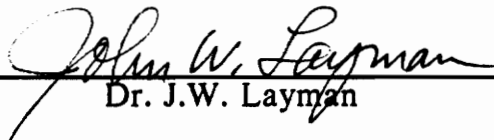
APPROVED:

_____
Dr. A.G. Phadke, Co-Chairman

_____
Dr. K-S. Tam, Co-Chairman

_____
Dr. S. Rahman

_____
Dr. R.P. Broadwater

_____
Dr. J.W. Layman

October 1991

Blacksburg, Virginia

PROTECTION SYSTEM REPRESENTATION IN THE

ELECTROMAGNETIC TRANSIENTS

PROGRAM

by

Arvind K.S. Chaudhary

Dr. A.G. Phadke, Co-Chairman

Dr. K-S. Tam, Co-Chairman

the Bradley Department of Electrical Engineering

(ABSTRACT)

This work concerns the addition of the few critical elements of a protection system to the Electromagnetic Transients Program (EMTP). The EMTP is one of the most widely used programs for the simulation of transients in power systems. The EMTP contains models for almost every major power system component. A protection system consists of instrument transformers, relays, and circuit breakers.

Models for current transformers and capacitor voltage transformers are developed, validated, and incorporated in EPRI/DCG EMTP Version 2.0. The user can define the values of the current transformer and capacitor voltage transformer parameters. Total Fortran capability has been added to EMTP; new subroutines and an inbuilt structure to allow the linking of user defined Fortran subroutines with the main EMTP are explained. This capability is necessary to

simulate computer relay algorithms. The outputs of the algorithms can be passed to the EMTP, which enables the study of the dynamic interaction between the power system and the protection system. Models of specific relays for line protection (SLY12C) and transformer differential protection (BDD15B) are also available. The relay models can be used with different settings.

These new features in EMTP together constitute the critical elements of a protection system. Thus, it is now possible to simulate the dynamic interactions between a power system and a protection system.

Dedication

This work is dedicated to family, friends, and faculty who have contributed to my growth as a person and as an engineer.

Acknowledgements

Thanks are due to all the students of the Power Systems Laboratory for contributing to a congenial atmosphere. Virgilio Centeno helped develop the relay testing apparatus. Nitin Vichare has helped me in innumerable ways. I also owe a large debt to Mr. Viruru Phaniraj who has always provided counsel on many matters, including the inner mechanics of EMTP.

It is an onerous task to select names amongst the many individuals who have influenced me for the better. From St. Joseph's B.H. School I remember Mr. Luke D'Souza (deceased), Mr. A. Alvarez (deceased), Ajit Bhide, and Gerard Kamath. At St. Joseph's College -- Mr. S. Srinivasan, Mr. B.D. Anantharaman, Pradeep Vellodi (deceased), Mahesh Chandra, Janaki Nair, and Tara D'Souza. At the Indian Institute of Science -- Dr. D.P. Sengupta, Dr. K. Parathasarathy, Dr. J.J. Vithayathil, Dr. K.S. Prabhu, and Rajen Borgohain. At Bharat Heavy Electricals Limited -- Mr. D. Suryanarayana, Narendra Varma, and Subhash Saxena. At North Carolina State University -- Dr. A.J. Goetze, Dr. A.A. Girgis, and Dr. B.K. Aggarwal.

But, one must begin at the beginning. My father and mother have instilled in me many qualities, but the impetus to be half as decent a person as my father is the strongest. My brother's selfless support in this endeavor is diminished by mentioning it. To my large and extended family I can only say "thank you". Last but not least, Sandhya is thanked for her courage and fortitude and support.

Table of Contents

List of Illustrations

List of Tables

Chapter I

1.0 INTRODUCTION

A protection system consists of instrument transformers, relays, and circuit breakers. Protection systems are critical power system components, and their behavior often determines the response of a power system to a transient event.

Power system response to faults and other sudden disturbances includes "transient" and "steady-state" components. For low speed protection systems, the transient component is generally ignored; only the steady-state component is used for analysis. For high-speed protection systems, the transient and steady-state components must be considered, because the relays operate during the transient regime, which creates a serious risk to protection system security and dependability. Security refers to the fact that the relay does not operate erroneously, e.g., for faults outside its zone of protection. Dependability refers to the fact that the relay must operate for a fault in its zone of protection.

Designers of protection equipment have developed miniature system models to determine relay response under selected system conditions. As with other studies using miniature system models, it is not possible to include substantial portions of the power system in the model. Also, it is not possible to easily vary parameters, such as the remanent flux in the current transformer, or the magnetization curve of the current transformer, or the inertia of the machines in the system. The dynamics of the interaction between the power system and the protection system cannot be studied. The time and cost of such studies may also be prohibitive.

The Electromagnetic Transients Program (EMTP) is a large computer program for simulating electromagnetic, electromechanical, and control system transients on multiphase electric power systems. This large (over 100,000 lines) and complex Fortran code has been developed over the last 25 years by many individuals. Almost every major power system component is modeled including nonlinear elements such as circuit breakers and surge arresters. The capabilities of this program for conducting engineering studies are enormous and include insulation coordination, equipment ratings, and solving operating problems such as unexplained events or equipment failures. The EMTP is also one of the most widely used packages in the electric utility industry. (Ref. [1.])

Thus, there is a need to study the transient response of the protection system in conjunction with the transient response of the power system, because of the strong interaction between the two systems. For example, a fault on one of the

two parallel transmission lines leads to the opening of the faulted line, with the consequent overload and opening of the unfaulted line, which in turn leads to system overvoltages. It is indeed critical for relays to isolate faults, but it is equally important that only the desired relays operate and not the backup relays. With the ever growing importance of sophisticated computer relay algorithms, a technique must be developed which will allow the algorithms to process the power system data and feedback the relay decisions to affect the state of the power system. There is no tool at present which can simulate the dynamic interactions between a power system and a protection system. This work is an effort contributing to the development of a few critical protection system components and their integration within EMTP, leading to an enhanced simulation capability.

Chapter 2 is a review of protection system simulation techniques. The Transient Network Analyzer (TNA) and its limitations are described. The trend towards digital simulation of the protection system is shown. A brief description of the EMTP algorithm and of the need for enhancing EMTP to incorporate protection system simulation is explained.

Chapter 3 dwells on the need for accurate models of instrument transformers -- current transformers and capacitor voltage transformers -- particularly in the transient regime. The current transformer model development, validation, and incorporation in EMTP are expanded upon. In EMTP, the development, validation, and incorporation of the capacitor voltage transformer model are dealt

with. Finally, the limitations of the current transformer and capacitor voltage transformer models are listed.

Chapter 4 deals with the addition of the total Fortran capability to EMTP, which is required to implement computer relay algorithms. The present status of Fortran capability in EMTP is examined, and various alternatives to implementing these features are explored. The changes made to EMTP are documented, and the structure of the new EMTP subroutines is defined. With the addition of Fortran capability, relay models can be developed in Fortran and included within EMTP. The relay models are not limited to computer relay algorithms. Thus, Fortran relay models can be developed for any relay (e.g., an overcurrent relay).

Chapter 5 deals with the models for the SLY12C (a three phase, static mho distance relay) and BDD15B (a single phase transformer differential relay with harmonic restraint). The details are given for each of the models, and the modeling of the important functions of the relays is given. The validation of the relay models is performed using the test data from actual tests done on the models by American Electric Power (AEP). The incorporation of these models with user defined settings within EMTP is explained.

Chapter 6 contains an example data case incorporating the models developed in this dissertation, which includes the dynamic interaction between the power system and the protection system.

Chapter 7 summarizes the contributions of this work and lists some of the recommended future work.

Chapter II

2.0 PROTECTION SYSTEM SIMULATION
AND EMTP

2.1 INTRODUCTION

The simplest method of testing relays consists of supplying the relays with steady-state currents and voltages and plotting the steady-state relay operating characteristics and operating time. No dc offset or reflection transients are applied to the relay. However, in the field a relay initially "sees" the normal power system currents and voltages, and on the occurrence of a fault "sees" the changes in currents and voltages applied to it--the dynamic operating characteristics are applicable. The relay in the field is subjected to both the dc offset and the re-

flection transients. The actual field current and voltage waveforms are essential to testing the relay correctly.

Figure 1 on page 8 is similar to Fig. 2 of Ref. [2.] and lists some of the methods of the relay testing. One method of testing the relay is to take the EMTP data case output, convert the output to analog signals, amplify the signals through current and voltage amplifiers, and feed the relay with these signals. Another method consists of using the TNA.

These methods are useful for testing individual relays in relatively simple configurations. It is often desirable to test a complete protection system, within a complex multi-terminal power system network, through a series of events. It is extremely difficult to achieve this capability using TNAs or digital computers, because it involves the interactive modeling of both the power system and the protection system. This chapter shows one approach to achieve this capability.

2.2 SURVEY OF PROTECTION SYSTEM SIMULATION AND RELAY TESTING

As the speed of operation of modern relays becomes faster and the relay bandwidth increases, the dynamic or transient response of **all** the elements of the protection system must be studied in greater detail. Thus, it is no longer valid to test
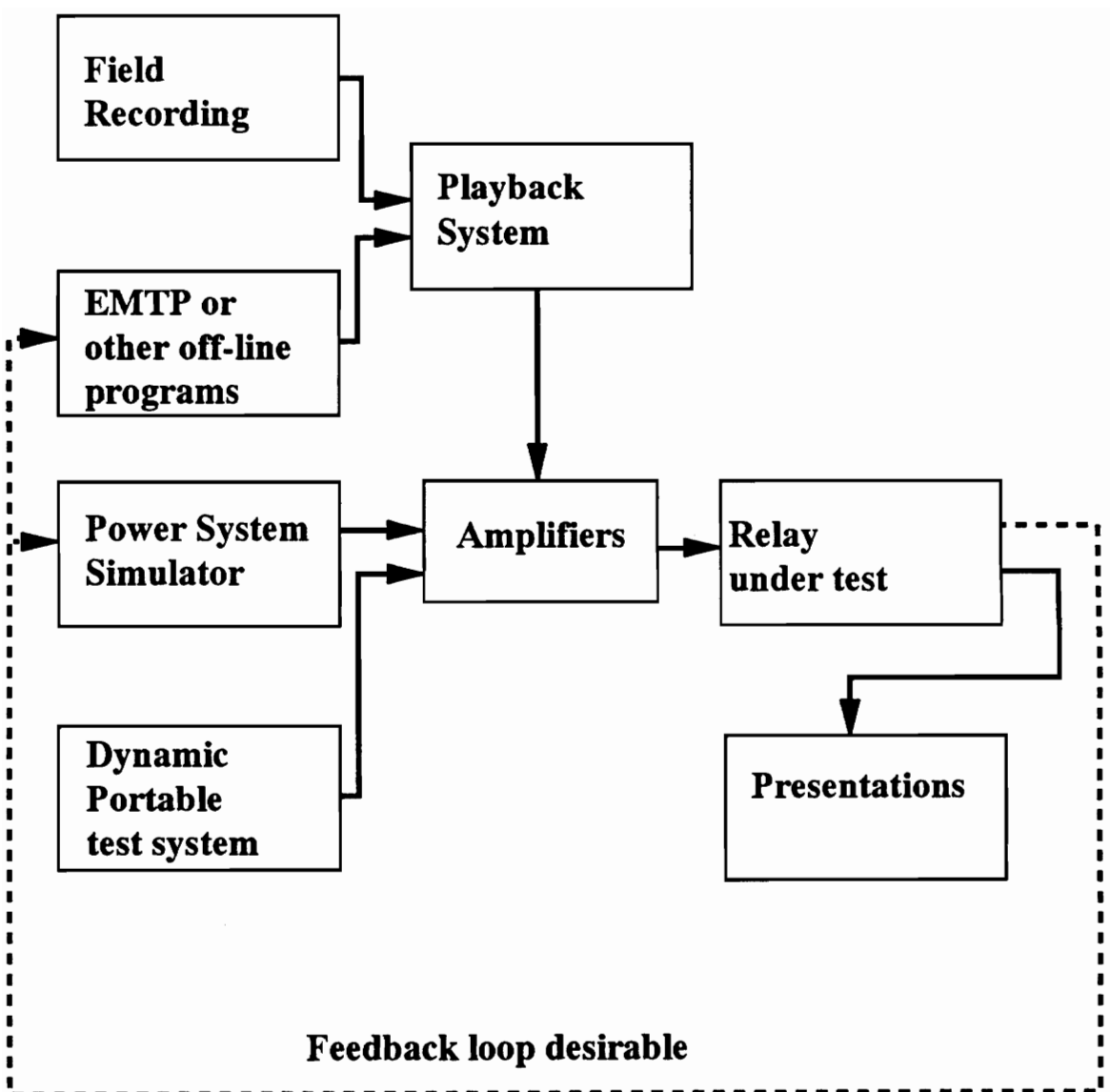
Figure 1. Methods of relay testing

the protection system or the relays under steady state fault conditions. It is important to test not only the relays that operate, but also those relays that "see" the fault but do not operate initially on the fault. And, most importantly, the relay decisions should reflect into the power system and initiate tripping or reclosing of the circuit breakers.

A brief discussion of the TNA is given because of its importance in relay testing. This device consists of scaled analog models which represent, up to a few kHz, the transient behavior of the actual power system components. The models are accurate and can represent the magnetic nonlinearities of the transformers and reactors. Because of the physical models, the influence of remanence in transformers, which can pass unobserved in a digital simulation (Ref. [3.]), has been observed and studied. Synchronous machine models are available in which d and q axis flux dynamics, exciter, and governor dynamics can be simulated. Transmission lines with frequency dependent parameters can also be modeled. The disadvantages of the TNA are listed below :-

1. The parameters of the transmission line or transformer cannot be changed easily, if at all.

2. The study is limited to the components available -- not all configurations can be studied.

3. The TNA is not accessible to all users. Also, the maintenance cost is quite high.

One of the earlier works on power system protective equipment modeling is given in Ref. [4.]; this work employs the analog models of the required components. Analog models of current transformers, summation-transformers, and pilot wires have been built. An electromechanical relay's equation is simulated on an analog computer. The digital computer simulation method is not adopted because of the length and complexity of the problem.

Ref. [5.] digitally simulates generators, transmission lines, current transformers, capacitor voltage transformers, and relays. An extensive program has been written mainly based on the EMTP solution method and successfully demonstrated. The authors envision adding models for the long transmission lines and incorporating remanence in the current transformer model.

The principal author of Ref. [6.] is also the principal author of Ref. [4.], but the digital computer simulation method is now adopted for the modeling of current transformers and relays. A transient analysis of a restricted earth fault protective scheme is implemented, and a resistive relay is shown to have a large margin of safety.

Ref. [7.] uses a TNA to test the protection for two parallel, mutually coupled series-compensated lines. The protection of the series compensator consisting of

the spark gaps which flashover and bypass switches in parallel with the capacitor is also included in the model. An equivalent tie impedance and two source impedances are also included in the simulation. The TNA outputs are amplified and fed to the relay under test. The configuration was used to prove the relay performance under transient conditions.

Electricité de France (Ref. [8.]) employs digital simulation to compute the transient electrical values of each network element at each time step. The trapezoidal integration rule is used to compute the transient behavior of inductances, and capacitances; the solution method is similar to that employed in EMTP. The digital signals are then converted to analog signals, filtered, and amplified before feeding the relays. At GEC Measurements in England, a similar procedure is used to test relays, except that the digital simulation employed is EMTP (Ref. [9.]).

The Ph.D. thesis of Dr. B.W. Garrett (Ref. [10.]) demonstrates the use of digital simulation for analyzing protection system performance. The "sequential" rather than a "simultaneous" approach to the power system and the protection system simulation is employed. The power system simulation is first performed using EMTP, or digitized TNA waveforms, or fault recordings. The Transient Response Processor (TRP) has complete models for an overcurrent relay and a memory-polarized mho relay. The TRP reads in the digital data and solves the state equations of the input filters and transactors using the method of central differences. A technique called "numerical logic replacement", which makes

near-misoperation visible from simulations, e.g., how close the timer was to issuing a trip, is introduced.

A most important contribution to the field of protection system simulation is given in Ref. [11.]. This simulator consists of a digital computer which controls the configuration and parameters of an electronic real time analog model of a power system, including most of the important power system components. The outputs of the power system simulator are fed through amplifiers to the relays. Closed loop real time testing is achieved, with the relay initiating tripping and reclosing of breakers. The main disadvantages of this approach are :

1. A finite number of components have been built -- three current transformers, three capacitor voltage transformers, three two winding transformers, one three winding transformer, four loads, four series capacitors, seven transmission lines, and 17 circuit breakers. Thus, there are finite limits to the level of complexity of the power system that can be simulated.

2. The maximum short circuit level that can be simulated is 50,000 MVA.

3. HVDC systems cannot be integrated with this system.

2.3 INTRODUCTION TO EMTP

The first version of an electromagnetic transients program was developed by Dr. Hermann W. Dommel in Germany in the early 1960's. Dr. Dommel, together with Dr. W. Scott Meyer, made further developments to EMTP at the Bonneville Power Administration (BPA) till 1973, when Dr. Dommel left for the University of British Columbia, where he continues to improve the EMTP. Over the years, as a result of the contributions of many individuals, EMTP has developed from an original 5,000 lines to over 100,000 lines of code today.

This section aims to give a brief description of solution method of EMTP; it is impossible to explain all or even most of the solution techniques and model details of all EMTP components and features within this dissertation. The main references of EMTP are given, which in turn point to the more specific references for specific techniques and devices.

The seminal reference for the theory of EMTP is Ref. [12.]. This book explains the solution methods used in EMTP for linear and nonlinear elements, linear coupled elements, transmission lines, cables, transformers, synchronous machines, surge arresters, and switches. This book, published in 1986, contains 192 references. Other important references are Ref. [1.], Ref. [13.], and Ref. [14.].

2.3.1 EMTP Solution Method

The EMTP solution method consists of the formulation of the nodal admittance matrix of the network being solved, and the solution of the node voltages of the network. The differential equations of the elements (L and C) are transformed to algebraic equations using the trapezoidal integration rule.

Thus, for an inductance connected between nodes 1 and 2, the differential equation is :-

$$v_1 - v_2 = L\frac{di_{12}}{dt}$$

Applying the trapezoidal rule of integration from time $(t - \Delta t)$ to time t (assuming that the solution of the voltages and currents is known up to time $(t - \Delta t)$):

$$\int_{t-\Delta t}^{t} (v_1(t) - v_2(t))\, dt = L(i_{12}(t) - i_{12}(t - \Delta t)),$$

which can be written as

$$i_{12}(t) = \frac{\Delta t}{2L}[v_1(t) - v_2(t)] + I_{12}(t - \Delta t), \qquad (2.3.1)$$

where $I_{12}(t - \Delta t) = i_{12}(t - \Delta t) + \frac{\Delta t}{2L}[v_1(t - \Delta t) - v_2(t - \Delta t)].$

If a capacitor is connected between nodes 1 and 3, the equation for the branch current can be written as

$$i_{13}(t) = \frac{2C}{\Delta t} [v_1(t) - v_3(t)] + I_{13}(t - \Delta t), \tag{2.3.2}$$

where $I_{13}(t - \Delta t) = -i_{13}(t - \Delta t) - \frac{2C}{\Delta t} [v_1(t - \Delta t) - v_3(t - \Delta t)].$

Applying Kirchoff's Current Law at node 1,

$$\left(\frac{\Delta t}{2L} + \frac{2C}{\Delta t}\right) v_1(t) - \left(\frac{\Delta t}{2L}\right) v_2(t) - \left(\frac{2C}{\Delta t}\right) v_3(t) = i_1(t) - I_{12}(t - \Delta t) \atop - I_{13}(t - \Delta t), \tag{2.3.3}$$

where $i_1(t)$ is the current injection at node 1.

Similar equations can be obtained at other nodes to form the nodal admittance matrix, with the node voltages as the unknown quantities.

$$[Y][v(t)] = [i(t)] - [I(t - \Delta t)] \tag{2.3.4}$$

where,

$[Y] = n \times n$ symmetric nodal admittance matrix;

$[v(t)] = $ vector of n node voltages;

$[i(t)] = $ vector of n current injections;

$[I(t - \Delta t)] = $ vector of n known "history" terms.

The initial conditions of the network can be determined for linear elements. Nonlinear resistances are ignored in the steady-state solution for initial condi-

tions. Steady-state values can be defined for time-varying resistances. Nonlinear inductances are included with their specified steady-state values to calculate the initial conditions.

The vector $[v(t)]$ is solved by the triangular factorization of the $[Y]$ matrix, using optimal ordering which exploits the sparsity of the $[Y]$ matrix (Ref. [15.]). The $[Y]$ matrix is re-formed and re-factorized for changes in switch positions. The $[Y]$ matrix can also be subdivided, based on the number of known voltages in the network. Both of these techniques reduce the computational effort involved in obtaining the solution.

TACS (Transient Analysis of Control Systems) can be used to model the dynamic interaction between the power system and the various controllers.

Once again, it must be emphasized that this section is only a rudimentary introduction to the EMTP solution method and techniques.

2.4 EMTP ENHANCEMENT WITH PROTECTION SYSTEM REPRESENTATION

The preceding two sections point to the inevitability of the enhancement of EMTP with a protection system representation. The EMTP is perhaps one of the

most powerful and one of the most widely accepted transients programs in use today. The ability to simulate accurately the transient behavior of most power system components makes EMTP the ideal candidate to implement a complete protection system representation. The protection system should include models for instrument transformers, relays, and also total Fortran capability to allow the simulation of computer relay algorithms. The protection system decisions should initiate the tripping or reclosing of breakers. Thus, at each time step the power system transient solution is obtained. The currents and voltages at the relay location are supplied through instrument transformers, whose transient solution must be obtained. The relay dynamics must now be solved and relay decisions reflected in the possibly new (if a trip occurs) power system equations, which are solved for the next time step. This procedure is repeated till the end of the study period.

There are three main motivating reasons for developing the protection system representation in EMTP.

1. In relay system simulation problems, ideally it is not acceptable to study the protection system response in an off-line mode. Relay system models must respond to transient events and participate in influencing their course by taking appropriate sequences of control actions. Instances when this interaction is crucial are numerous. For example: sequential phase opening when single phase relaying is used; studies of evolving faults and relay responses to

them. It is often necessary to examine a complex transient event in its natural order, and this order is partially determined by the protection system.

2. Utility engineers (as well as relay designers) need a tool which can be used to analyze relay responses under specific system conditions. There is no single tool which can be used by such a broad group of potential users.

3. The advances in digital computer relaying have made it highly desirable that the simulations be in digital form. Since EMTP results are already in digital form, EMTP can readily interface with digital relay system representations.

Chapter III

3.0 CURRENT AND CAPACITOR VOLTAGE TRANSFORMER MODELS

3.1 INTRODUCTION

Instrument transformers -- current transformers, electromagnetic voltage trans-
formers, and capacitor voltage transformers -- constitute the first link of a pro-
tection system. The outputs of the instrument transformers supply the relays. The
transient performance of the instrument transformers affects the transient per-
formance of the relays and the protection system. This transient interaction has
been studied in Refs. [16.], [17.], [18.], [19.], [20.], [21.], and [22.]. The following
are some instances where this transient interaction occurs :

- The saturation of the current transformers reduces the magnitude of the secondary current, and hence the operating force or torque of the overcurrent or induction relays. The reduced force increases the speed of operation of the relay, and also reduces the reach. The dependability of the protection scheme is reduced.

- The saturation of current transformers affects the zero crossings of the current wave. This will affect schemes which depend on the zero crossings such as phase comparators (see Section 5.2 for details of the SLY phase comparison scheme).

- The relaxation current in the current transformer secondary is the current which flows when the primary circuit is de-energized. The relaxation current is more pronounced in the case of current transformers with an anti-remanent air gap. The relaxation current can delay the resetting of low set overcurrent relays and also cause the false operation of breaker-failure relays.

- Electromagnetic voltage transformers and capacitor voltage transformers can be subject to ferroresonance. Ferroresonance leads to overvoltages which in turn can lead to relay misoperation and thermal and dielectric failure of the voltage transformers.

- The reduction of the primary voltage to zero creates a subsidence transient on the CVT secondary, because of the stored energy in the capacitive and

inductive elements. This subsidence transient affects the speed of the protection scheme, and can cause relay misoperation for reverse faults.

Thus, it is evident that models for instrument transformers are necessary to simulate a protection scheme with a degree of fidelity. The instrument transformer models must represent the following phenomena :-

1. The nonlinear magnetization characteristic of the core material must be represented. This characteristic should include the hysteresis loop with capability to simulate the minor loops. CTs generally operate along minor hysteresis loops, and only during a fault do CTs operate along the major hysteresis loops. For example, if the dynamic major hysteresis loop operates with a flux density variation of $\pm$ 1.8 T, then the minor hysteresis loop operates with a flux density variation of $\pm$ 0.09 T, for an overcurrent factor of 20.0.

2. The ability to incorporate remanent flux in the current transformer model is critical. CTs can have large amounts of remanent flux in the core and yet operate satisfactorily during steady state unfaulted conditions. Primary fault currents can then drive the CT into saturation much more quickly than if the CT had been operating with zero remanent flux. Modelling of remanent flux is necessary to simulate high speed reclosing schemes which can be affected by the trapped flux in the CT core.

3. Relaxation transients occur when the primary current or primary voltage goes to zero, but the secondary current or secondary voltage does not do so immediately. The CT secondary current discharges unidirectionally through the burden. This current can delay the dropout of the breaker-failure relay and cause this relay to misoperate. The CVT model should be able to simulate the subsidence transient and its influence on the protection scheme.

4. The instrument transformer models should be valid for a frequency range of 0 - 3 kHz. This frequency range is selected because the relay input filters generally have a cut-off frequency of 3 kHz. This need not apply to travelling wave relays, which require the high-frequency surges to be faithfully transmitted from the CTs. The range of these high-frequency surges is "several kilohertz to megahertz depending upon the location of the fault," as mentioned in Ref. [23.]. The travelling wave relays should perhaps be used in conjunction with non-conventional CTs, such as magneto-optic CTs. Non-conventional instrument transformers are not the subject of this work; however, Refs. [24.], [25.], [26.], [27.], and [28.] provide a glimpse of the work in this area. The capacitance of high voltage iron-cored oil-impregnated paper dielectric CTs is of the order of 350 pF for 161 kV and increases with the voltage class (Ref. [29.]). This capacitance shunts the high-frequency surge to ground; consequently, the relay fails to "see" the surge, and hence the need for non-conventional CTs. The large capacitance of high voltage conventional CTs is inherent in achieving the Basic Insulation Level (BIL) corresponding to the CT's voltage class, and is in fact exploited through capacitance grading.

5. Burden characteristics, especially under transient conditions, should be modeled because the errors of instrument transformers directly depend upon the burden. The CT burden is connected in series, and the CVT burden is connected in parallel. The power frequency Thevenin equivalent for the total burden is an assumption. The burden varies with the secondary current and the frequency. The inductance in the burden varies non-linearly with the secondary current, decreasing with the increasing secondary current. Moving armature relays also have different inductances in the closed and open positions, because of the different reluctances in the two positions. The burden can also exhibit frequency dependent and voltage dependent behavior.

3.2 A DISCUSSION OF THE CT MODEL

3.2.1 Representation of a CT in EMTP

A good representation of a current transformer equivalent circuit for modeling purposes in EMTP is shown in Figure 2 on page 24. In this representation, the secondary winding resistance and the secondary winding leakage inductance are included with the lead impedance and the burden impedance. The nonlinear characteristics of the current transformer are represented by a Type 96 pseudononlinear hysteretic inductor (Ref. [30.]).
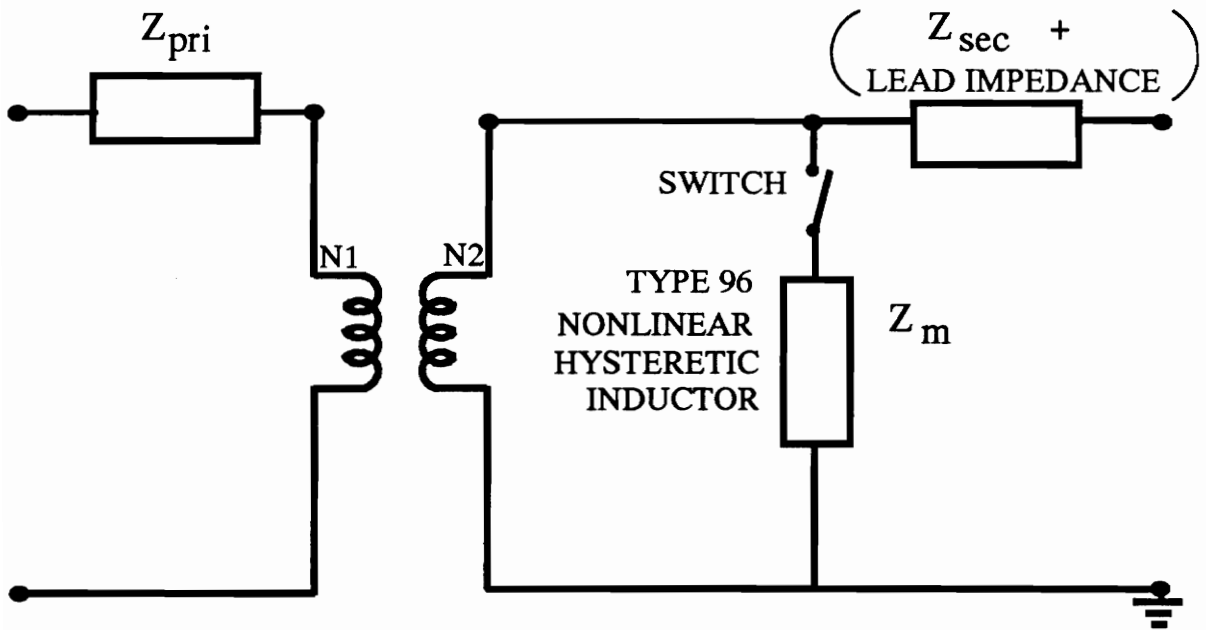
Z_{pri} : Transformer primary resistance and leakage inductance.

Z_{sec} : Transformer secondary resistance and leakage inductance.

Z_m : Transformer magnetizing impedance

Switch closes at T=0.0.

Figure 2. Representation of a CT model in EMTP

In this context, it is necessary to distinguish between a low reactance current transformer and a high reactance current transformer (Refs. [31.] and [32.]). A uniformly wound toroidal core CT with a centrally placed primary is considered a low reactance CT, with negligible secondary leakage reactance. The negligible leakage reactance implies that the CTs excitation characteristic can be used to predict its performance, particularly at high levels of flux density, corresponding to high overcurrents in the primary circuit. A wound primary CT is considered a high reactance CT, where tests have to be done to determine its performance. In high reactance current transformers, the primary exciting current is influenced by the leakage flux set up by the primary current and is not equal to the secondary exciting current multiplied by the turns ratio. The secondary excitation characteristic cannot be used to predetermine the current transformer's performance during primary fault conditions. Thus, the model shown in Figure 2 on page 24 is strictly valid for low reactance current transformers only.

3.2.2 EMTP Requirements

The EMTP representation of a current transformer is shown in Figure 3 on page 26. In this model, Z_m is placed after Z_{EMTP}, in parallel with ($Z'_{sec} + Z_{lead} + Z_{burden}$). This representation is required because finite values **must** be given for Z_{pri} and Z_{EMTP}. More precisely, L_{EMTP} must be non-zero, and R_{EMTP} can be zero; and either R_{pri} or L_{pri} can be zero, but not both. More details are given in Ref.

Figure 3. EMTP requirements of a CT model
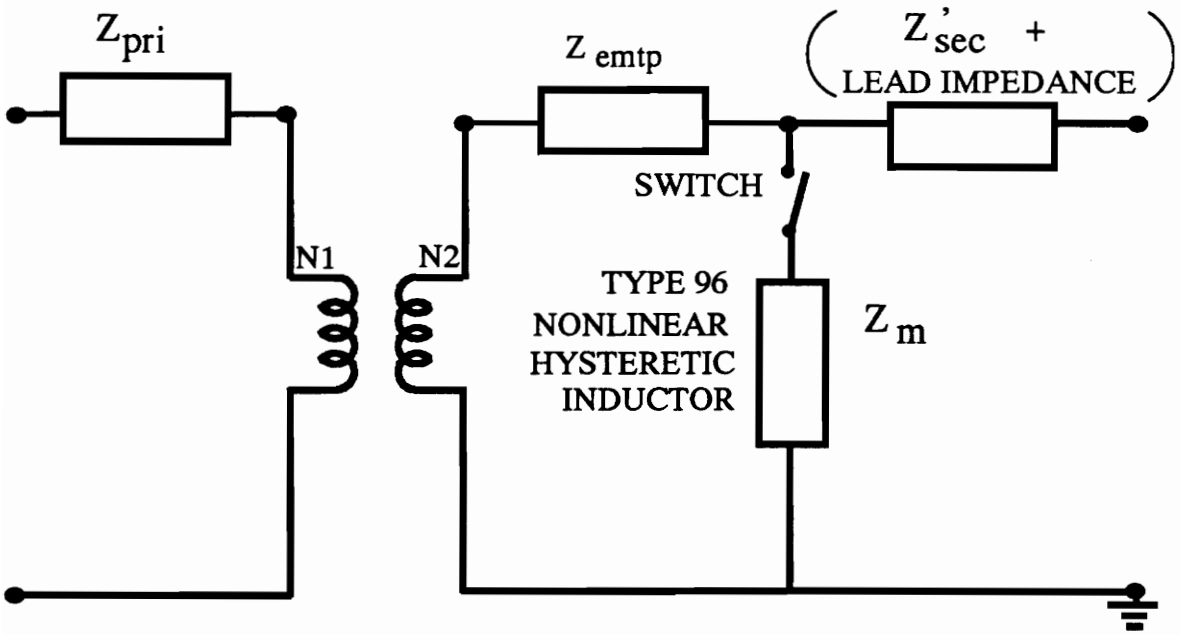
Z_{pri} : Transformer primary resistance and leakage inductance.

Z_{sec} : Transformer secondary resistance and leakage inductance.

Z_m : Transformer magnetizing impedance

Z_{emtp} : Transformer impedance required by EMTP

$Z'_{sec} = Z_{sec} - Z_{emtp}$

Switch closes at T=0.0.

[1.]. It must be mentioned that Z_{pri} does not affect the current transformer behavior. This data requirement of the EMTP transformer model can be satisfied by separating Z_{sec} into two parts -- Z_{EMTP} and Z'_{sec}. Z_{EMTP} should be small; however, very small values of Z_{EMTP} give rise to very large values of the admittance $\frac{1}{Z_{EMTP}}$ in the matrices [Y] and [G] -- the steady-state complex matrix and the real coefficient matrix within the time-step loop respectively. These large admittance values can "swamp out" the effects of other elements connected to Z_{EMTP}, leading to inaccurate results. It is not possible to give an absolute lower bound on the magnitude of Z_{EMTP}, because it depends on the floating-point word length of the computer system and on the relative ratio of Z_{pri} and Z_{EMTP}. The lower bound on Z_{EMTP} also depends on the magnitude of the other impedances in the network; this dependence is due to the different multipliers used in the forward reduction of the matrices [G] and [Y], which affect the diagonal element corresponding to the node being eliminated. TOLMAT is a near-zero tolerance, which is used to check the singularity of the steady-state complex matrix [Y]. If Z_{EMTP} is very small, then EMTP will give the disconnected subnetwork error message. EPSILN is a near-zero tolerance, which is used to check the singularity of the real coefficient matrix [G] within the time-step loop, where

$$[G]V_{node}(t) = I_{node}(t) \,.$$

If Z_{EMTP} is very small, then EMTP will give the disconnected subnetwork error message in the steady-state solution, or it will give the floating network error message in the time-step solution. With the approximation of placing Z_m as it is

placed in Figure 3 on page 26, the secondary side of the current transformer can be represented by a current source in series with Z_{EMTP}. Because of the current source behavior of the CT, the value of Z_{EMTP} does not affect the secondary voltage drop or the onset of saturation.

3.2.3 Open Circuit Magnetization Characteristics

The determination of L_{sec} from secondary open circuit tests is difficult. The waveforms of currents and voltages are required, because for impressed sinusoidal voltages the currents are non-sinusoidal. Thus, the I_{rms} is only a measure of the effective magnitude of the current. The secondary open circuit test is used to plot the magnetization characteristic: the (V_{rms} - I_{rms}) curve, which is the data that is available most of the time. This characteristic is measured from the secondary terminals, and hence measures ($Z_{sec} + Z_m$), as shown in Figure 2 on page 24. In the unsaturated region ($Z_{sec} << Z_m$), and in the saturated region Z_{sec} is of the same order of magnitude as Z_m.

One procedure of separating Z_{sec} from the measurement of ($Z_{sec} + Z_m$) is as follows:-

1. Subroutine CONVERT in the Auxiliary part of the EMTP Version 2.0 is used to convert the (V_{rms} - I_{rms}) to the (ψ_{peak} - I_{peak}). Subroutine CONVERT assumes that there is no voltage drop across the secondary winding resistance

and the secondary winding leakage reactance. R_{sec} can be measured easily. A value of L_{sec} is assumed. The assumed voltage drop across Z_{sec} can be calculated using I_{rms}. This assumed voltage drop is subtracted from V_{rms} to give a new (V'_{rms} - I_{rms}) curve. The new (V'_{rms} - I_{rms}) curve is converted to the (ψ_{peak} - I_{peak}) curve.

2. The value of I_{peak} can be read from the test current oscillogram.

3. Corresponding to I_{peak} in Step (2), the value of ψ_{peak} can be read from the (ψ_{peak} - I_{peak}) curve generated in Step (1).

4. The ψ_{peak} read in Step (3) can be converted to V_{peak}. This V_{peak} represents the voltage drop across Z_m.

5. The value of V_{peak} in Step (4) is subtracted from the value of V_{peak} which is impressed across the secondary terminals to give the voltage drop across Z_{sec}.

6. The voltage drop across Z_{sec} in Step (5) is compared to the assumed voltage drop in Step (1) converted to its peak value. If there is a significant difference between the two voltage drops, then the procedure is repeated from Step (1), till there is no significant difference between the assumed and calculated voltage drops.

7. When the assumed and calculated voltage drops are equal, then the value of L_{sec} can be calculated. This procedure can be repeated for other points on the (V_{rms} - I_{rms}) curve and the corresponding oscillograms.

The magnetization characteristic should ideally be used with the value of Z_m separated from the measurement of ($Z_{sec} + Z_m$). This separated value of Z_m should be used to compute the hysteresis curve, and then it should be included in the current transformer model. When this is done, the value of Z_{sec} should be included with the secondary burden. The model we have used does not preclude this exact procedure from being followed.

3.2.4 CT Model for EMTP

For low reactance current transformers, generally ($Z_{sec} < (Z_{lead} + Z_{burden})$), and it can be included as shown in Figure 4 on page 31. When there is no fault on the primary circuit of the current transformer, the voltage drop across Z_{sec} is not significant. The small voltage drop does not influence the exciting current and the pseudononlinear hysteretic inductor significantly. When there is a fault on the primary circuit of the current transformer, the voltage drop across Z_{sec} can be significant. The large voltage drop across the secondary terminals (including $Z_{sec} + Z_{lead} + Z_{burden}$) demands a large flux in the core. This large flux causes a sharp increase in the exciting current and a reduction in the value of the
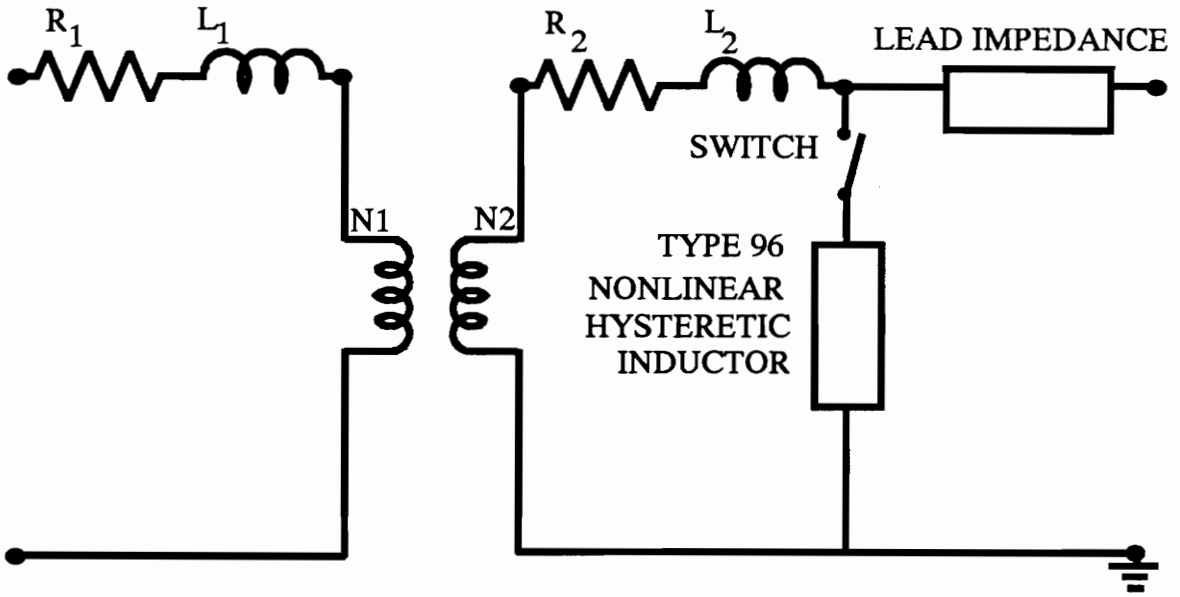
R_1,L_1 : Transformer primary resistance and leakage inductance.

R_2,L_2 : Transformer secondary resistance and leakage inductance.

Switch closes at T=0.0.

Figure 4. Current Transformer model

pseudononlinear hysteretic inductor. The addition of Z_{sec} to $(Z_{lead} + Z_{burden})$ does hasten the onset of saturation, depending on the relative magnitude of Z_{sec} and $(Z_{lead} + Z_{burden})$.

In summary, the model shown in Figure 4 on page 31 is used because of the following reasons: the data requirements for the EMTP transformer model, the difficulty of separating Z_m from the measurement of $(Z_{sec} + Z_m)$, and the low magnitude of Z_{sec} relative to $(Z_{lead} + Z_{burden})$ for low reactance current transformers. It is possible to use the model shown in Figure 2 on page 24 when the following is done: Z_m is separated from the secondary open circuit measurement of $(Z_{sec} + Z_m)$, and the data requirement of the EMTP transformer model can be satisfied by separating Z_{sec} into two parts, Z_{EMTP} and Z'_{sec}. Because of the difficulty of separating Z_m from the open circuit measurement, it may in practice be possible to achieve the data requirement of the transformer model only.

3.3 VALIDATION OF THE CURRENT TRANSFORMER MODEL

3.3.1 Validation method

TRANSMISSION LINE

SWITCH

CT
MODEL

L
O
A
D

BURDEN
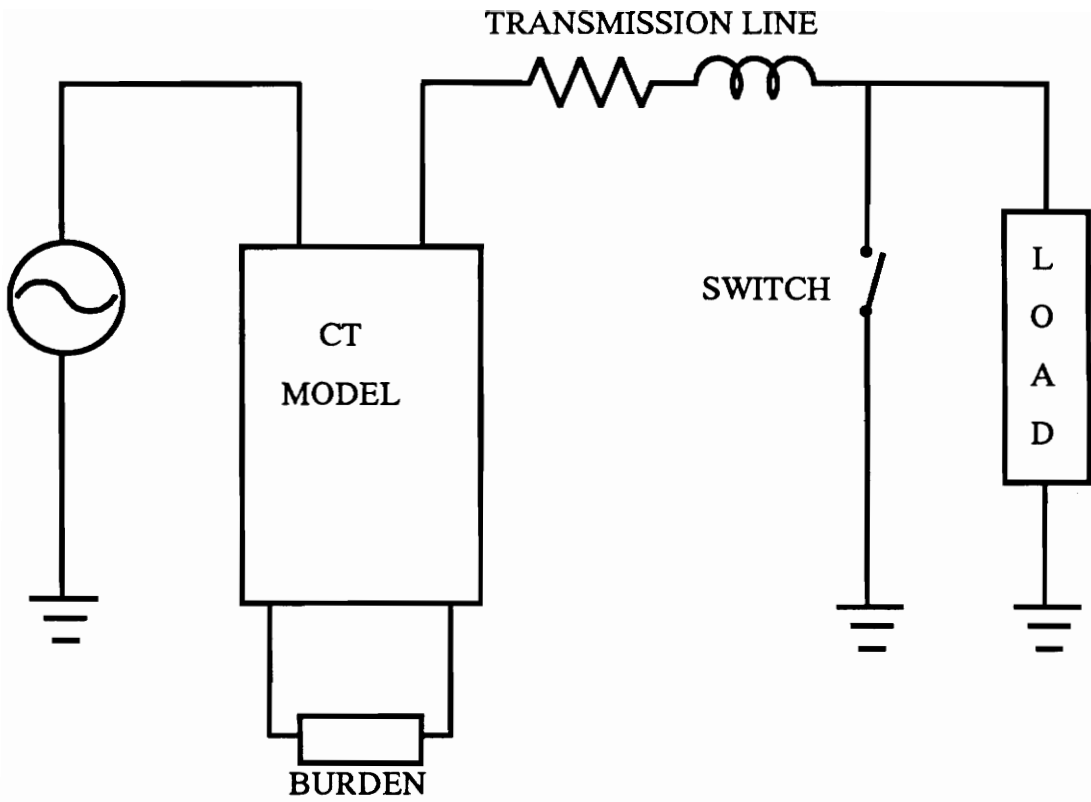
Figure 5.   CT Model Validation circuit

The CT model shown in Figure 4 on page 31 is included in the circuit shown in Figure 5 on page 33 to validate the CT model.

The secondary excitation curve of a 230 kV, 1200:5 A ratio, current transformer is given in Fig. 12 in Ref. [17.]. This excitation curve, the $(V_{rms} - I_{rms})$ curve, is converted by the EMTP subroutine SATURATION into the peak flux linkage vs. I_{peak} curve, the $(\psi_{peak} - I_{peak})$ curve. From the $(\psi_{peak} - I_{peak})$ curve, the coordinates of the saturation point $(\psi_{(saturated)}, I_{(saturated)})$ are determined. The coordinates of the saturation point, (FLXSAT, CURSAT) in EMTP parlance, are input into the EMTP subroutine HYSDAT to determine the hysteresis loop of ARMCO M4 oriented silicon steel. This hysteresis loop is included in the current transformer model for the Type 96 nonlinear inductance. The fault which occurs at a current zero and consequently produces the maximum dc offset is applied. The secondary current and the primary current transformed ideally to the secondary side are plotted.

By using different values of CURSAT and FLXSAT in the subroutine HYSDAT, different hysteresis loops are obtained. These curves are then included in the CT model and the fault is simulated. Increasing the value of FLXSAT increased the time to saturation of the core; it simulated the effect of a larger core. Increasing the value of CURSAT increased the magnetization current drawn by the CT, and thus the deviation between the ideal secondary current and the actual secondary current increased. It was found necessary to make the core draw a large magnetizing current at the saturation point, viz., to flatten

the magnetization curve in the saturation region. One reason for this decision is that the slope of the last two points in the hysteresis curve is extrapolated up to infinity to determine the operating point. The magnitude of this slope is calculated to be 66.7, the relative permeability (μ_r). This extrapolation is valid only for small excursions from the saturation point. During current transformer saturation, the magnetization current drawn can be extremely large, and extrapolation with a large slope is not valid. Another reason for this decision is that the material of the CT in Ref. [17.] may not be ARMCO M4 oriented steel. Increasing the current drawn at the maximum flux density leads to a sharper drop-off in the secondary current during saturation. This drop-off occurs because the rate of the change of flux is lowered, and thus a lower secondary voltage is generated.

3.3.2 Validation results

By varying the parameters CURSAT, FLXSAT, and the flatness of the magnetization curve in the saturation zone, the curves in Figs. 3a and 3b of Ref. [17.] have been simulated to a reasonable degree.

Fig. 2 of Ref. [17.] has also been simulated by varying the primary time constant, the secondary time constant, and the source voltage magnitude, and also by en-
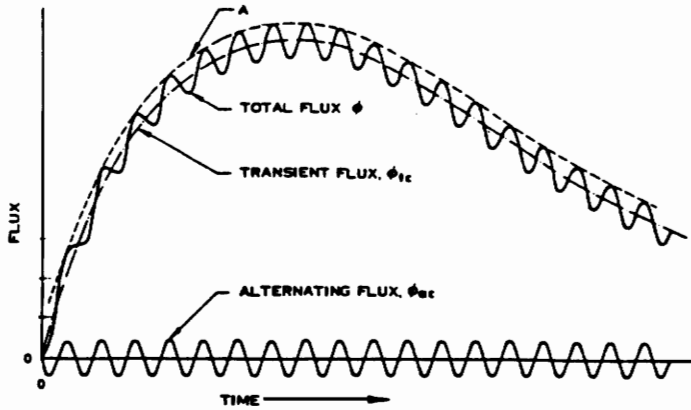
FIGURE 2: RISE OF FLUX IN THE CORE OF
A CURRENT TRANSFORMER
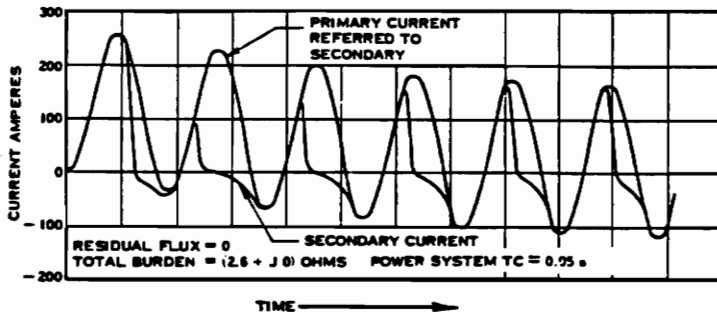
FIGURE 3a: DISTORTION IN SECONDARY CURRENT
DUE TO SATURATION
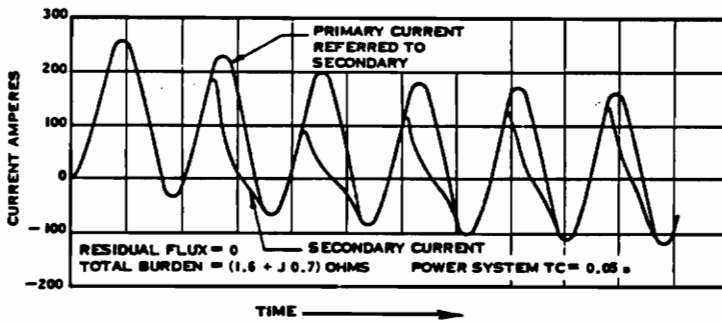
FIGURE 3b: DISTORTION IN SECONDARY CURRENT
DUE TO SATURATION

Figure 6.   Curves reproduced from Ref. [17.]

3.0 CURRENT AND CAPACITOR VOLTAGE TRANSFORMER MODELS   36
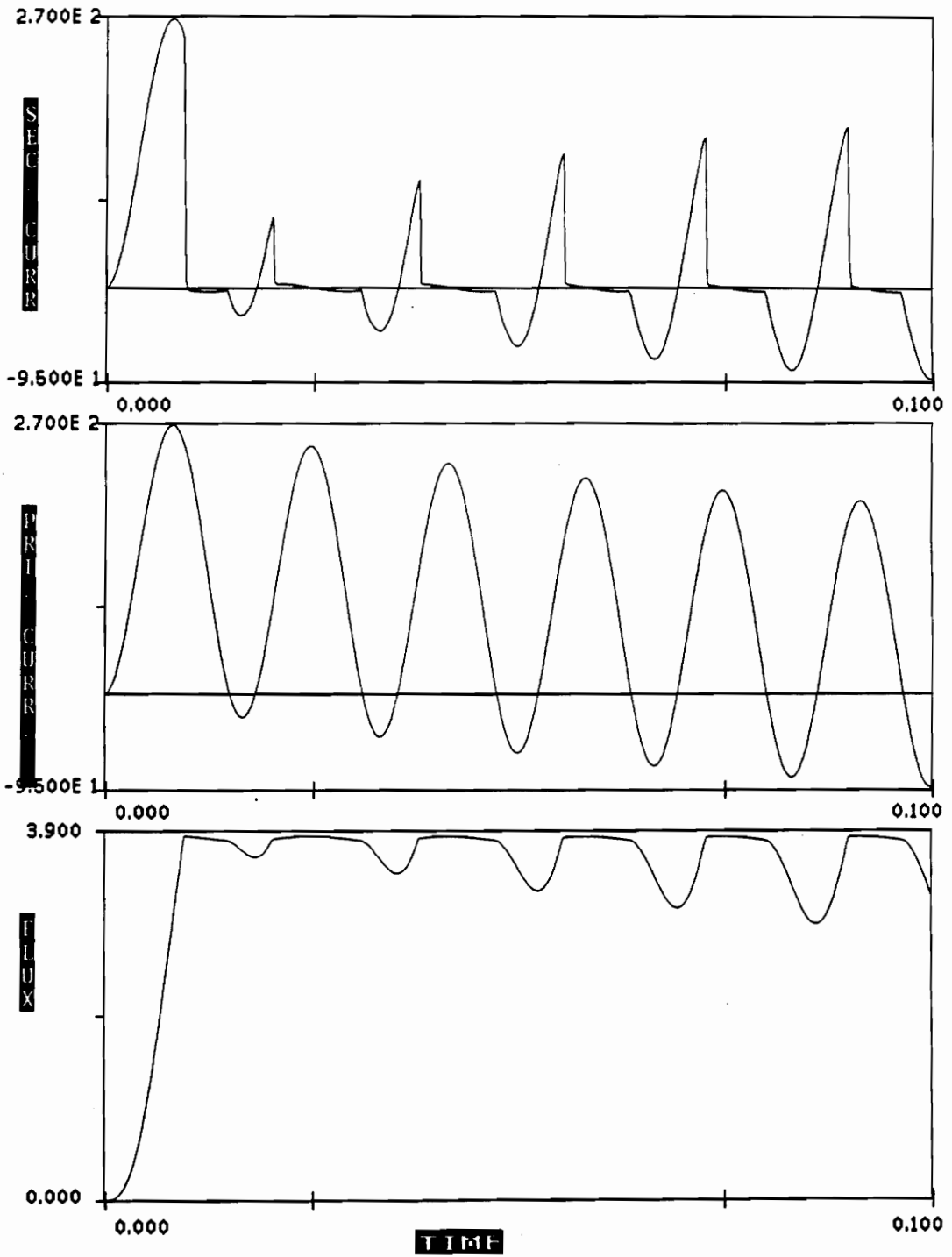
Figure 7. Simulation of Fig. 3a from Ref. [17.]

3.0 CURRENT AND CAPACITOR VOLTAGE TRANSFORMER MODELS
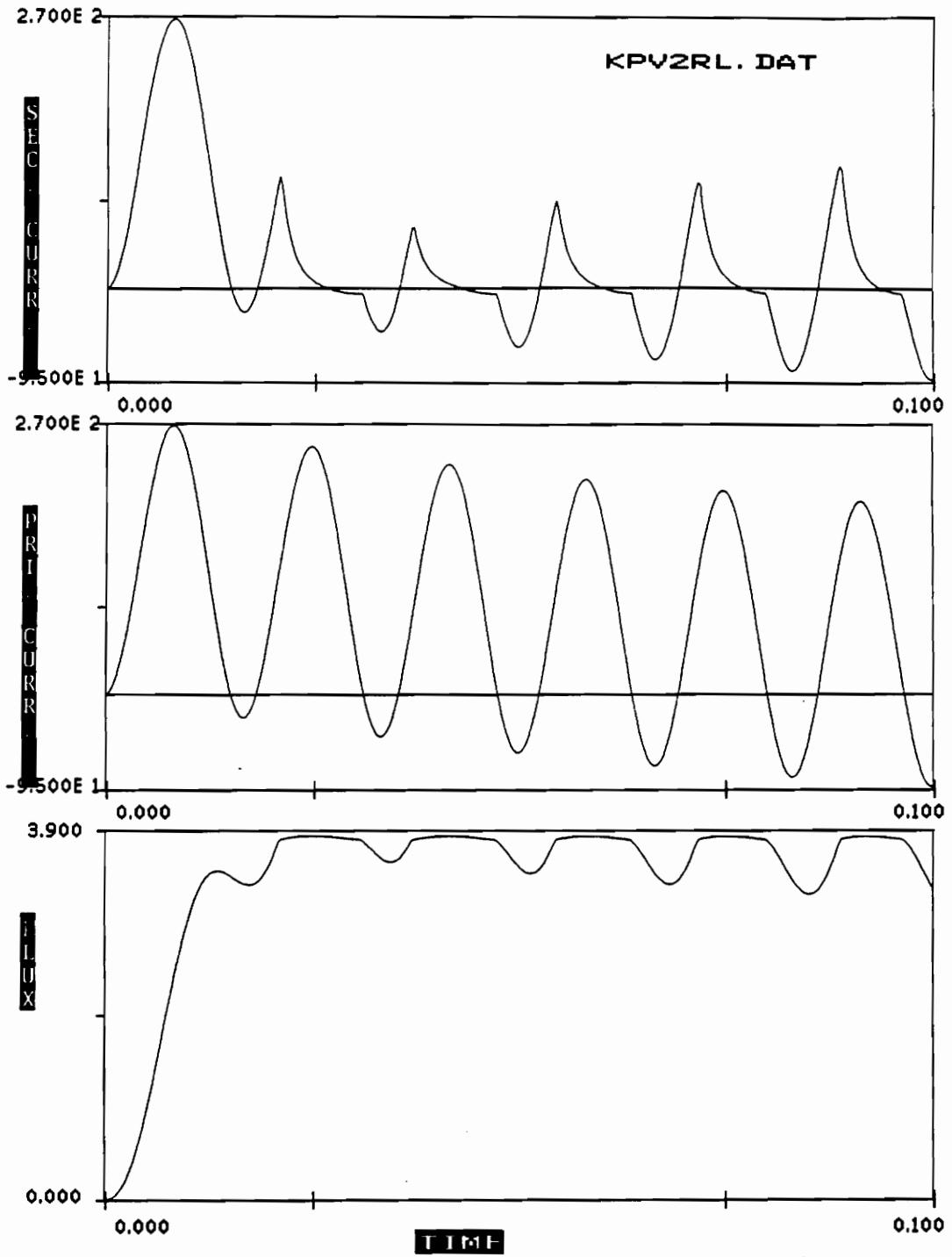
Figure 8. Simulation of Fig. 3b from Ref. [17.]
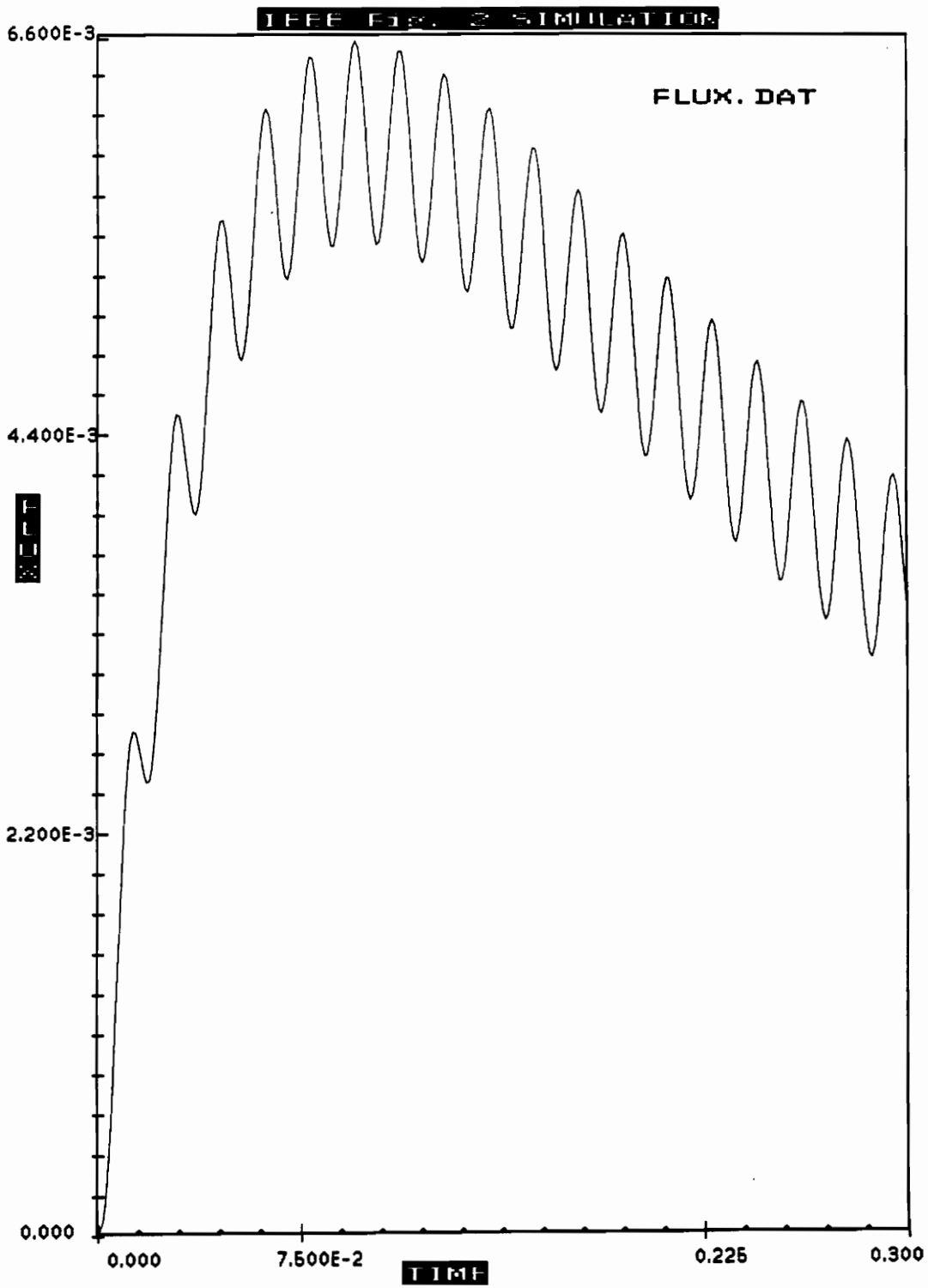
Figure 9. Simulation of Fig. 2 from Ref. [17.]

suring the fault occurred at a current zero. Fig. 2 of Ref. [17.] should be compared to the simulation results shown in Figure 9 on page 39.

The CT model was also validated with the oscillogram -- Fig. 1 of Ref. [33.]. This curve was obtained by increasing the source voltage, to cause saturation in the first cycle. The comparison is between the curves in Figure 10 on page 41 and those in Figure 11 on page 42.

The effect of remanence on the onset of saturation is also studied. With no remanent flux in the core, the time to saturation was 0.010 seconds (see Figure 12 on page 43). Adding a remanent flux linkage of 3.0 WbT (approximately 80% of the peak flux linkage) hastened saturation to approximately 0.005 seconds (see Figure 13 on page 44). If, for the same fault, a remanent flux linkage of -3.0 WbT is in the core, saturation is delayed to approximately 0.025 seconds (see Figure 14 on page 45). Thus, the validity of the model is further confirmed. It is worthwhile to note that the phenomenon of residual magnetic flux has been the subject of numerous studies over a long time span, as evidenced by Refs. [34.], [35.], and [36.].

3.3.2.1 CT Time to Saturation: Ref. [17.] plots a series of curves for the saturation factor K_s vs. Time to saturation. The saturation factor K_s is defined as follows :-

$$K_s = \frac{V_x \times N_2}{I_1 \times R_2} .$$

Figure 1. Waveforms of 150/5 ct subjected to 40 KA
Primary current with offset

Figure 10.   Fig. 1 from Ref. [33.]

3.0 CURRENT AND CAPACITOR VOLTAGE TRANSFORMER MODELS
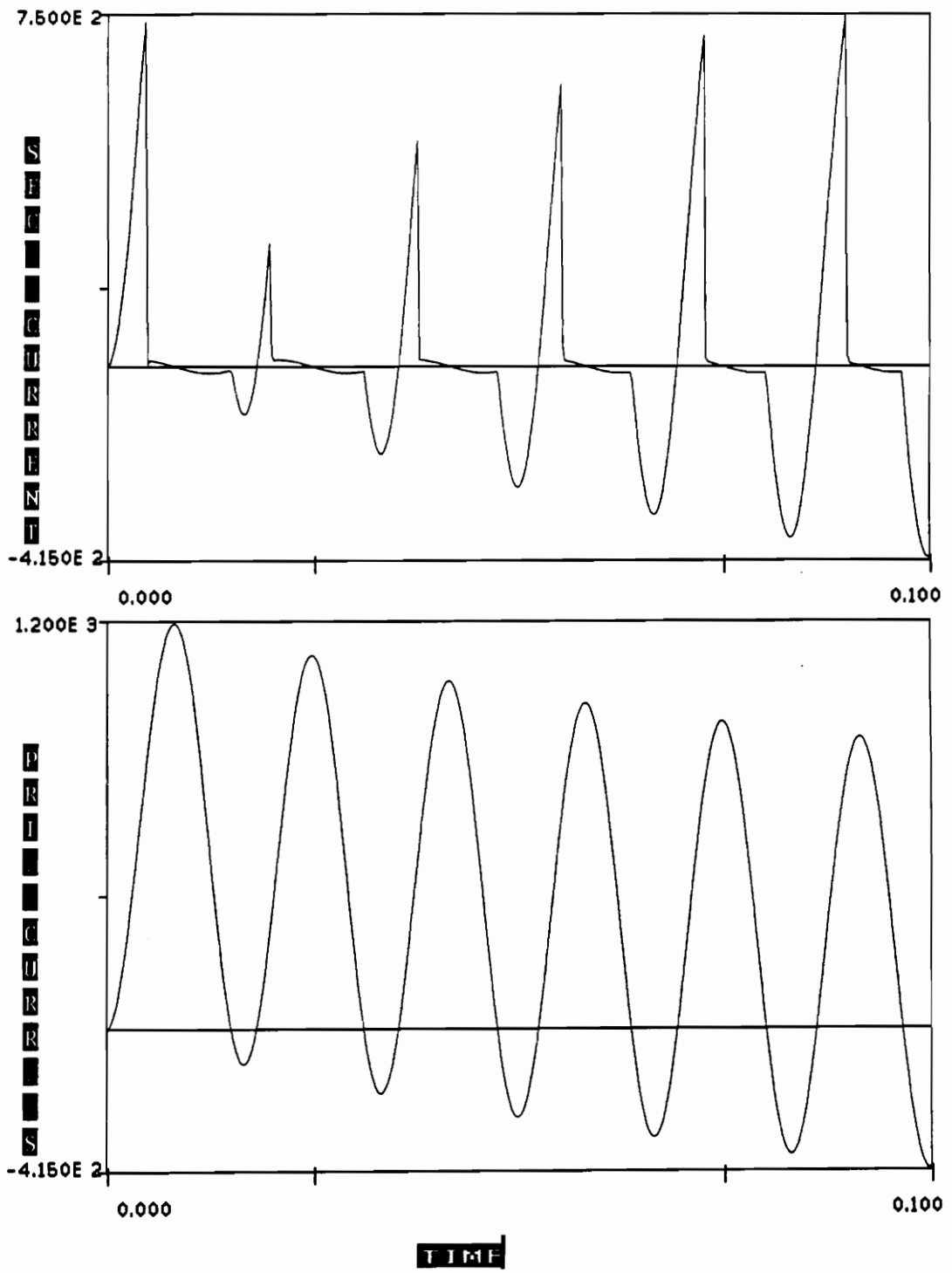
Figure 11. Simulation of Fig. 1 from Ref. [33.]
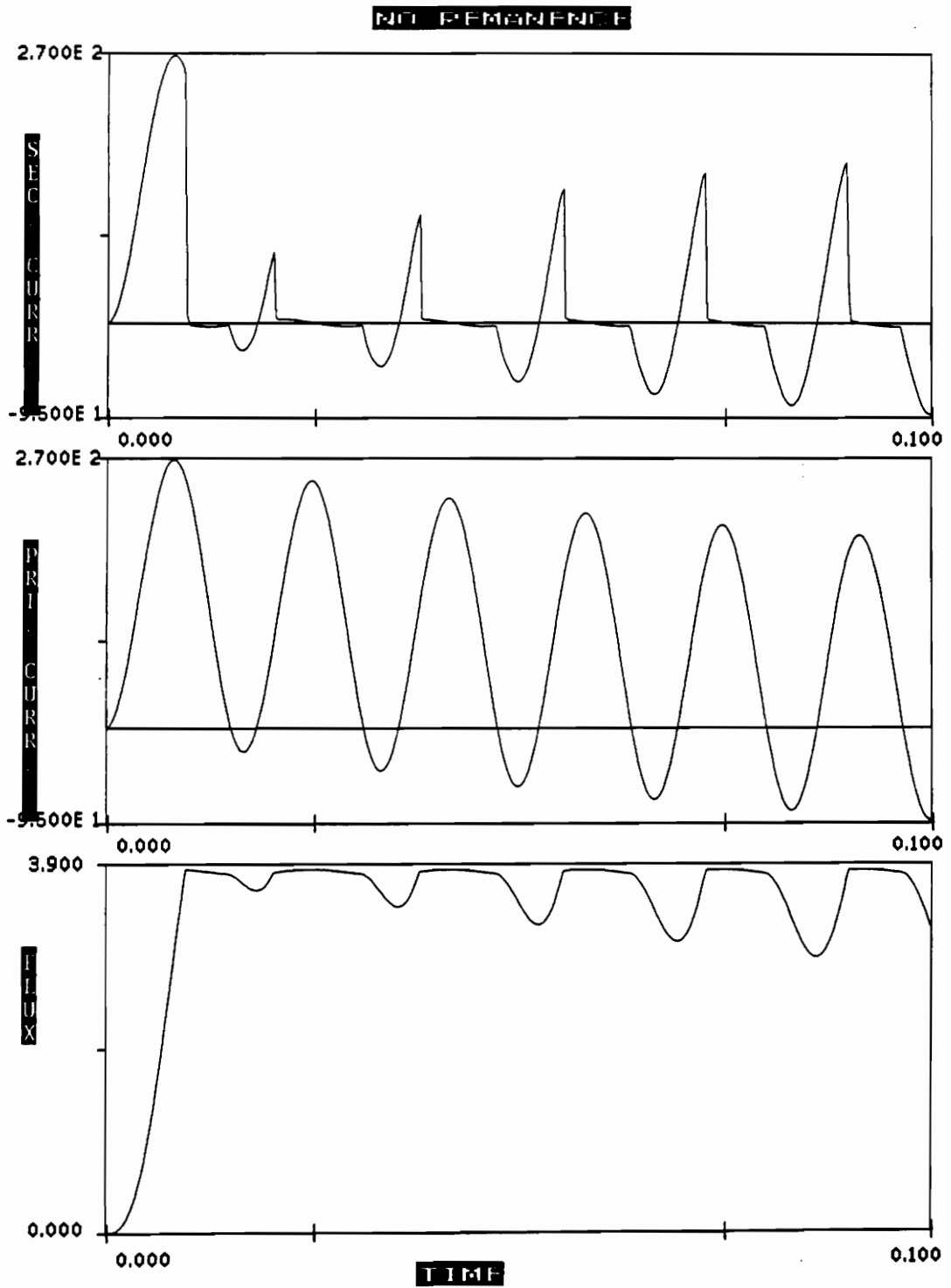
Figure 12. No remanence in CT core
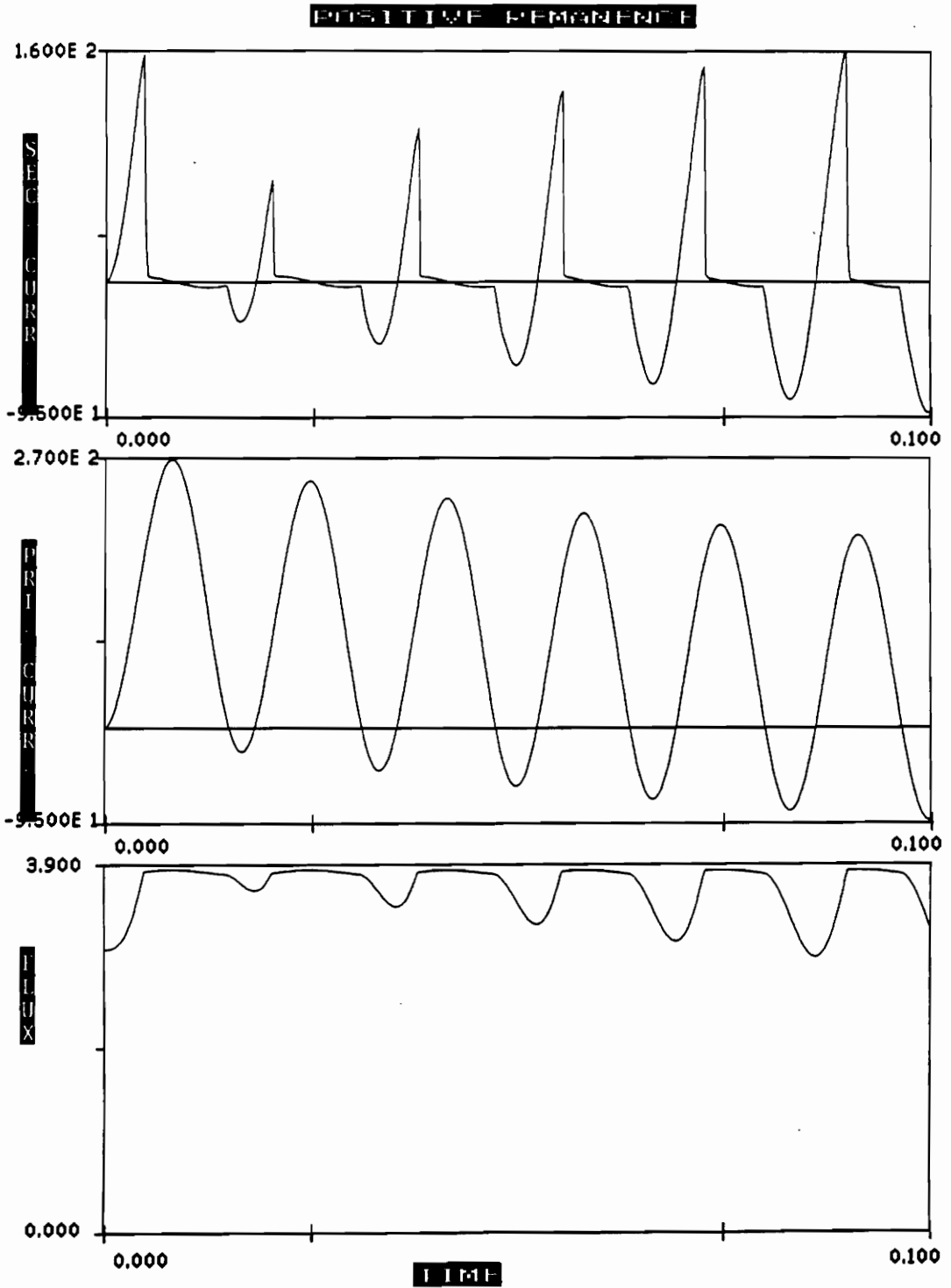
Figure 13. Positive remanence in CT core
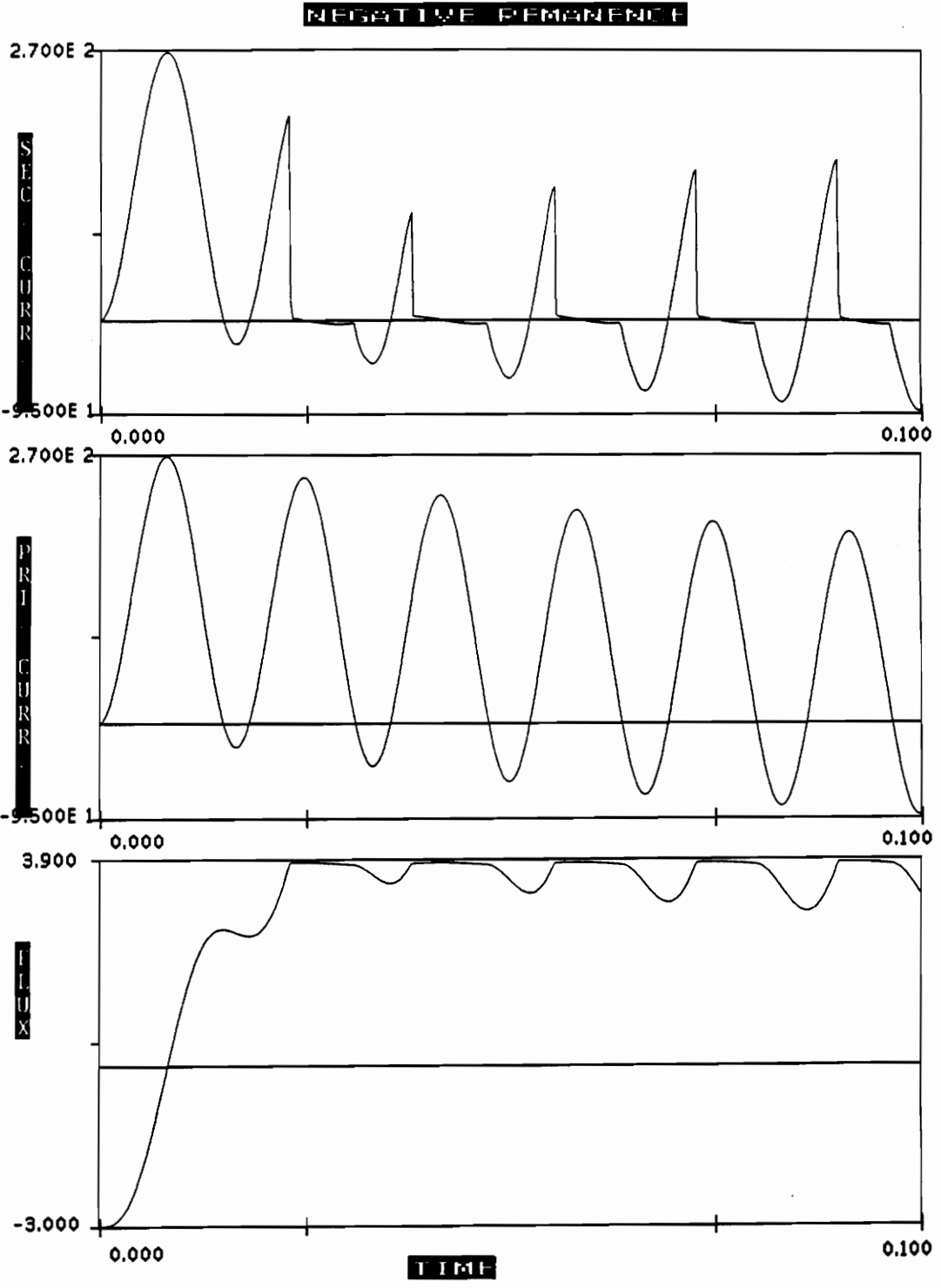
Figure 14. Negative remanence in CT core

where,

V_x is the saturation voltage (rms),

N_2 is the number of secondary turns,

I_1 is the ac current in the CT primary (rms),

R_2 is the resistance of the total CT secondary burden (winding plus external resistance).

It is important to note that I_1 is the rms primary current. For a particular value of the primary time constant (T_1), a series of curves are plotted for different secondary time constants (T_2). The aim is to determine how accurate the CT model is in predicting the time to saturation.

At the outset, it must be stated that the curves for K_s vs. Time to saturation of Ref. [17.] are approximations to reality. Hysteresis is not considered, and the flux wave is considered without any sinusoidal variations. Not considering the sinusoidal variations in the flux wave leads to pessimistic results in time to saturation.

The values of the time to saturate using the CT model in an EMTP test data case (with $T_1 = 0.06$ secs. and $T_2 = 10.0$ secs) and the time to saturate from Fig. 6 in Ref. [17.] are given in Table 1 on page 47.

The CT model, as expected, always gave larger time to saturation than the curves. Most results were within $+5\%$ of the theoretical curves of the report. A few results were up to $+21\%$ of the theoretical curves.

Table 1. Comparison of CT model's and Ref. [17.]'s time to saturation

K(s)	CT model's time to saturation (t in ms)	Ref. [17.]'s time to saturation (t in ms)
7.6	24.8	21.0
9.1	27.5	27.0
11.84	42.5	39.0
13.3	56.9	47.0
15.2	60.7	60.0
18.7	94.6	93.0
20.7	128.4	126.0

3.4 INTRODUCTION TO MODEL INCORPORATION IN EMTP

In EPRI/DCG EMTP Version 2.0, an important new feature of data modules has been introduced. A module is a functional frame which allows for variable node names, variable values of impedance, variable times for switch closing and opening, etc. This module can be included in a data case with the appropriate node names, numerical values, switch names, and time of switch closing and opening. Thus a function can be included many times in a data case through the 'SINCLUDE' card followed by the module name and the node names and other numerical data required in a data case. For example, a module can be made for a two stage R-C cascaded filter called FILTER2.INC. This module consists of

four node names (including the common node), and four numerical values for each of the resistances and capacitances. Whenever the user wishes to include the filter in a data case, a statement similar to the one below is sufficient: --

$INCLUDE FILTER2.INC INPUT1, MIDPNT, OUTPUT, COMMON, 1000.0, 0.1E-6, 2000.0, 0.1E-6

The user can include as many modules of name FILTER2.INC with different values of node names, resistances, and capacitances as desired in one data case. Thus, there can be one module for one function or device, such as a CT or a relay. The method of modules improves reliability because the modules can be tested individually. Once a module is tested, it can be employed in all studies involving the same function. Another **extremely** important advantage is that changes can be easily made to the module without changing the EMTP source code. The use of modules also improves the clarity and readability of large EMTP data cases, because of the grouping of functions.

This feature of modules is implemented in EPRI/DCG EMTP Version 2.0 by subroutine DATAIN. Subroutine DATAIN has three main functions:

1. To convert an input MODULE which contains the data of variable node names and variable numerical data to a *.INC file with the vectors KARD, KARG, KBEG, KEND, and KTEX. The five vectors are needed to process the $INCLUDE *.INC file in a data case. The vectors KARD, KARG, KBEG, KEND, and KTEX identify the card number, the argument number, the beginning column number for the argument being substituted, the ending

column number for the argument being substituted, and the numeric or alphanumeric character of the data being substituted.

2. To read in the *.INC file, and the vectors KARD, KARG, KBEG, KEND, and KTEX using the $INCLUDE card. The EMTP data case is now expanded to include all the cards of the module and the node names and numerical values required by the module. After all the modules have been read in, EMTP data case is sorted according to the order of the cards, i.e., /TACS, /BRANCH, /SWITCH, and then /SOURCE. The data case is now ready to be read; processing the input data in Overlays 2 and 5 begins.

3. To use the module concept in the interactive mode of EMTP, subroutine DATAIN contains the code to achieve this.

In subroutine DATAIN, after the code to process a data case in the interactive mode, EMTP input data case is copied to an array named FILE6. The code then proceeds to read a *.INC file and expand it. Before it begins this procedure, a call is made to Subroutine INSTFR to process the input CT and CVT data and include the appropriate CT and CVT modules in the data case, if required. Just after the call to subroutine INSTFR, another call is made to subroutine RELAYS to process the input relay data and include the appropriate relay modules. Subroutine INSTFR is used to process the CT and CVT input data and to write within the array FILE6 the appropriate current transformer module with **all** of the data required by that particular module.

Although the next three paragraphs refer specifically to the CT model and its incorporation, similar reasoning applies to the CVT model, the SLY relay, and the BDD relay. The details of the incorporation of these components in EPRI/DCG EMTP Version 2.0 are given in Sections 3.8, 5.2, and 5.3.

Because no capacitances are included in the EMTP transformer model, it is valid up to a few kHz (Ref. [12.]). There is a model for a Type 96 Nonlinear hysteretic inductor. This element has the ability to model the hysteresis curve for ARMCO M4 grade cold rolled grain oriented silicon steel. Minor hysteresis loops can also be simulated. Remanent flux can be included in the model by switching the Type 96 element at time $t = 0.0^+$. This element requires the peak flux linkage vs. peak exciting current characteristic. There are also models for resistance, inductance, and capacitance. Thus, all the components required to model the instrument transformers are already incorporated within EMTP.

Since the concept of modules has been used, there is no necessity to include additional code for the current transformer model. Thus, there is no need to repeat the transformer model and the Type 96 Nonlinear Hysteretic Inductor code. If the source code of EMTP were changed and the code for the CT model were added, there would be a large increase in the source code, with no corresponding enhancement in the functions of EMTP. There would be unnecessary duplication of code. The EMTP has grown enormously in the last two decades, to the point of being almost unmanageable, and this duplication is undesirable.

Another alternative would be to read in the CT model data, and perform the conversion of the (V_{rms} - I_{rms}) curve to the (ψ_{peak} - I_{peak}) curve. Then the CT model data, together with the internal node names of the CT model, could be embedded in EMTP **[Y]** matrix formulation. This embedding is an extremely complex task, as it entails modifying large parts of EMTP code. It would then be necessary to test not only the new CT model, but also all other EMTP components to ensure that the changes did not affect other models. This task can be accomplished only by a large team working in concert.

3.5 INCORPORATION AND DATA FORMAT OF THE CT MODEL IN EMTP

3.5.1 Incorporation method

As mentioned in Sec. 3.4, subroutine DATAIN calls subroutine INSTFR for the processing of CT and CVT input data. If the keyword CTMODEL is found, subroutine INSTFR then includes the appropriate CT module with all the required data. The flowchart of subroutine INSTFR is given in Figure 15 on page 52. As discussed before, the (V_{rms} - I_{rms}) has to be converted to the (ψ_{peak} - I_{peak}) curve. This conversion is done by subroutine RMSHYS, which is a combination
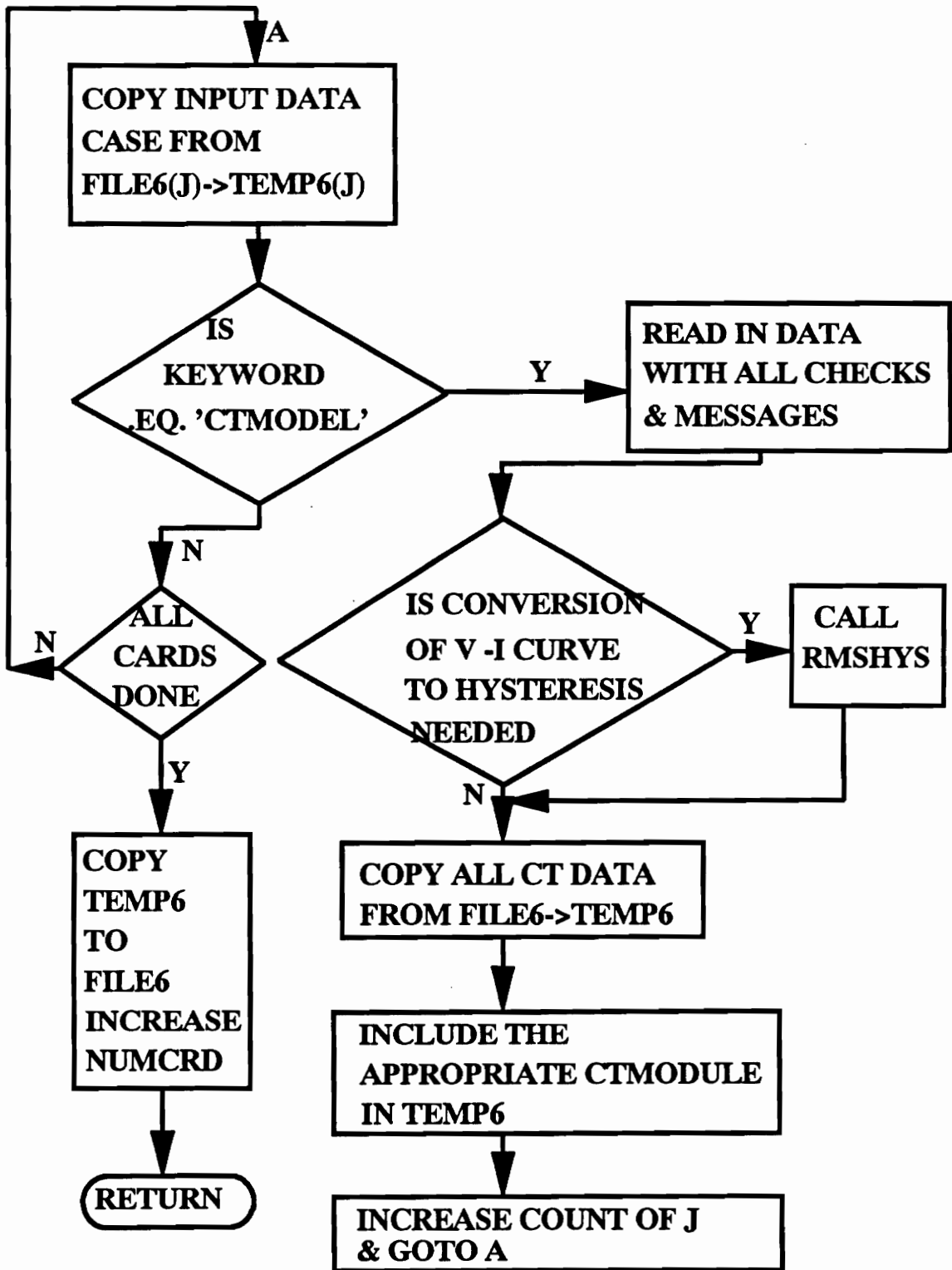
Figure 15. Flowchart of Subroutine INSTFR for CTs
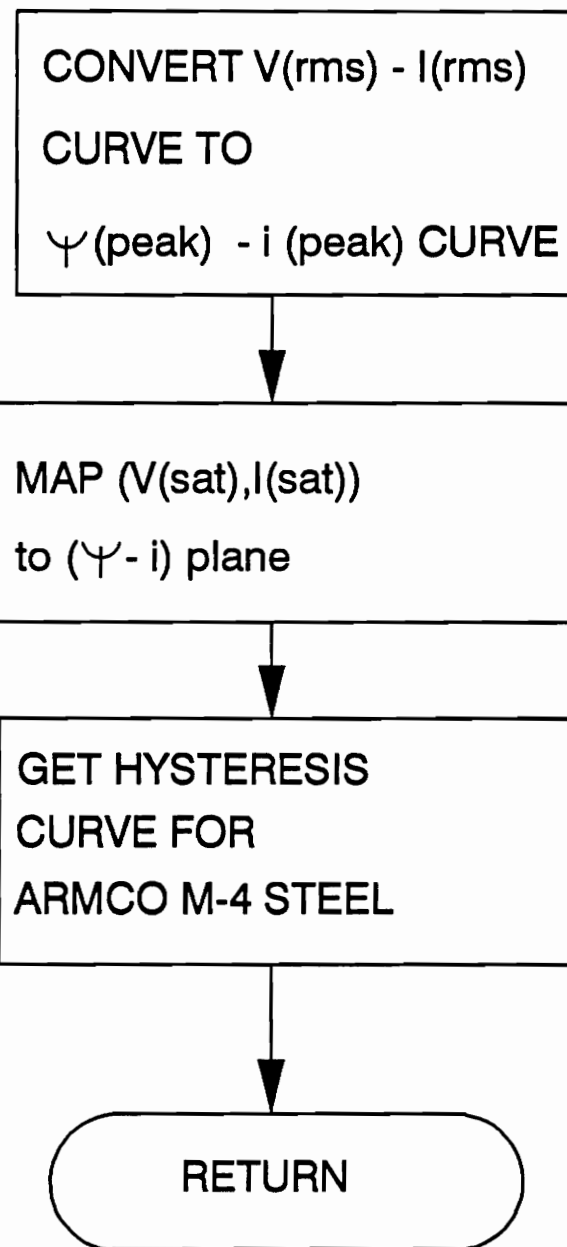
Figure 16.   Flowchart of Subroutine RMSHYS

of subroutines CONVERT and HYSDAT in the Auxiliary part of EPRI/DCG EMTP Version 2.0. The flowchart of subroutine RMSHYS is given in Figure 16 on page 53.

The CT has been modeled by creating the following modules :- CTBL.INC, CTNBL.INC, CTBNL.INC, and CTNBNL.INC. The modules are created by running AUX on the data files CTBL.DAT, CTNBL.DAT, CTBNL.DAT, and CTNBNL.DAT. It is not necessary for the user to create the modules. They must be present in the EMTP directory, and the user must have read access to the modules. The four modules represent the following cases :-

CTBL.INC   this module is included by EMTP when the user inputs IBURFG = 01 and ILEDFG = 01. This is the Burden and Lead module. The values of the burden resistance, burden inductance, and burden capacitance are given by the user and connected within the CT model on the ct secondary side. An internal node for the lead impedance is created, and the values for the lead resistance, lead inductance, and lead capacitance are given by the user and connected in the ct model.

CTNBL.INC   this module is included by EMTP when the user inputs IBURFG = 00 and ILEDFG = 01. This is the No Burden, Lead module. The burden values must be connected by the user on the ct secondary side. An internal node for the lead impedance

is created, and the values for the lead resistance, lead inductance, and lead capacitance are given by the user and connected in the ct model.

CTBNL.INC   this module is included by EMTP when the user inputs IBURFG = 01 and ILEDFG = 00. This is the Burden, No Lead module. The values of the burden resistance, burden inductance, and burden capacitance are given by the user and connected within the CT model on the ct secondary side. No provison is made for the lead impedance.

CTNBNL.INC   this module is included by EMTP when the user inputs IBURFG = 00 and ILEDFG = 00. This is the No Burden, No Lead module. The burden values must be connected by the user on the ct secondary side. No provison is made for the lead impedance.

The modules represent the basic structure of the CT model. The details needed by this module are the following :-

* the names of the primary nodes to which the current transformer is connected;

* the names of the secondary nodes of the current transformer;

- the parameters of the transformer, such as the primary and secondary resistance and leakage inductance, and number of turns on each winding;

- the details of the burden and lead impedances;

- the remanent flux, the frequency, and the coordinates of the saturation point;

- the magnetization curve, either V(rms)-I(rms) or ψ(peak)-i(peak) hysteresis curve;

- flags for selecting default current transformer values, the burden connection, the lead impedance, and the magnetization curve options.

EMTP processes the input data case and computes the hysteresis curve for ARMCO M4 oriented silicon steel required by the Type 96 nonlinear hysteretic element. It then inserts the appropriate CT module with the required inputs, including the hysteresis curve in the data case. This module is then sorted and included in the data case. The outputs of the CT model are the current through the burden and the voltage across the burden.

3.5.2 CT Model Data Format

The data format of the ct model is shown in Figure 17 on page 57.

C CTMODEL

```
    (I2)      (A6)      (A6)      (A6)      (A6)      (A6)
C IDEFLG CTPRI1 CTPRI2 CTOUT1 CTOUT2 CTRIDN

    (A6)      (A6)      (A6)      (A6)      (A6)      (A6)
C RNPRIM RNSEC PRIRES PRILEK SECRES SECLEK

    (I2)      (A6)      (A6)      (A6)      (I2)      (A6)      (A6)
C IBURFG BURRES BURIND BURCAP ILEDFG RLDRES RLDIND ...

        (A6)
    ... RLDCAP

    (I2)      (A6)      (E8.0)  (E8.0)  (E8.0)
C IHYSFG REMFLX  FREQ  RISAT  VSAT

    (E16.0)       (E16.0)
C RIRMS        VRMS

C .....              ...

C       9999.
```

IDEFLG = 00 => USER SUPPLIES ALL DATA
        = 01 => ALL DEFAULT VALUES USED BY EMTP

IBURFG = 00 => USER WILL CONNECT THE BURDEN ACROSS
                  THE OUTPUT TERMINALS
        = 01 => BURDEN VALUES SUPPLIED BY USER AND
                  CONNECTED BY EMTP

ILEDFG = 00 => NO LEAD IMPEDANCE
        = 01 => LEAD IMPEDANCE VALUES SUPPLIED BY USER
                  AND CONNECTED BY EMTP

IHYSFG = 00 => USER SUPPLIES V(rms)-I(rms) CURVE, REMFLX,
                  FREQ, RISAT, VSAT
        = 01 => USER SUPPLIES FLUX(peak)-I(peak) CURVE,
                  and REMFLX

Figure 17.   Current Transformer Data Format

```
BEGIN NEW DATA CASE
C  THIS DATA CASE IS TO TEST THE CT MODULE WITH A PRIMARY CIRCUIT FAULT
C  CT MODEL IN VERSION 2.0 - USING THE MODULE CTNBNL.INC
C  NO BURDEN (NB) MEANS USER CONNECTS THE BURDEN
C  NO LEAD (NL) MEANS NO LEAD IMPEDANCE IN THIS CASE.
5.E-5 .100000
     5        -1        1
C 3456789012345678901234567890123456789012345678901234567890
C          1         2         3         4         5         6         7         8
C  IDEFLG = 00
C  IBURFG = 00
C  ILEDFG = 00
C  IHYSFG = 00
C CTMODEL
C 00CTPRI1CTPRI2CTSEC1#####UNI
C 5.00001200.00.001515.0001.00003.2000
C 002.60000.00000.0000000.50000.00000.0000
C 000.000060.0000025.000001250.000
C    0.5000000E+00   0.4000000E+03
C    0.1100000E+01   0.8000000E+03
C    0.1260000E+02   0.1200000E+04
C    0.1007500E+03   0.1300000E+04
C          9999
/BRANCH
C 3456789012345678901234567890123456789012345678901234567890
C          1         2         3         4         5         6         7         8
  CTPRI4ENDLIN              0.338 16.875                                  3
  CTPRI2CTPRI4              0.001
  ENDLIN                   150.0  3.75                                    1
  ENDLINSHSWTH              .001
C THIS IS THE BURDEN.
  CTSEC1                     2.6                                          3
BLANK ENDS BRANCH CARDS
/SWITCH
  BEGLINCTPRI1+.00000        5.9
  SHSWTH   +.00000           5.0
BLANK ENDS SWITCH CARDS
/SOURCE
14BEGLIN  405000.00  60.0        274.48            -1.0        5.0
BLANK ENDS SOURCE
BLANK CARD ENDING SELECTIVE NODE VOLTAGE OUTPUT REQUESTS
BLANK CARD ENDING PLOT CARDS
BEGIN NEW DATA CASE
BLANK
BLANK
```

Figure 18. CT Model Test Data Case

An example of an EMTP data case employing the CT model is given in Figure 18 on page 58. For an explanation of the data format and the various terms employed in the CT model see Appendix A.

3.5.3 Outputs

The outputs of the CT Model are the current through the burden and the voltage across the burden. These outputs are available in the cases where the user has selected the option IBURFG = 01.

3.6 CVT MODEL DEVELOPMENT

The Capacitor Voltage Transformer (CVT) model is shown in Figure 19 on page 60. This model is applicable for subsidence transient studies. The following are the overvoltage protection devices used in one high voltage coupling capacitor potential device (See Ref. [37.] for more details). The actual CVT usually has a protective network across the capacitor C_2 as shown in Figure 19 on page 60. This protective network consists of an arcing gap in series with a parallel R-C network. This network provides overvoltage protection and ferroresonance suppression. Another arcing gap is placed across the inductor L_1, protecting its insulation from high voltages. A ferroresonant suppression circuit is connected across

LEAD IMPEDANCE

L_2

SWITCH

R_2

TYPE 96 NONLINEAR HYSTERETIC INDUCTOR

N2

N1

L_1

R_1

L_0

C_1

C_2
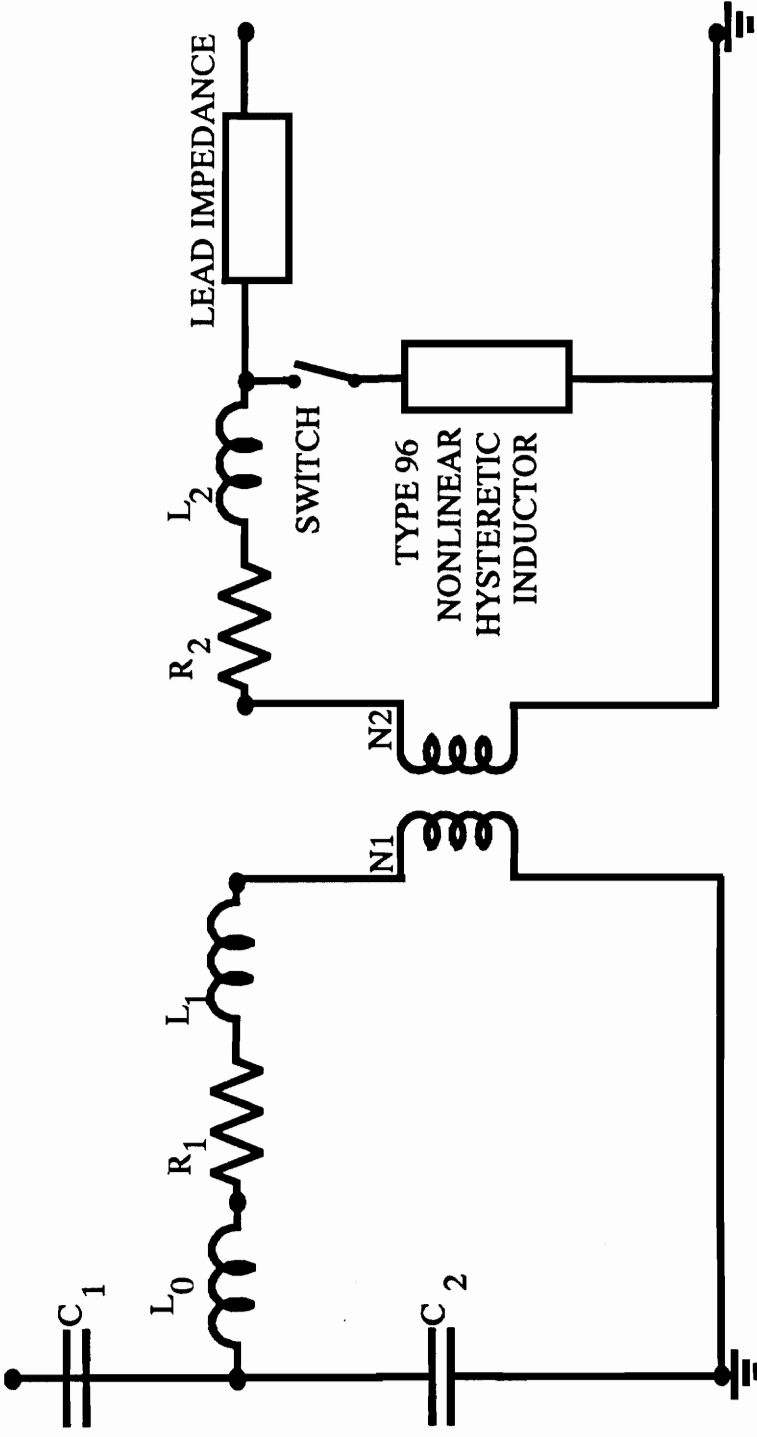
C_1, C_2: Capacitor Divider

L_0: Tuning Inductor.

R_1, L_1: Transformer primary resistance and leakage inductance.

R_2, L_2: Transformer secondary resistance and leakage inductance.

Switch closes at T=0.0.

Figure 19. Capacitor Voltage Transformer Model

the secondary terminals of the CVT. An arcing gap with a series R-C network is placed across the transformer primary. During an overvoltage, the gap breaks down and protects the transformer's primary insulation. Thus, a model for a CVT which represents it for overvoltages will need data for the Type 99 Pseudononlinear Resistance, which includes the flashover voltage and the (V - I) characteristic of the arcing gap. Alternatively, the arcing gap can be modeled by a Class 2 voltage-controlled flashover switch. Usage and data requirements of both of these components are elaborated upon in Ref. [1.]. When models for the arcing gaps are included in the CVT model, then the model will be applicable for overvoltage studies.

3.6.1 A Discussion of the CVT model

3.6.1.1 Good Representation of a CVT in EMTP

A good representation of a capacitor voltage transformer equivalent circuit for modeling purposes in EMTP is shown in Figure 20 on page 62. In this representation, the secondary winding resistance and the secondary winding leakage inductance are included with the lead impedance and the burden impedance.

3.6.1.2 EMTP Requirements
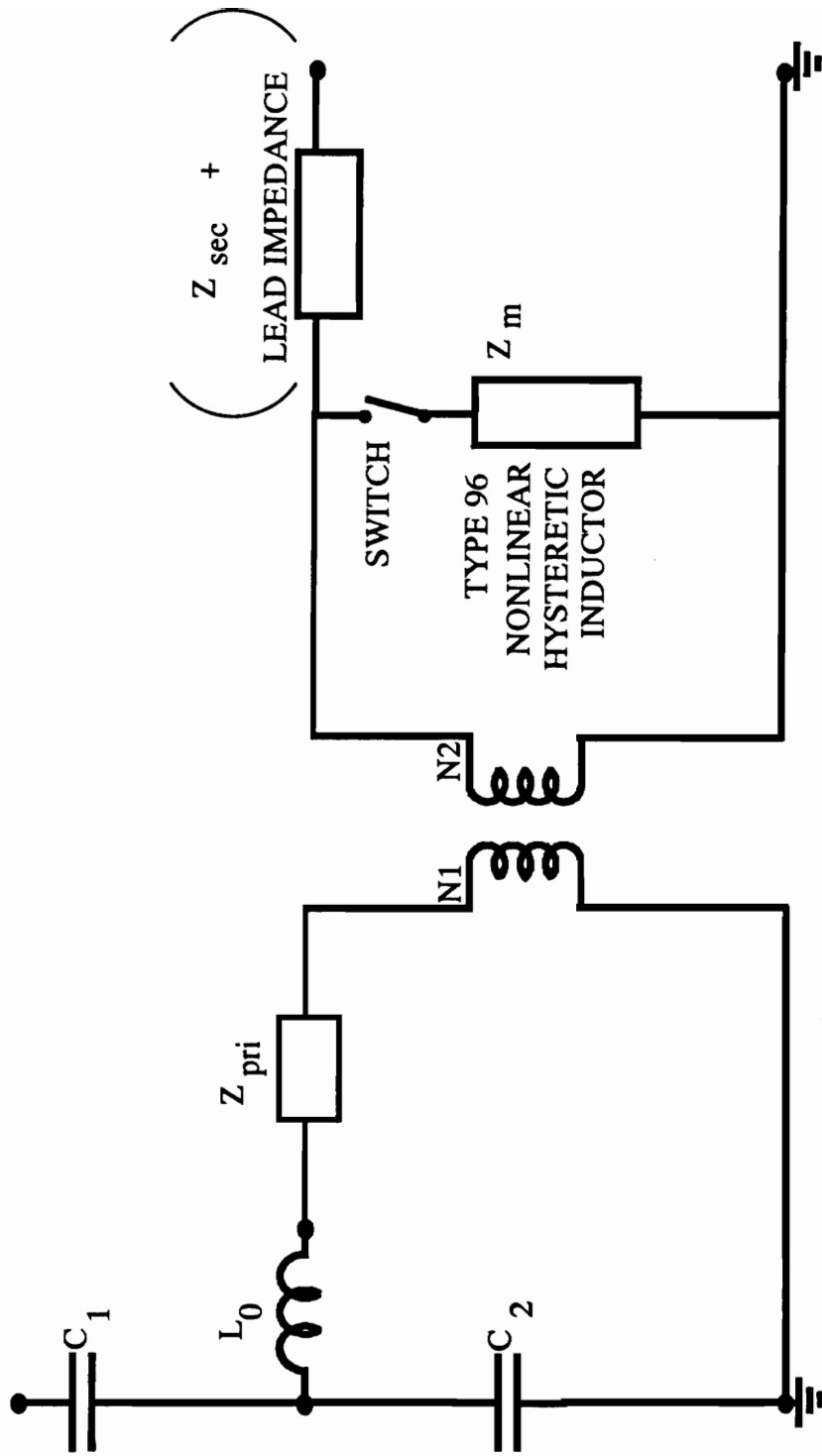
Figure 20. Representation of a CVT model in EMTP
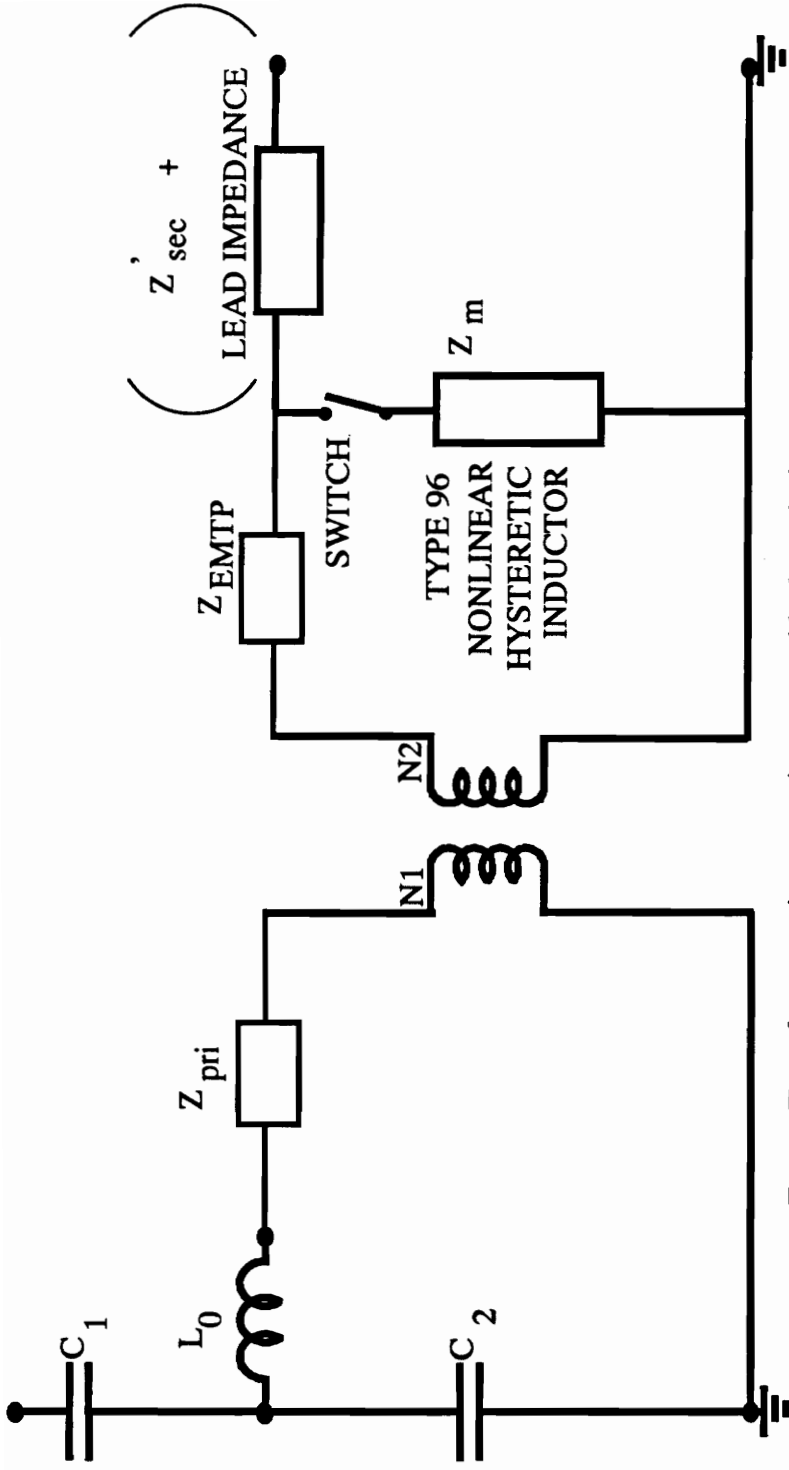
Z_{pri} : Transformer primary resistance and leakage inductance.

Z_{sec} : Transformer secondary resistance and leakage inductance.

Z_m : Transformer magnetizing impedance

Z_{pri} : Transformer primary resistance and leakage inductance.

Z_{sec} : Transformer secondary resistance and leakage inductance.

Z_m : Transformer magnetizing impedance

Z_{EMTP} : Transformer impedance required by EMTP

$Z'_{sec} = Z_{sec} - Z_{EMTP}$

Figure 21. EMTP requirements of a CVT model

The EMTP representation of a capacitor voltage transformer is shown in Figure 21 on page 63. In this model, Z_m is placed after Z_{EMTP}, in parallel with ($Z'_{sec} + Z_{lead} + Z_{burden}$). This representation is required because finite values **must** be given for Z_{pri} and Z_{EMTP}. More precisely, L_{EMTP} must be non-zero, and R_{EMTP} can be zero; and either R_{pri} or L_{pri} can be zero, but not both. More details are given in Ref. [1.]. This data requirement of the EMTP transformer model can be satisfied by separating Z_{sec} into two parts -- Z_{EMTP} and Z'_{sec}. For a discussion on the allowed magnitude of Z_{EMTP}, see Section 3.2.2. With the approximation of placing Z_m as in Figure 21 on page 63, there is no appreciable change in the voltage seen by the relays. The magnitude of Z_m can be as high as six megohms, as mentioned in Ref. [38.]. The magnitude of Z_{burden} for which CVTs are tested varies from 40 Ω (corresponding to 100 VA) to 160 Ω (corresponding to 25 VA) for a 63.5 V(rms) secondary rating. There is a lower bound on the magnitude of Z_{burden}, but there is no upper limit on the connected Z_{burden}. The order of magnitude of Z_{sec} is 1 Ω. The magnitude of Z_{sec} is much smaller than those of both Z_{burden} and Z_m. Thus, the position of Z_{sec} does not affect the relay voltage in any significant manner.

3.6.1.3 Open Circuit Magnetization Characteristics: A similar discussion to that conducted in the case of current transformers (Section 3.2.3) applies here to the exact procedure for the determination of L_{sec}, and the separation of Z_m from the measured value of ($Z_{sec} + Z_m$). However, in the case of the capacitor voltage transformer it is not necessary to do this because the difference in the subsidence

voltage transient with and without the Z_m is negligible in most cases, and is extremely small (around 3%) in those cases where it exists for one particular CVT.

3.6.2 CVT model for EMTP

For capacitor voltage transformers, generally $(Z_{sec} << (Z_{lead} + Z_{burden}))$, and it can be included as shown in Figure 19 on page 60, which does not change the voltage seen by the relays both in the steady-state and during the subsidence transient. The relay voltage does not change, because the magnitude of Z_m is much larger than Z_{burden} and has a negligible influence both during steady-state operation, and during the subsidence transient regime. Z_m has been included in the CVT model because the nonlinear magnetization characteristic is essential to simulating ferroresonance.

In summary, the model in Figure 19 on page 60 is used because of the following reasons: the data requirements for the EMTP transformer model, the difficulty of separating Z_m from the measurement of $(Z_{sec} + Z_m)$, and the low magnitude of Z_{sec} relative to Z_m and $(Z_{lead} + Z_{burden})$ for capacitor voltage transformers. It is possible to use the model shown in Figure 20 on page 62 when the following is done: Z_m is separated from the secondary open circuit measurement of $(Z_{sec} + Z_m)$, and the data requirement of EMTP transformer model can be satisfied by separating Z_{sec} into two parts, Z_{EMTP} and Z'_{sec}. Because of the difficulty

of separating Z_m from the open circuit measurement, it may in practice only be possible to achieve the data requirement of the transformer model.

In most cases, the CVT will be used to simulate the subsidence transient and its effect on connected relays. For such an application, the user need not include Z_m in the CVT model, with negligible difference in the voltage at the relay terminals. The user can include the different CVT models without the nonlinear hysteretic inductor option.

3.7 CVT MODEL VALIDATION

Ref. [39.] is the AEP test data. Full scale tests have been conducted on a 500 kV GE CD31 CVT. A model for the CVT has been developed by AEP, which has been validated against the full scale tests. What we have done is built an EMTP circuit of the AEP model. For a burden of 0.0 Watts, a primary line to ground fault was applied at the instant V = MAX and at the instant V = 0. Compare Figure 22 on page 67 to Figure 23 on page 68 and Figure 24 on page 69. Again for a burden of 150W +j120 VARS, a primary line to ground fault was applied at the instant V = MAX and at V = 0. Compare Figure 25 on page 70 to Figure 26 on page 71 and Figure 27 on page 72. There is a reasonable match between the full scale tests and the EMTP simulations, which establishes the validity of the CVT model developed by AEP.
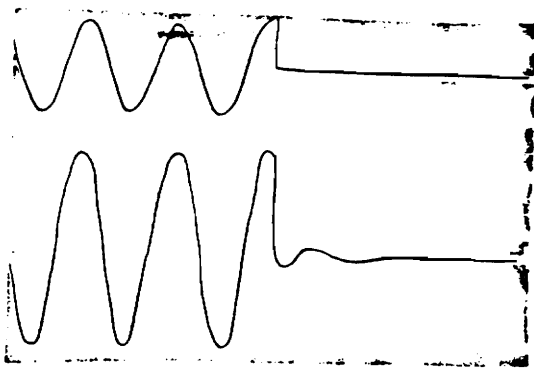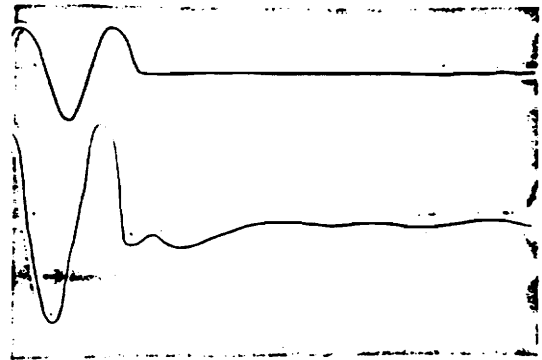
Figure 22.   GE CD31 full scale tests — no burden
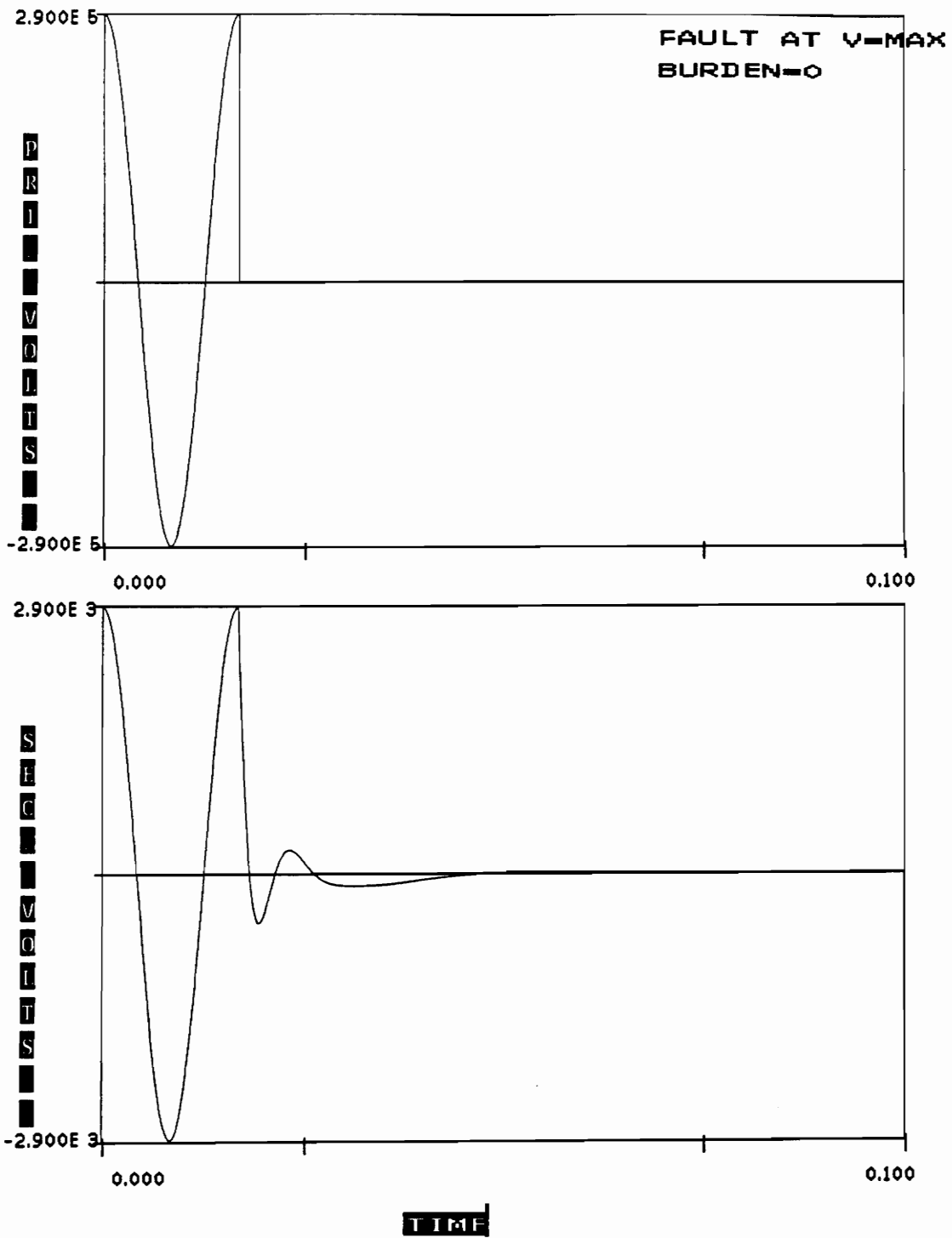
Figure 23.   Simulation – fault at V = max and no burden

FAULT AT V=0
BURDEN=0
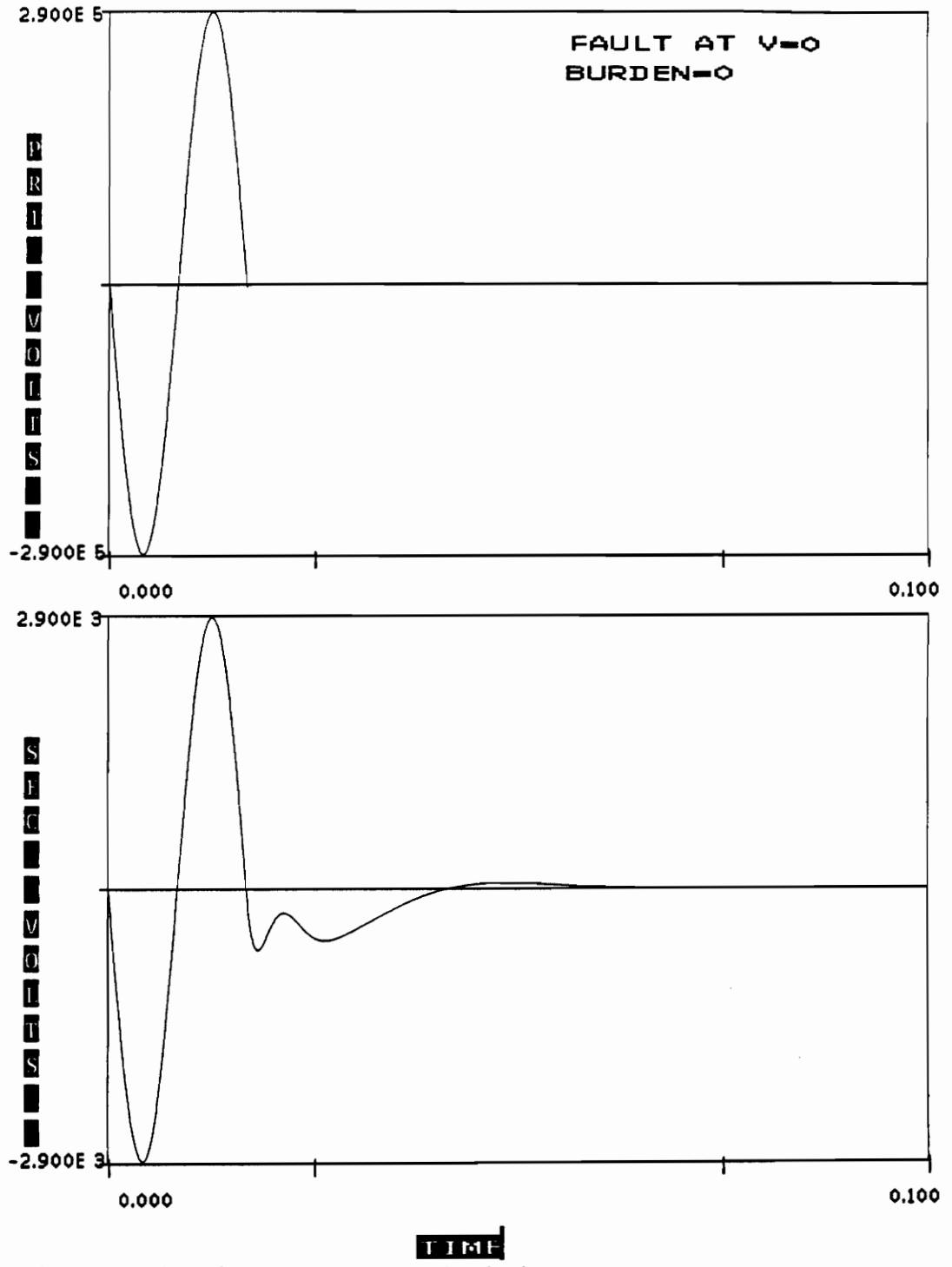
Figure 24.   Simulation — fault at V = 0 and no burden

Figure 25.   GE CD31 full scale tests - with burden
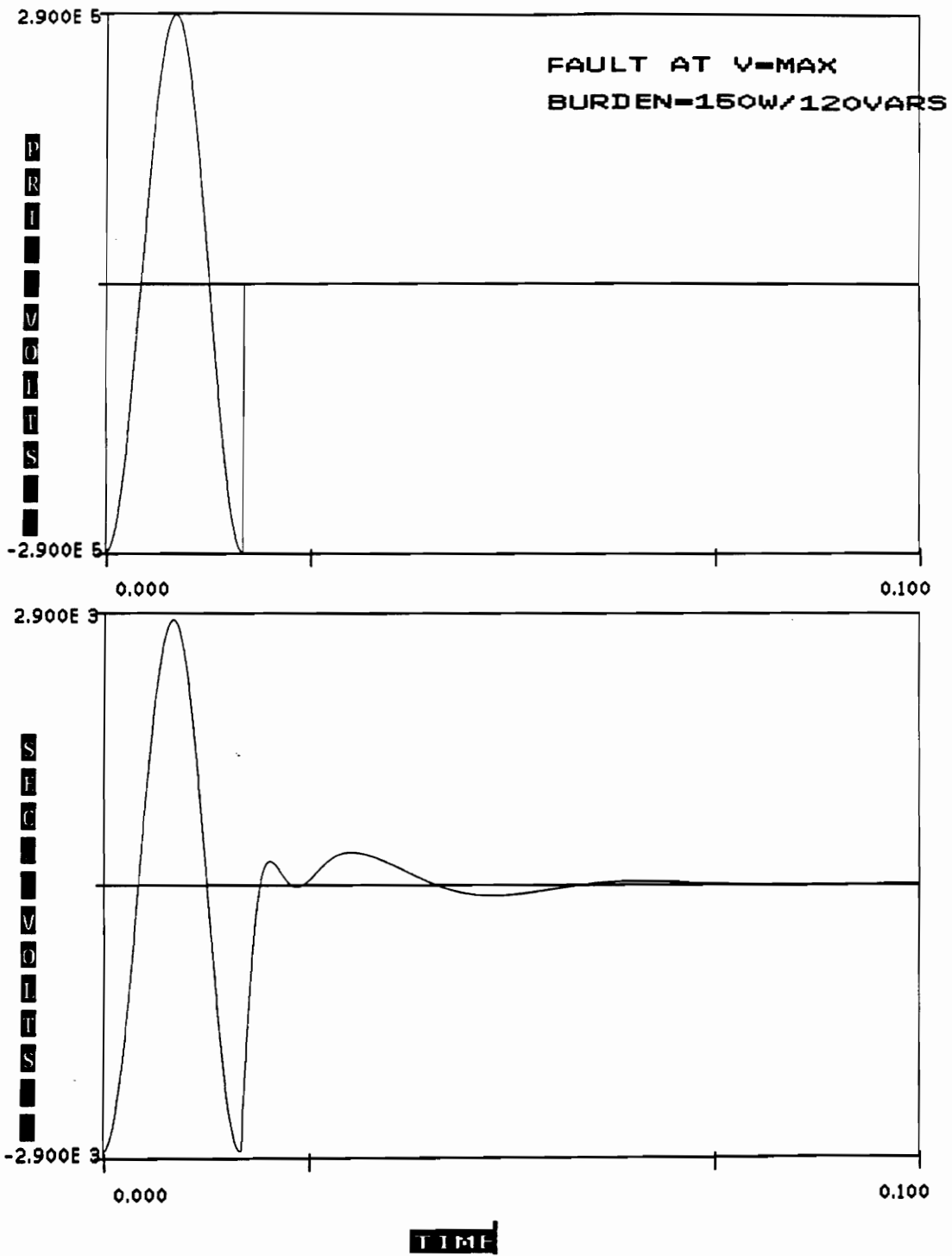
Figure 26.   Simulation — fault at V = max and with burden

3.0 CURRENT AND CAPACITOR VOLTAGE TRANSFORMER MODELS   71
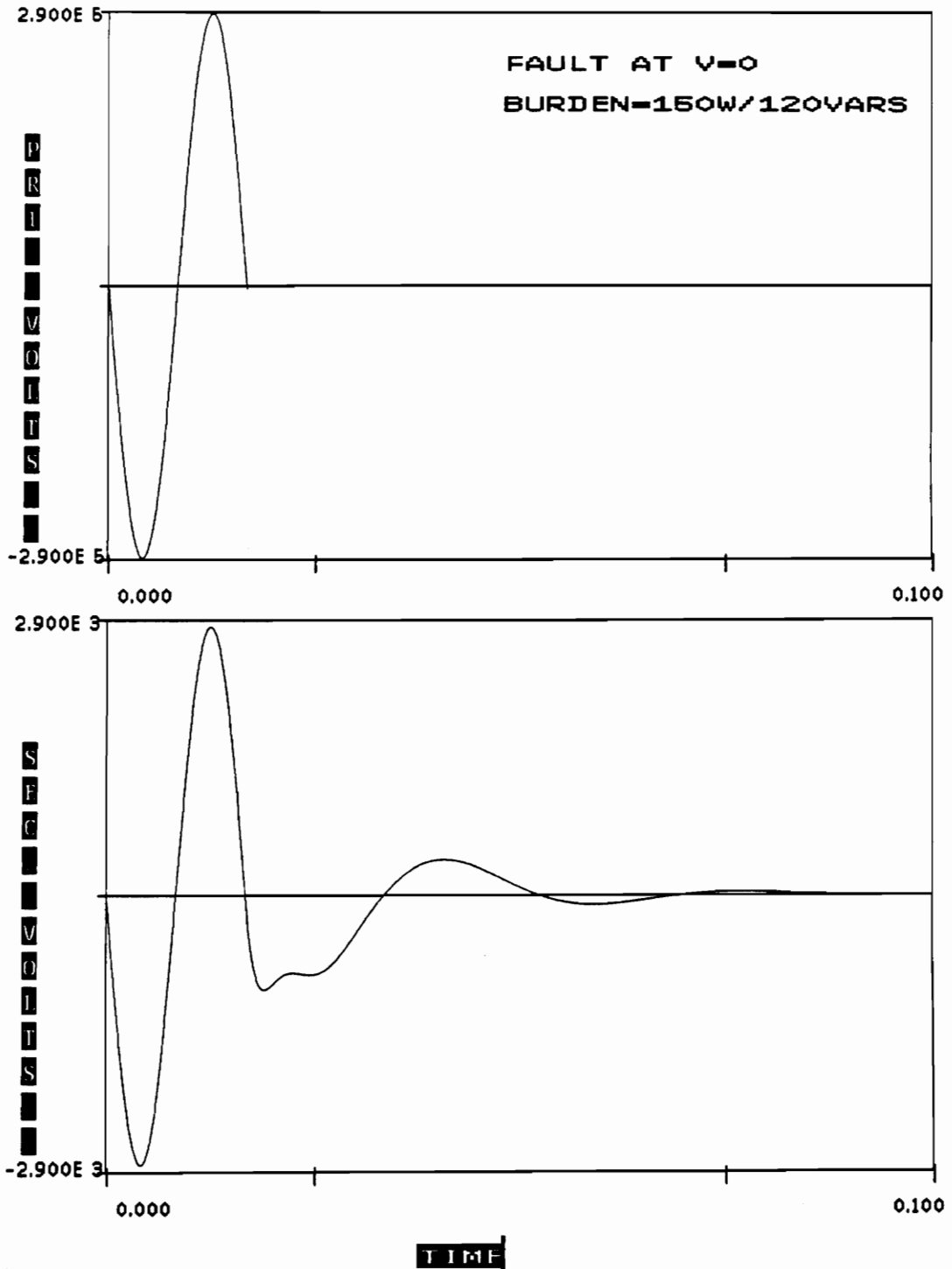
Figure 27. Simulation — fault at V = 0 and with burden

3.0 CURRENT AND CAPACITOR VOLTAGE TRANSFORMER MODELS   72

Ref. [40.] is a comprehensive study involving the modeling and the behavior of the CVT model. Ref. [40.] also contains data of a 110 kV CVT. This data was used to test the CVT model for the following cases :-

3.7.1 Effect of the instant the primary short circuit occurs

The subsidence transient has the largest magnitude and lasts the longest time when the fault occurs at a primary voltage zero. This result is expected -- see Ref. [38.] for a lucid explanation for why this is expected -- and poses a serious threat to reliable Zone 1 distance relay operations. This result was also obtained with EMTP simulations of the CVT model. This can be observed from Figure 28 on page 74 and Figure 29 on page 75.

3.7.2 Influence of the burden magnitude

With increased burden, the magnitude of the subsidence transient increases. This behavior is expected because of the increased primary current, and hence the increased energy stored in the inductances and the capacitances of the circuit. This result was also obtained with EMTP simulations of the CVT model.
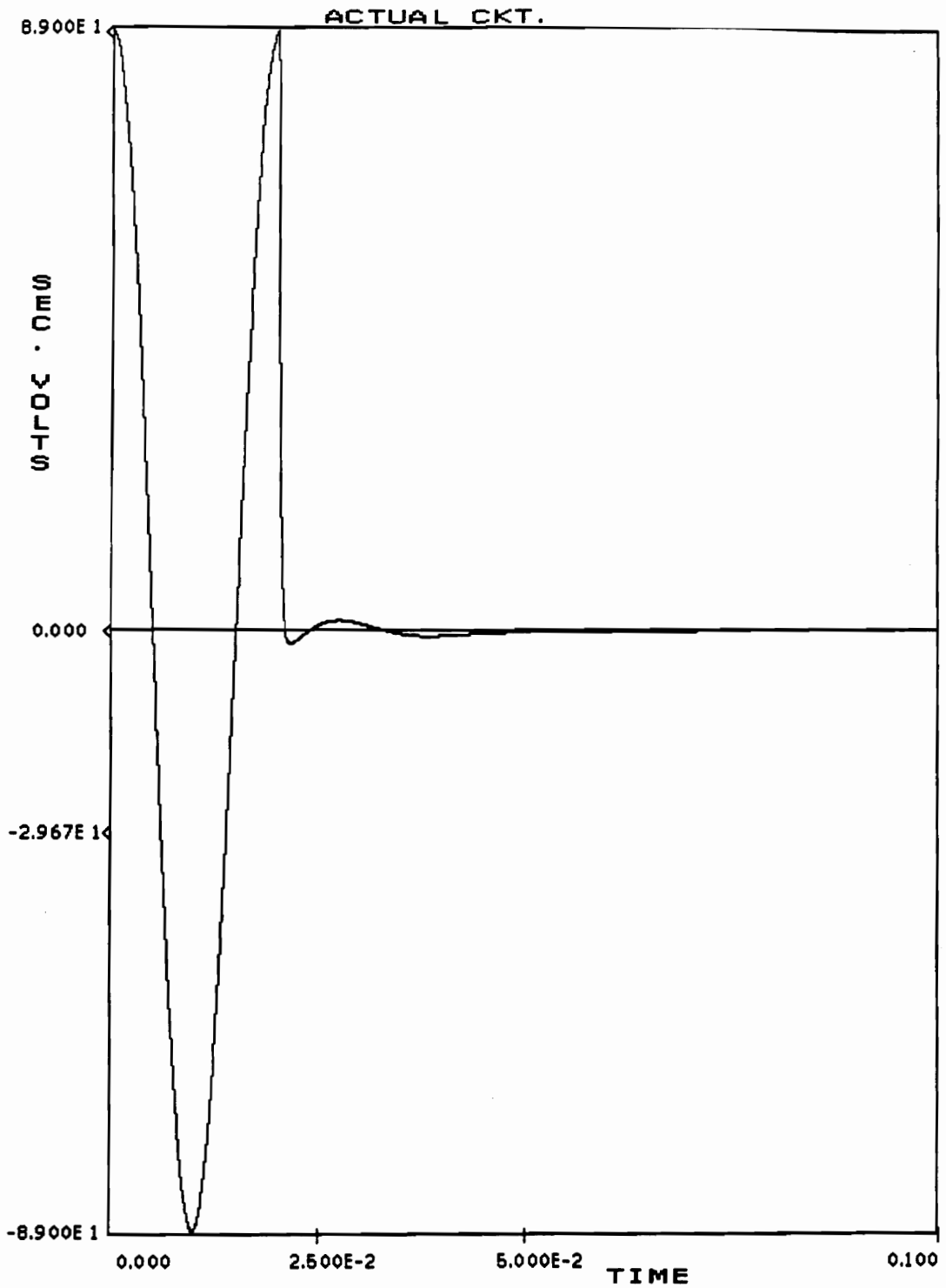
Figure 28. Simulation -- Ref. [40.] data and fault at V = max & with burden

3.0 CURRENT AND CAPACITOR VOLTAGE TRANSFORMER MODELS
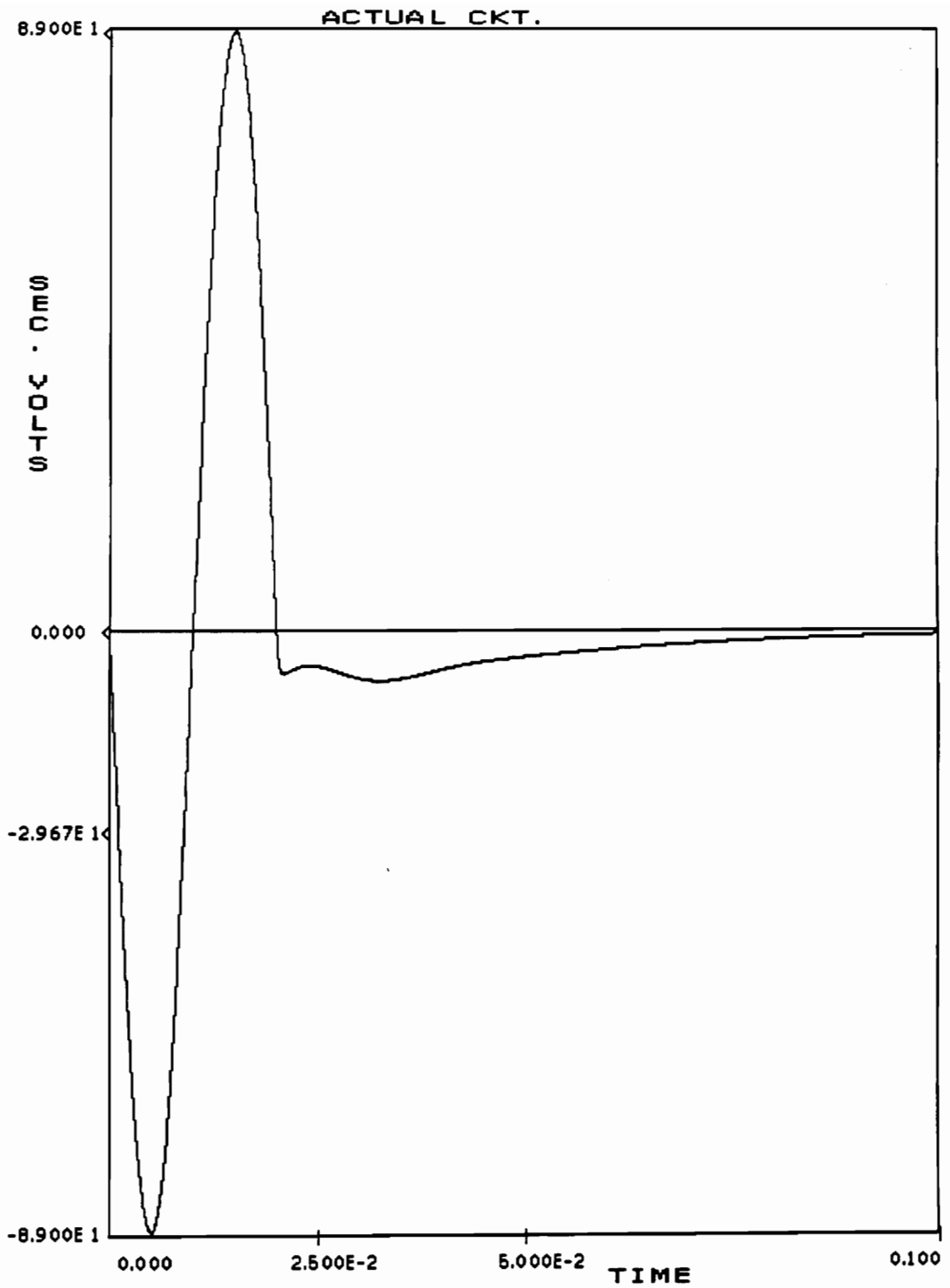
Figure 29.   Simulation -- Ref. [40.] data and fault at V = 0 & with burden

3.7.3 Effect of the value of the capacitance

Decreasing the value of the capacitances of the divider increases the magnitude of the subsidence transient. The reduction of the capacitance implies an increase in X_c ($= \dfrac{1.0}{j\omega C}$). For the same burden current, the voltage drop across X_c increases. The larger voltage drop implies larger energy storage ($\dfrac{1}{2} CV^2$) which has to be dissipated through the burden. This result was also obtained with EMTP simulations of the CVT model.

3.7.4 Effect of the magnetizing inductance

Tests were conducted with and without the magnetizing inductance. There is negligible difference in the subsidence transient between the two cases in most of the simulations. In those cases where there was a difference, the maximum difference observed was 3.0%. This result is expected and is similar to the results in Refs. [38.] and [40.].

3.7.5 Conclusions

At the moment, what we are lacking is both full scale test data and CVT data simultaneously, which will enable us to validate our model with even greater confidence. For the present, we can state that with a linear circuit to model the

CVT for subsidence transients, there are no known problems with EMTP components, which are used to form the CVT model. Most importantly, the results of the CVT model simulations are in accordance with the results in Refs. [22.], [38.], [40.], and [41.].

3.8 INCORPORATION OF THE CVT MODEL IN EMTP

3.8.1 Incorporation method

The general principles of incorporating the CT, CVT, and the relay models are explained in Section 3.4. Subroutine DATAIN calls subroutine INSTFR for the processing of CT and CVT input data. If the keyword CVTMODEL is found, subroutine INSTFR then includes the appropriate CVT module with all the required data. The flowchart of subroutine INSTFR is given in Figure 30 on page 78. As discussed before, the (V_{rms} - I_{rms}) has to be converted to the (ψ_{peak} - I_{peak}) curve. This conversion is done by subroutine RMSHYS, which is a combination of subroutines CONVERT and HYSDAT in the Auxiliary part of EPRI/DCG EMTP Version 2.0. The flowchart of subroutine RMSHYS is given in Figure 16 on page 53.
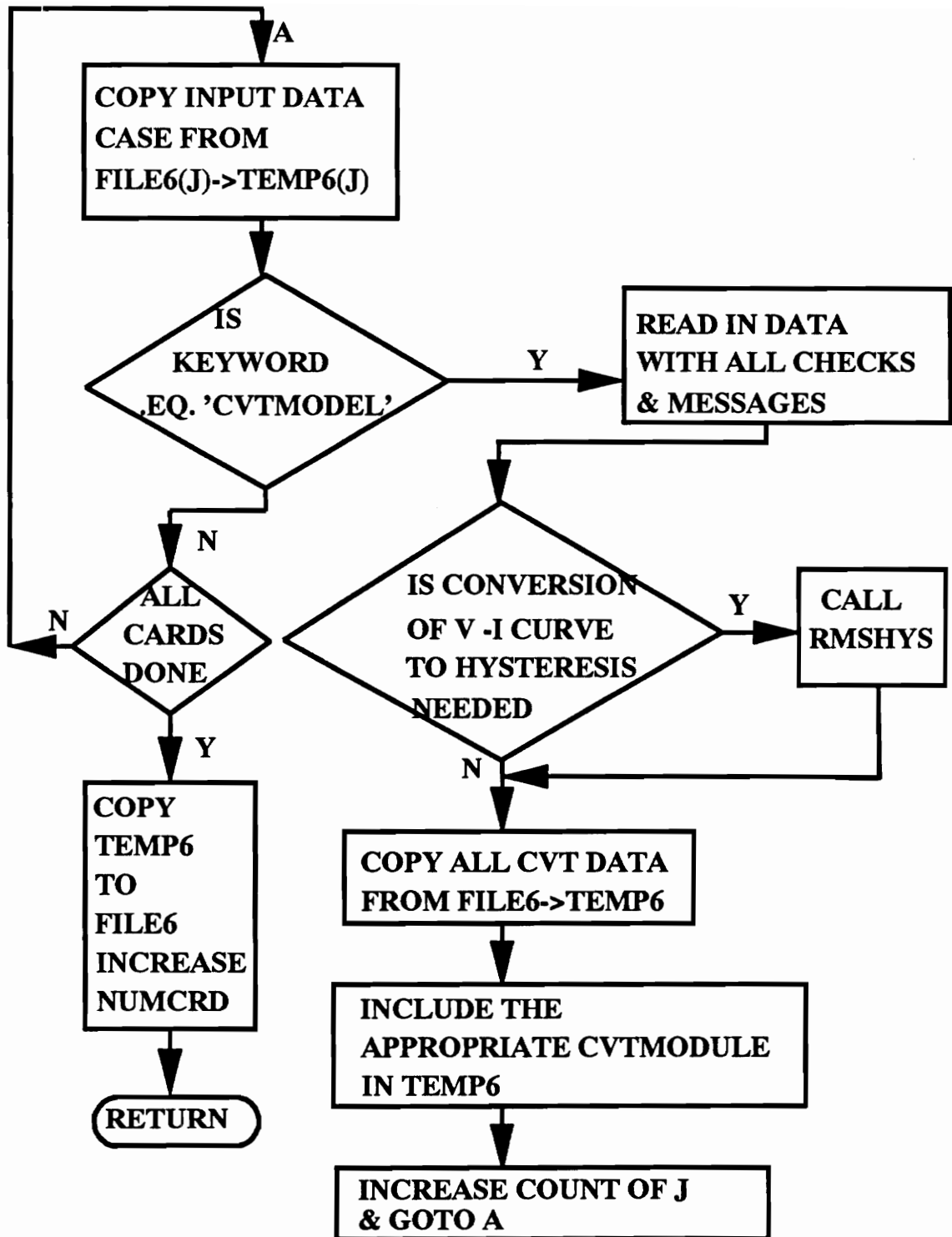
Figure 30. Flowchart of Subroutine INSTFR for CVTs

The CVT has been modeled by creating the following modules:- CVTBLH.INC, CVTNBLH.INC, CVTBNLH.INC, CVTNBNLH.INC, and CVTBLNH.INC, CVTNBLNH.INC, CVTBNLNH.INC, and CVTNBNLNH.INC. The modules are created by running AUX on the data files CVTBLH.DAT, CVTNBLH.DAT, CVTBNLH.DAT, CVTNBNLH.DAT, and CVTBLNH.DAT, CVTNBLNH.DAT, CVTBNLNH.DAT, and CVTNBNLNH.DAT. It is not necessary for the user to create the modules. They must be present in the EMTP directory, and the user must have read access to the modules. The eight modules represent the following cases :-

CVTBLH.INC   this module is included by EMTP when the user inputs IBURFG = 01, ILEDFG = 01, and IHYSFG = 00 or 01. This is the Burden, Lead, and Hysteresis module. The values of the burden resistance, burden inductance, and burden capacitance are given by the user and connected within the CVT model on the cvt secondary side. An internal node for the lead impedance is created, and the values for the lead resistance, lead inductance, and lead capacitance are given by the user and connected in the cvt model. The hysteresis curve is either computed from the V(rms)-I(rms) curve or 22 points of the ψ(peak)-i(peak) curve are given.

CVTNBLH.INC   this module is included by EMTP when the user inputs IBURFG = 00, ILEDFG = 01, and IHYSFG = 00. This is

the No Burden, Lead, and Hysteresis module. The burden values must be connected by the user on the cvt secondary side. An internal node for the lead impedance is created, and the values for the lead resistance, lead inductance, and lead capacitance are given by the user and connected in the cvt model. The hysteresis curve is computed from the V(rms)-I(rms) curve.

CVTBNLH.INC   this module is included by EMTP when the user inputs IBURFG = 01, ILEDFG = 00, and IHYSFG = 00. This is the Burden, No Lead, and Hysteresis module. The values of the burden resistance, burden inductance, and burden capacitance are given by the user and connected within the CVT model on the cvt secondary side. No provision is made for the lead impedance. The hysteresis curve is computed from the V(rms)-I(rms) curve.

CVTNBNLH.INC   this module is included by EMTP when the user inputs IBURFG = 00, ILEDFG = 00, and IHYSFG = 00. This is the No Burden, No Lead, and Hysteresis module. The burden values must be connected by the user on the cvt secondary side. No provision is made for the lead impedance. The hysteresis curve is computed from the V(rms)-I(rms) curve.

CVTBLNH.INC this module is included by EMTP when the user inputs IBURFG=01, ILEDFG=01, and IHYSFG=02. This is the Burden, Lead, and No Hysteresis module. The values of the burden resistance, burden inductance, and burden capacitance are given by the user and connected within the CVT model on the cvt secondary side. An internal node for the lead impedance is created, and the values for the lead resistance, lead inductance, and lead capacitance are given by the user and connected in the cvt model. No hysteresis curve is required by this module.

CVTNBLNH.INC this module is included by EMTP when the user inputs IBURFG=00, ILEDFG=01, and IHYSFG=02. This is the No Burden, Lead, and No Hysteresis module. The burden values must be connected by the user on the cvt secondary side. An internal node for the lead impedance is created, and the values for the lead resistance, lead inductance, and lead capacitance are given by the user and connected in the cvt model. No hysteresis curve is required by this module.

CVTBNLNH.INC this module is included by EMTP when the user inputs IBURFG=01, ILEDFG=00, and IHYSFG=02. This is the Burden, No Lead, and No Hysteresis module. The values of the burden resistance, burden inductance, and burden

capacitance are given by the user and connected within the CVT model on the cvt secondary side. No provision is made for the lead impedance. No hysteresis curve is required by this module.

CVTNBNLNH.INC this module is included by EMTP when the user inputs IBURFG = 00, ILEDFG = 00, and IHYSFG = 02. This is the No Burden, No Lead, and No Hysteresis module. The burden values must be connected by the user on the cvt secondary side. No provision is made for the lead impedance. No hysteresis curve is required by this module.

The modules represent the basic structure of the CVT model. The details needed by this module are the following :-

* the names of the primary nodes to which the CVT is connected.

* the names of the secondary nodes of the CVT.

* the values of the capacitor divider (C1 and C2), and the values of the inductance, resistance, and capacitance of the tuning inductor.

* the parameters of the transformer, such as the primary and secondary resistance and leakage inductance, and the number of turns on each winding.

- the details of the burden and lead impedances.

- the remanent flux, the frequency, and the coordinates of the saturation point.

- the magnetization curve, either the V(rms)-I(rms) or the ψ(peak)-i(peak) hysteresis curve.

- flags for selecting default CVT values, the burden connection, the lead impedance, and the magnetization curve options.

The EMTP processes the input data case and computes the hysteresis curve for ARMCO M4 steel required by the Type 96 nonlinear hysteretic element. It then inserts the appropriate CVT module with the required inputs, including the hysteresis curve in the data case. This module is then sorted and included in the data case. The outputs of the CVT model are the current through the burden and the voltage across the burden.

If IDEFLG = 01, then the default values of a particular CVT are chosen. When the IDEFLG = 01, then the CVT model does not use the Type 96 nonlinear hysteretic element (IHYSFG = 02). The values of ILEDFG = 01, and IBURFG = 01 are chosen. Thus, the values of the Lead impedance and Burden impedance are assigned and connected internally by EMTP. The default values of the CVT model are for a 110 kV CVT. These values have been obtained from Ref. [40.].

3.8.2 Data Format

The data format of the cvt model is shown in Figure 31. Many numerical quantities are read in as characters. An explanation similar to the explanation given in Appendix A is applicable in the case of CVTs.

One example of an EMTP input data case employing the CVT model is given in

3.8.3 Outputs

The outputs of the CVT Model are the current through the burden and the voltage across the burden. These outputs are available in the cases where the user has selected the option IBURFG = 01.

```
C CVTMODEL

   (I2)      (A6)      (A6)      (A6)       (A6)       (A6)
C IDEFLG CVTPRI1 CVTPRI2 CVTOT1 CVTOT2 CTRIDN

   (A6)      (A6)      (A6)      (A6)       (A6)
C CPDIV1 CPDIV2 SLFIND RESIND CAPIND

   (A6)      (A6)      (A6)      (A6)       (A6)       (A6)
C RNPRIM RNSEC PRIRES PRILEK SECRES SECLEK

   (I2)      (A6)      (A6)      (A6)       (I2)       (A6)       (A6)
C IBURFG BURRES BURIND BURCAP ILEDFG RLDRES RLDIND ...
      (A6)
   ... RLDCAP

   (I2)      (A6)      (E8.0)  (E8.0)  (E8.0)
C IHYSFG REMFLX  FREQ  RISAT  VSAT

   (E16.0)          (E16.0)
C RIRMS          VRMS

C .....                ...
C      9999.
```

IDEFLG = 00 => USER SUPPLIES ALL DATA
       = 01 => ALL DEFAULT VALUES USED BY EMTP

IBURFG = 00 => USER WILL CONNECT THE BURDEN ACROSS
               THE OUTPUT TERMINALS
       = 01 => BURDEN VALUES SUPPLIED BY USER AND
               CONNECTED BY EMTP

ILEDFG = 00 => NO LEAD IMPEDANCE
       = 01 => LEAD IMPEDANCE VALUES SUPPLIED BY USER
               AND CONNECTED BY EMTP

IHYSFG = 00 => USER SUPPLIES V(rms)-I(rms) CURVE, REMFLX,
               FREQ, RISAT, VSAT
       = 01 => USER SUPPLIES FLUX(peak)-I(peak) CURVE,
               and REMFLX
       = 02 => TYPE 96 ELEMENT NOT INCLUDED IN MODEL

Figure 31.   Capacitor Voltage Transformer Data Format

```
C USING MODULE CVTNBNLH.INC
C NB (NO BURDEN) MEANS USER CONNECTS THE BURDEN.
C NL (NO LEAD) MEANS THE LEAD IMPEDANCE NOT CONNECTED.
C H (HYSTERESIS) MEANS TYPE 96 HYSTERETIC INDUCTOR CONNECTED.
BEGIN NEW DATA CASE
.000050    .100000
       3          -1           1           1           0
C IDEFLG = 00
C IBURFG = 00
C ILEDFG = 00
C IHYSFG = 00
C ##### = THE GROUND NODE
C CVTMODEL
C 00NODINP######NODOUT#####FIR
C 8.3E-37.5E-21216+40.00010.0000
C 200.001.00002772.00.00000.00001.0E-3
C 0032.27077.0700000.0000.00010.00000.0000
C 000.00000050.00003.7140000126.00
C 0.0507        91.0
C 0.136         98.0
C 0.300        105.0
C 0.850        112.0
C 3.714        126.0
C 9999.0
/BRANCH
NODOUTNODEA3         12.0
NODEA3               1.0     33.8
        NODEA3                      300.
C 345678901234567890123456789012345678901234567890123456789012345678901234567890      3
C THIS IS THE BURDEN
NODOUT               32.27 77.07
BLANK ENDS BRANCH CARDS
/SWITCH
NODINP       .020         .3
BLANK ENDS SWITCH CARDS
C GENERATOR REPRESENTED AS AN IDEAL VOLTAGE SOURCE
C 345678901234567890123456789012345678901234567890123456789012345678901234567890
/SOURCE
14NODINP   178000.4    50.       90.0                        -1.
BLANK ENDS SOURCE CARDS
NODINP
BLANK CARD ENDING SELECTIVE NODE VOLTAGE OUTPUT REQUESTS
BLANK CARD ENDING PLOT CARDS
BEGIN NEW DATA CASE
BLANK
```

Figure 32. CVT model Test Data Case

3.9 LIMITATIONS OF THE CT AND THE CVT MODELS

3.9.1 Limitations of the CT model

1. Since no capacitances are included in the transformer model, the CT model is valid up to a few kHz. Thus, simulation results which have high frequency surges impinging on the CT model may not be accurate. The loss of accuracy will increase with higher frequencies. Most relays generally have input filters with a cutoff frequency of 3 kHz. Hence, at high frequencies simulations involving a combination of a CT model together with a relay will be more accurate than simulations involving a CT model only.

2. It is not possible to predict the remanent flux in the CT core after the fault is cleared.

3. For CTs with air gaps, the hysteresis curve is tilted at a smaller angle with respect to the positive x axis, and a lower remanent flux in the CT core is obtained after fault clearance. The hysteresis loop employed in the CT Model is valid only for ARMCO M4 oriented steel with no air gaps.

4. CTs with different core materials (notably Nickel Iron alloys) will need that particular metal's hysteresis curve for greater accuracy in the simulation results.

3.9.2 Limitations of the CVT model.

1. Strictly, the CVT model response is not valid for high frequency surges. However, since the input L-C circuit of the CVT equivalent circuit is tuned to the fundamental frequency, and the capacitance C_2 provides a low impedance path to the high frequency surge, this limitation is less serious than in the case of the CT model.

2. The CVT model's response to over-voltages -- two times rated L-N voltage -- is not accurate. The reason for the inaccuracy is that arcing gaps across C_2, across L_1, and across the transformer primary terminals are not included in the CVT model. These gaps flashover and protect the components from dielectric failure. These gaps can be modeled using a Type 99 Resistance or a Voltage-controlled Flashover Switch. These components can be included in a CVT model for an overvoltage study for accurate results.

Chapter IV

4.0 TOTAL FORTRAN CAPABILITY IN EMTP

4.1 INTRODUCTION

The EMTP also has an important feature for the solution of control systems called TACS -- an acronym for Transient Analysis of Control Systems. This capability to interface EMTP electrical network variables and TACS signals to form a hybrid EMTP-TACS interactive configuration is shown in Figure 33 on page 91. Thus, network variables such as voltage at a node, current through a switch, etc., are passed to TACS. TACS will in turn pass signals for switch operation or converter valve firing. The signals from TACS are unavoidably delayed by one time step, as explained below. In advancing the network solution from time $(t - \Delta t)$ to time t, the TACS control signals are known at time $(t - \Delta t)$. The network solution at time t is then used to advance the TACS solution from time

$(t - \Delta t)$ to t. Ideally, the TACS solution should be known at time t, to advance the network solution from time $(t - \Delta t)$ to t. This solution method is the cause for the one time step delay between TACS and the network. This delay is generally acceptable, because of the small time steps used in the simulation of transients (Δt is of the order of magnitude of 50 $\mu secs$). The TACS program has the capability to solve differential equations, transfer functions, model special application devices such as integrators, nonlinear elements, relays, and allow limited Fortran processing of EMTP variables. Using TACS, power system transients and control systems can be modeled simultaneously; most importantly, the dynamic interaction between them can be studied.

4.2 PRESENT STATUS IN EMTP

At present there is limited capability to add Fortran code to EMTP. This limited Fortran capability to interact with EMTP variables is provided in TACS. The limitations are :-

1. Intrinsic functions accept only one argument.

2. GOTO Statements and DO Loops are not allowed.

3. SUBROUTINE and FUNCTION subprograms are not allowed.

Electrical Network

Voltage at a node

Current in a branch

Sync. mc. variable

Switch status

Control Signals :-
open breaker,
Switch ON/OFF signal
(one time step delay)
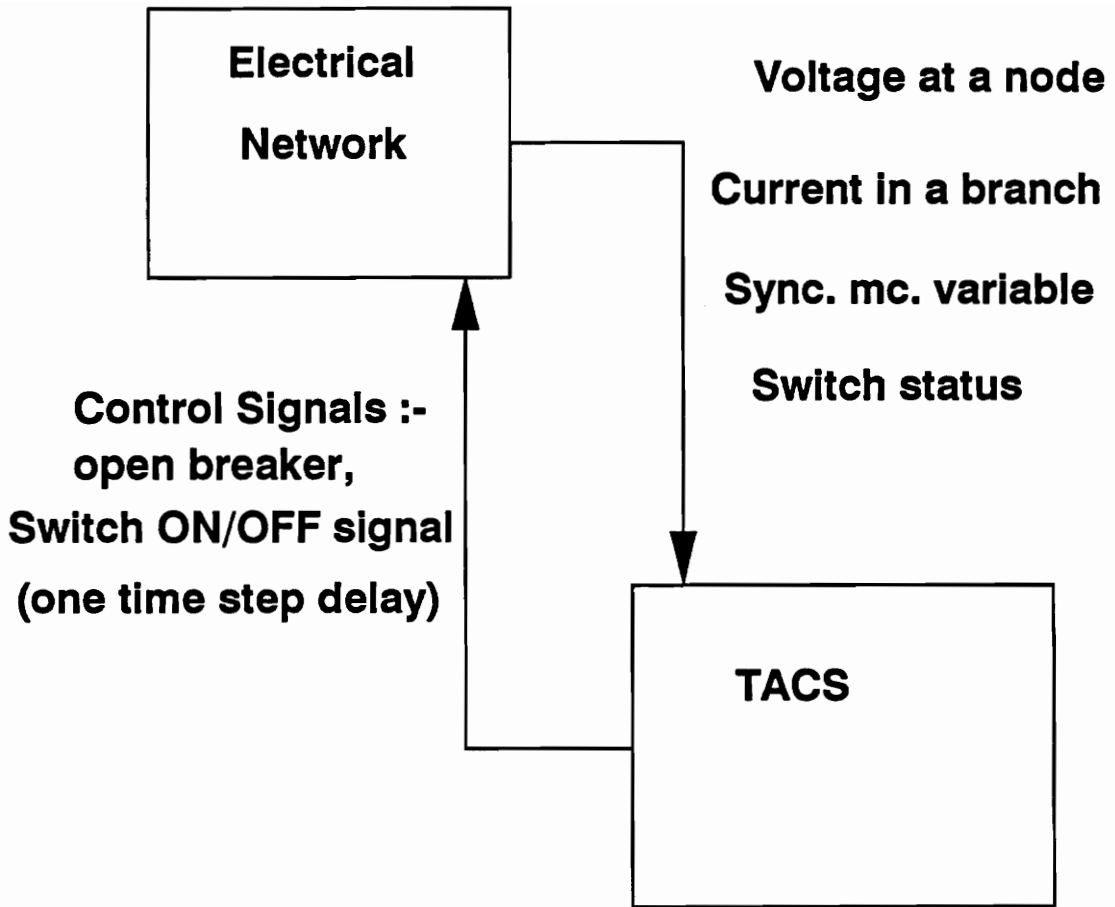
TACS

Figure 33. EMTP-TACS Interface

For many applications such as computer relay algorithms, controllers for HVDC converters, stabilizers for synchronous machines, the above limitations are not acceptable. Therefore, several alternatives for adding generic computer relay models to EMTP were examined.

4.3 ALTERNATIVES EXAMINED

This section is a summary of possible approaches, and their respective advantages and disadvantages.

4.3.1 Program Development Method

The program development method is similar to the program development stage in EMTP. The method consists of writing the relay model as a Fortran subroutine, which must include **all** the necessary common blocks. The common blocks must contain data such as the currents, voltages, switch status, and synchronous machine data required for the computer relay algorithm. This computer relay subroutine must be called by an appropriate existing EMTP subroutine. This computer relay subroutine must be compiled, and saved as an object file. Then, both the existing EMTP *.OBJ files and the relay subroutine object file must be linked to create a run time executable version. This method is summarized in

Figure 34 on page 94. The method poses a fair degree of difficulty for the average EMTP user.

4.3.2 Dynamic Linking

Ref. [42.] elaborates on the need and the internal operating system procedure to implement dynamic linking. Normally, all subroutines that a program might call are linked before the program is executed. This "static linking" does not take advantage of the full capabilities of the virtual memory. Many programs have subroutines for compiling rarely used statements, and procedures for handling error conditions that seldom occur. Dynamic linking is a flexible feature which enables linking separately compiled procedures the first time the procedure is called.

In EMTP, the separately written Fortran routine **must** have the necessary common blocks. The common blocks must contain data such as the currents, voltages, switch status, and synchronous machine data required for the computer relay algorithm. An appropriate calling sequence must be included in EMTP to invoke the computer relay subroutine. The advantage of this method is that the process of linking is not necessary before the EMTP data case is run. The computer relay algorithm is linked only if the relay model is invoked. This method does not create different executable versions of EMTP. Dynamic linking capability is available on the IBM/CMS operating system. In the operating system
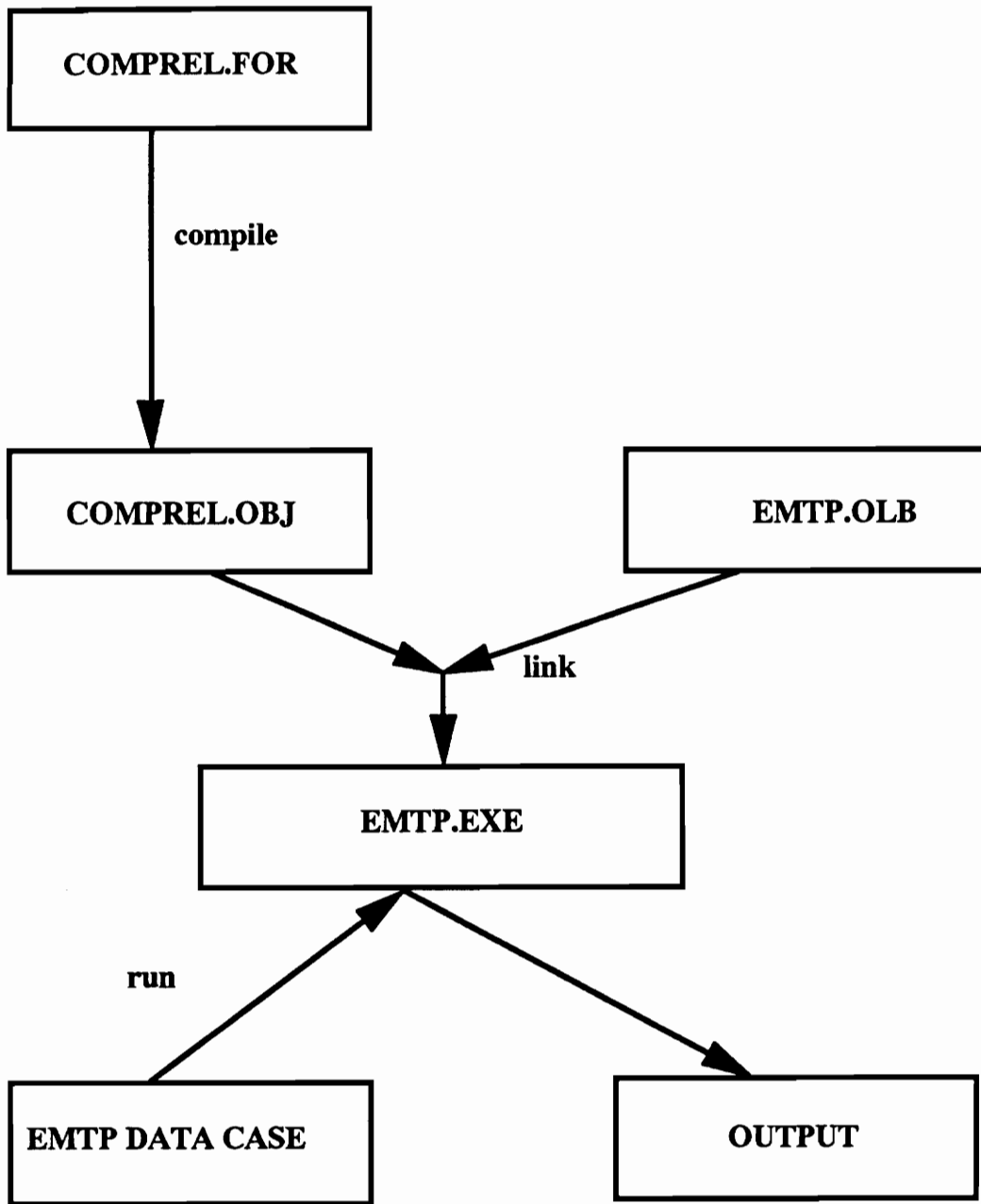
Figure 34. Program Development Flow Chart

at Virginia Tech Power Systems Lab, VAX/VMS 5.2, dynamic linking is not allowed. It is reported that dynamic linking will be introduced in VAX/VMS 5.3.

4.3.3 Fortran Interpreter

A Fortran interpreter reads in a Fortran program, converts it to a readily executable form, and performs a controlled execution. There are no steps of compiling and linking the program. Refs. [43.] and [44.] elaborate on compiler and interpreter design. The interpreter approach is suitable for the running of an EMTP data case. The Fortran code can be included in the TACS portion of the data case. This code would then be executed at each time step.

Two major requirements of this approach are :-

* Writing the Interpreter.

* Interfacing it to EMTP.

Writing the Interpreter: A special Fortran Interpreter is needed for EMTP. An Interpreter already exists in EMTP subroutines TACS1A and CSUP, but it implements only a subset of FORTRAN statements. A much more comprehensive interpreter is needed. In its present form, the existing TACS interpreter is extremely difficult to understand and modify. The language normally used in the

writing of interpreters/compilers is C. This might lead to problems of EMTP program maintainability.

Interfacing the Interpreter to EMTP: This interpreter has to be interfaced to EMTP carefully. Perhaps a two pass interpreter is needed. On the first pass, the Lexical Analyser and Parser can work to set up the Run time Symbol Table. At $T = 0(-)$, the initial conditions can be calculated. At each time step the Run time Symbol table can be updated.

4.4 METHOD ADOPTED

For the reasons given above, we have chosen the Program Development Method to implement total Fortran capability. This is the method which can be implemented now. Two Fortran subroutines are written which allow the user to write his/her own Computer Relay Algorithm. We use the term "Computer Relay Algorithm" to give a concrete example. Any Fortran routine for the control of HVDC converters or stabilizers for synchronous machines can be implemented. The Fortran subroutines implement the following functions :-

1. Pass EMTP variables of interest to this Computer Relay subroutine, i.e. the values of currents, voltages, switch status, and the internal variable of special EMTP components required should be passed as needed.

2. Move the results of the Computer Relay Subroutine into EMTP.

These Fortran routines are called from the TACS portion of EMTP. These routines will be in EMTP EPRI/DCG Version 3.0. Provision is made to call the Computer Relay Algorithm (named subroutine COMPREL) from subroutine TACS3A which is in the time step loop of EMTP.

The user will have to compile his/her Computer Relay Algorithm and then link the corresponding object file to EMTP.OLB. The abbreviation OLB in VAX/VMS systems stands for the object library.

4.5 EMTP STRUCTURE AND CALLING ROUTINES

The EMTP source code documentation is elaborated upon in Ref. [13.]. Details of the TACS code are documented in Ref. [45.]. Figure 35 on page 99 explains the call tree of the Main Driver MAIN00 for TACS routines. SUBR10 calls the many overlays. Only those overlays relevant for TACS solutions are given in Fig. 2. OVER1's main function is processing and checking the input data. OVER1 calls the routine TACS1 to read TACS input data. TACS1 calls TACS1A to read the input data for supplemental variables and devices. (TACS components that have a Type 98, 99, or 88 code). TACS1 also calls TACS1B which orders all the TACS variables and puts this new order in TACS array ILNTAB. TACS1 also calls TACS1C to check if the user-requested TACS EMTP source exists.

OVER12 processes branch tables and switch tables in preparation for the time step loop. OVER12 calls TACS2 to perform the steady state initialization of TACS. The system matrix is triangularized and forward/backward substitutions are executed to calculate the initial conditions.

OVER16 is the driver for the time step solution. It calls routines SUBTS1, SUBTS2, SUBTS3, and SUBTS4 to perform the time step solution. If it is a TACS hybrid case, after each EMTP time step solution routine SUBTS1 calls TACS3 to execute the time step solution for the TACS system. The results are placed in array XTCS. Figure 36 on page 100 shows the relationship between OVER1, OVER12, OVER16, and TACS routines.

4.6 CHANGES MADE TO EMTP

The changes made to EMTP can be classified as follows:-

1. Changes made to existing EMTP routines. These changes are made with the intent to have the minimum impact on the existing TACS code. The TACS code in EMTP Version 2.0 is complex, and this complexity is compounded by the lack of documentation. Ref. [45.] serves to reinforce and clarify this author's understanding of the code and is a valuable contribution.

MAIN CODE OVERLAYS   **SOLUTION**
                                OVERLAYS

MAIN00 ········ MAIN10 ······ SUBR10 ········ OVER1

                                          ······ OVER12

                                          ······ OVER16
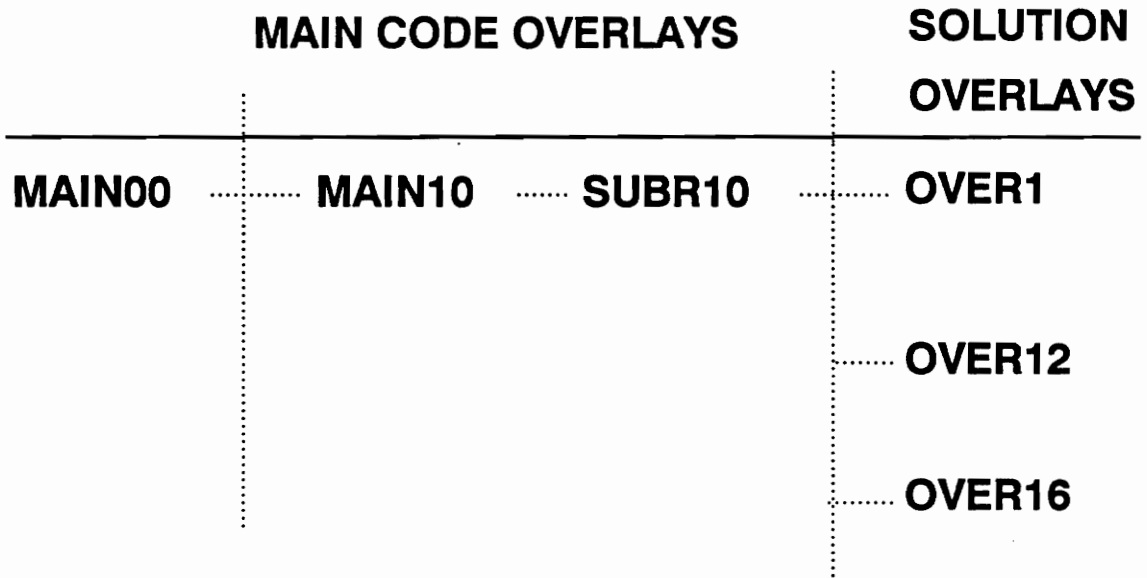
CALL TREE OF MAIN DRIVER MAIN00

FOR TACS ROUTINES

Figure 35.   Call Tree of subroutine MAIN00
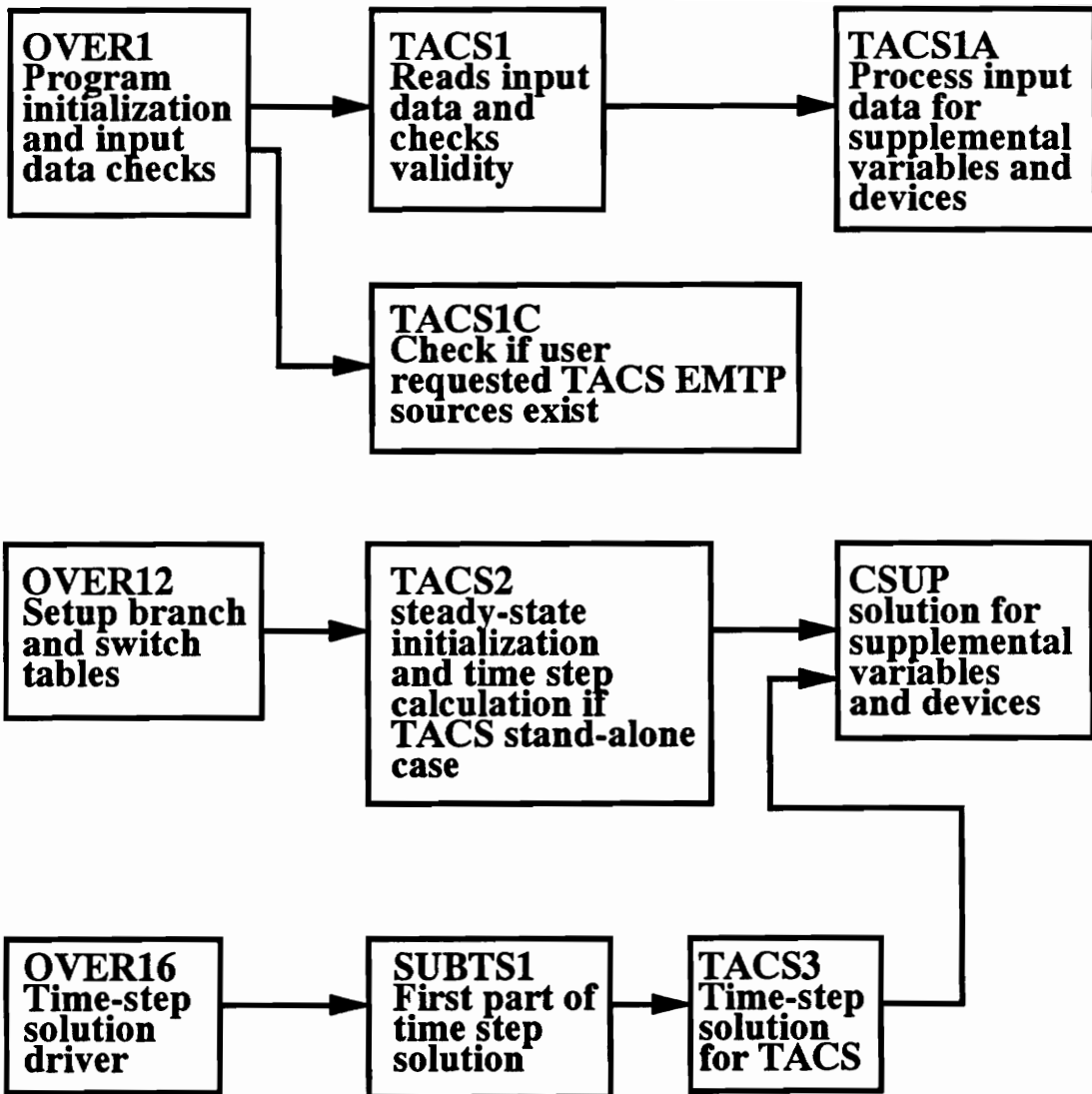
Figure 36. Relationship of TACS routines in EMTP.

2. Addition of new subroutine COMPREL. This subroutine is used only if the user wishes to interface a Fortran routine to EMTP.

3. Addition of new subroutine SOURCES. This subroutine serves as a support routine to COMPREL. Its function is to get EMTP data needed by the user.

4. Addition of new subroutine OUTPUT. The function of this support subroutine is to pass data from COMPREL to TACS and, if the user desires, into the network part of EMTP.

4.6.1 Changes made to existing EMTP routines

Subroutine TACS1 reads and processes all the TACS input data, including source data. Subroutine TACS1 also performs the initial checks for the validity of the input data. Previously, the TACS source Types allowed were up to Type 93. If the TACS source Type is greater than 93, a fatal error message is produced and the data case execution is terminated. The card is read as a transfer function block of order 94, if 94 was the intended source Type. This subroutine is changed to accept a Type 94 source. A source was chosen to do this function because this "device" impacts the least number of TACS elements. Type 94 is the new source type which will allow us to move variables from the subroutine COMPREL (Computer Relay) to TACS. This Type 94 source can be used in a data case as

any other TACS variable, for example it can be used with a time delay to turn on/off a TACS controlled switch.

Subroutine TACS3 is in the time step loop of EMTP. In OVER16, SUBTS1 calls TACS3 at each time step to solve for the TACS variables. A triangular factorization of the [A] matrix for the TACS system is performed before entering the time step. Subroutine TACS3 updates input sources, forms the right hand side of the system matrix, does a downward operation on it, and backsolves for the TACS variables. The solution is stored in array XTCS. In subroutine TACS3, after the input sources are updated (all input sources except Type 94), a call to SUBROUTINE COMPREL is made. This is the logical position to call subroutine COMPREL, because the new source Type 94 will be computed within COMPREL. Thus, when the user written subroutine COMPREL returns to TACS3, **all** input sources will have been updated. TACS3 can then perform its usual tasks as explained above.

4.6.2 New Subroutine COMPREL

Subroutine COMPREL is a dummy routine; it has the necessary common blocks for the user to write his/her Fortran routine. The common blocks contain data such as the time which the simulation has reached, and the time step. If there is no neccessity to run an EMTP case with a Fortran algorithm, then COMPREL will have a single statement RETURN. To run an EMTP data case with a

Fortran algorithm, the user has to write his/her code in subroutine COMPREL. Two support routines, SOURCES and OUTPUT, will be needed by the user. Subroutine SOURCES will be needed to get the inputs required by the relay algorithm. Subroutine OUTPUT will be needed to move the variables from COMPREL to TACS, and then if necessary from TACS to EMTP.

After a call to SOURCES, the user has access to the values of the sources at time = T. The computer relay algorithm can be run at this time, if T corresponds to a sampling instant. It is more efficient to call SOURCES at a sampling instant. The variable T is the time the simulation has reached and is contained in the common blocks. The user can now write the Fortran code for the relay. The user has to compile subroutine COMPREL and link it, along with subroutine SOURCES and subroutine OUTPUT, to EMTP.OLB.

4.6.3 New Subroutine SOURCES

The user will need subroutine SOURCES to obtain the inputs such as TACS sources Types 90 - 93. These sources can be the current and voltage seen by the relay, or the status of some switch, or some synchronous machine variable. These inputs at a particular time step are of course vital for any algorithm.

Subroutine SOURCES is called as follows:

```
CALL SOURCES(NCRSRC,CRSRCS,SVALUE)

NCRSRC = Number of sources of Types 90 - 93.

CRSRCS(NCRSRC) = Array defining the names of the sources,

               format = A6.

SVALUE(NCRSRC) = Array of values of corresponding sources

               at time = T.
```

The inputs to this subroutine are NCRSRC and CRSRCS(NCRSRC). The value

of the sources at time = T is returned in array SVALUE.

4.6.3.1 Details of Subroutine SOURCES

Figure 37 on page 105 explains the structure of the subroutine SOURCES. In

this section, a brief background of the relevant EMTP and TACS arrays and

variables that are accessed in SOURCES is given. Then, a brief explanation of

SOURCES is given. All the TACS arrays and variables are in common block

TACSAR.

UD1   The array that contains data of sources in TACS. Five consecutive

             cells are required for each source. Cell 2 contains the node number

             if the source is Type 90, and it contains the switch number if the

             source is Type 91 or Type 93. Cells 4 and 5 contain the time the

             source starts and the time the source stops, respectively.
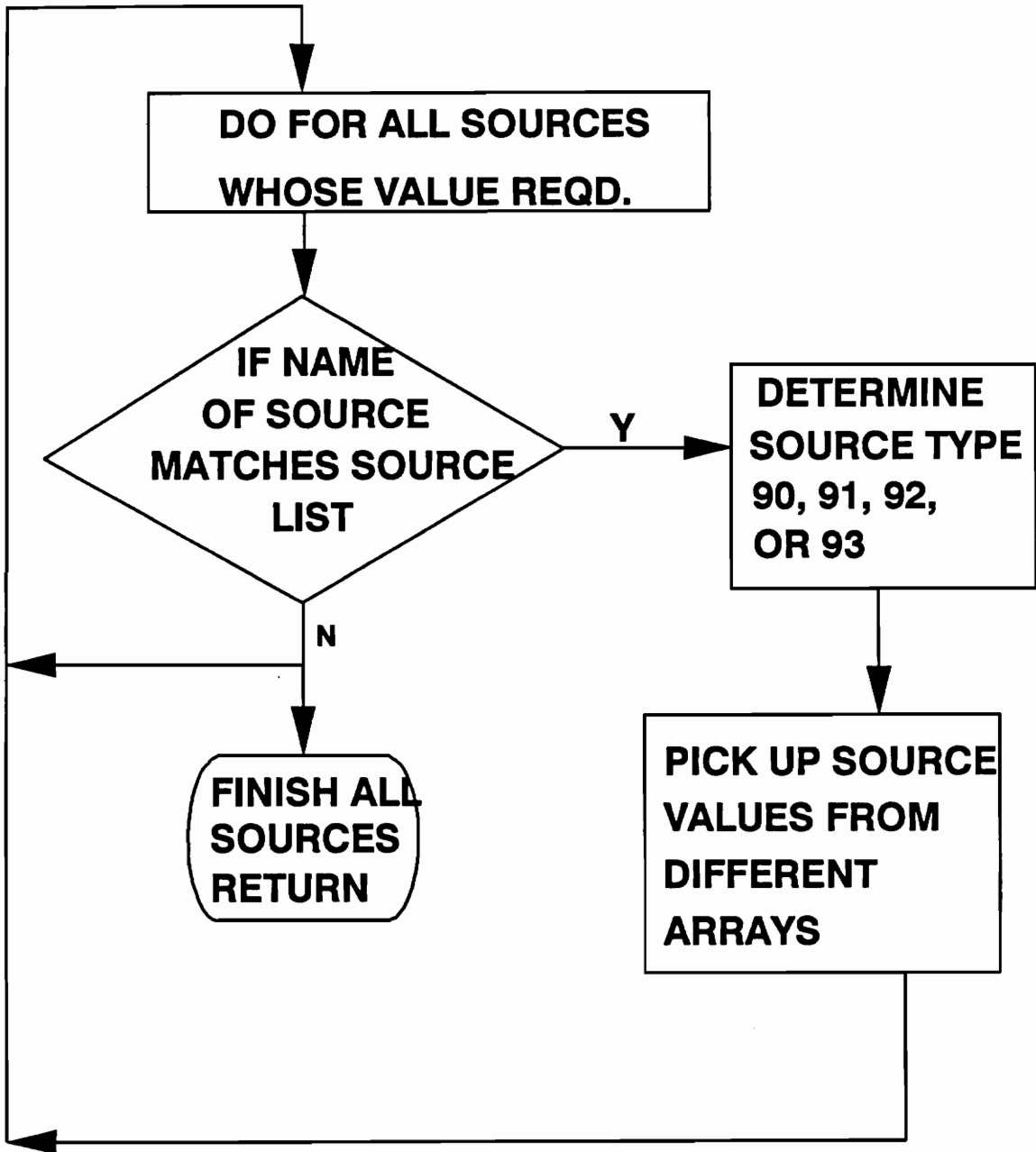
Figure 37. Flow chart of Subroutine SOURCES

KUD1   This is the offset address in array SPTACS, which indicates the starting address of array UD1.

IUTY   This array contains the TACS source type information (if Type 90, 91, etc.).

KIUTY   The offset address into array SPTACS which indicates the starting address of array IUTY.

ILNTAB   TACS source names are stored in array TEXVEC, and their addresses are stored in array ILNTAB.

NIURNS   Address of first user supplied source at IUTY $=12$. The first 11 cells are reserved for built-in TACS sources.

TEXVEC   An array containing alphanumeric names of TACS variables and Type 59 Synchronous Machine output variables.

KONSCE   Variable equal to the total number of sources (including the built-in sources) in a data case.

E   Array E contains the node voltages at the present time step. This array is in the Labeled Common (LABCOM) block.

KPOS   This array contains flags indicating the status of switches. A negative value of KPOS indicates a request for the output of the current

through the switch. If (L .LE. 3) = > the switch is closed (the permanently closed switch, the voltage controlled switch, the time controlled switch, and the diode are all closed). This array is in the Labeled Common (LABCOM) block.

TCLOSE   Array TCLOSE contains the switch currents in the time step loop. Subroutine SUBTS1 of Overlay 16 loads current values in TCLOSE, once the switch is closed. This array is in the Labeled Common (LABCOM) block.

ETAC   This array is in the common block SMTACS. SMTACS contains variables associated with the interface of the Type 59 Synchronous Machine to TACS. The values contained in ETAC(1) through ETAC(NTOTAC) are synchronous machine variables being passed to TACS.

SPTACS   This array contains **ALL** TACS arrays. It belongs to labeled common block LABCOM (/COB025/). SPTACS is divided into 16 sections by using EQUIVALENCE statements in common block TACSAR.

In subroutine SOURCES, the name of the source whose value is desired is in array CRSRCS. The addresses of the sources are stored in array ILNTAB. The name of the source in CRSRCS is compared to the name of the source in

TEXVEC. If there is a match, then a valid source is encountered, and the value of that source has to be located in the different EMTP arrays. The Type of the source is determined from array IUTY, using the proper offset into IUTY. Cell 2 of array UD1 contains the number of the node if the source Type is 90. Cell 2 of array UD1 also contains the switch number if the source Type is 91 or 93. Cell 2 of array UD1 also contains the number of the Synchronous Machine variable being passed to TACS. Depending on the Type of the source, the relevant EMTP array is accessed.

For a Type 90 source, the value of SVALUE(M) is determined from array E. For a Type 91 source, the value of the current is read from the array TCLOSE and put in array SVALUE. For a Type 92 source, the value of SVALUE(M) is determined from array ETAC. For a Type 93 source, the value of SVALUE(M) is equal to 1.0, if the switch is closed. Array KPOS contains flags indicating the status of the switches. If the switch is open, the value of SVALUE(M) is equal to 0.0.

The above procedure is repeated for all sources in array CRSRCS. Thus, after a call to subroutine SOURCES, COMPREL has all the input data required for its algorithm. This data corresponds to the particular time step at which SOURCES is called.

4.6.4 New Subroutine OUTPUT

After the algorithm of subroutine COMPREL is executed, if it is necessary to pass variables from the subroutine COMPREL to TACS, the user should have defined a TACS Type 94 source of any name in the user's EMTP data case. The user should use the same name to pass the value of this variable to TACS from COMPREL. The user can call SUBROUTINE OUTPUT as follows:

```
CALL OUTPUT(NOUTPT,CROTPT,CRVLOT)

NOUTPT = Number of outputs.

CROTPT(NOUTPT) = Array defining the names of the outputs,

                 format = A6

CRVLOT(NOUTPT) = Array defining the corresponding outputs

                 at time = T.

for example if, CROTPT(1) = 'NODEA1'

and   CRVLOT(1) = 5.3.
```

Then, the value assigned to a TACS Type 94 source NODEA1, is 5.3, at time = T. (Note that NODEA1 must be previously defined in EMTP data case).

This assignment is achieved by determining the location in array XTCS for this particular source and assigning the value of 5.3 to this particular location in array XTCS. This Type 94 source can be used in a data case as any other TACS variable, e.g., it can be used with a time delay to turn on/off a TACS controlled

switch. It can be printed in EMTP output file by using the Type 33 designation for TACS outputs. It can also be passed into the main EMTP by using the Type 60 Slave Source which is controlled by TACS variables having the same six character name.

4.6.4.1 Details of Subroutine OUTPUT

Figure 38 on page 111 explains the structure of the subroutine OUTPUT. In this section, a brief background of the relevant EMTP and TACS arrays and variables that are accessed in OUTPUT and not described in Section 4.5.3.1 is given. It is followed by a brief explanation of OUTPUT. All the TACS arrays and variables are in common block TACSAR.

XTCS　　In the time step solution array XTCS is used to store the values of all TACS variables at each time step solution. The output values of devices, TACS sources, supplemental variables, and function blocks are stored here.

KXTCS　　This represents the offset address into array SPTACS which indicates the starting address of array XTCS in the main TACS array SPTACS.

NUK　　Number of function blocks in a data case.
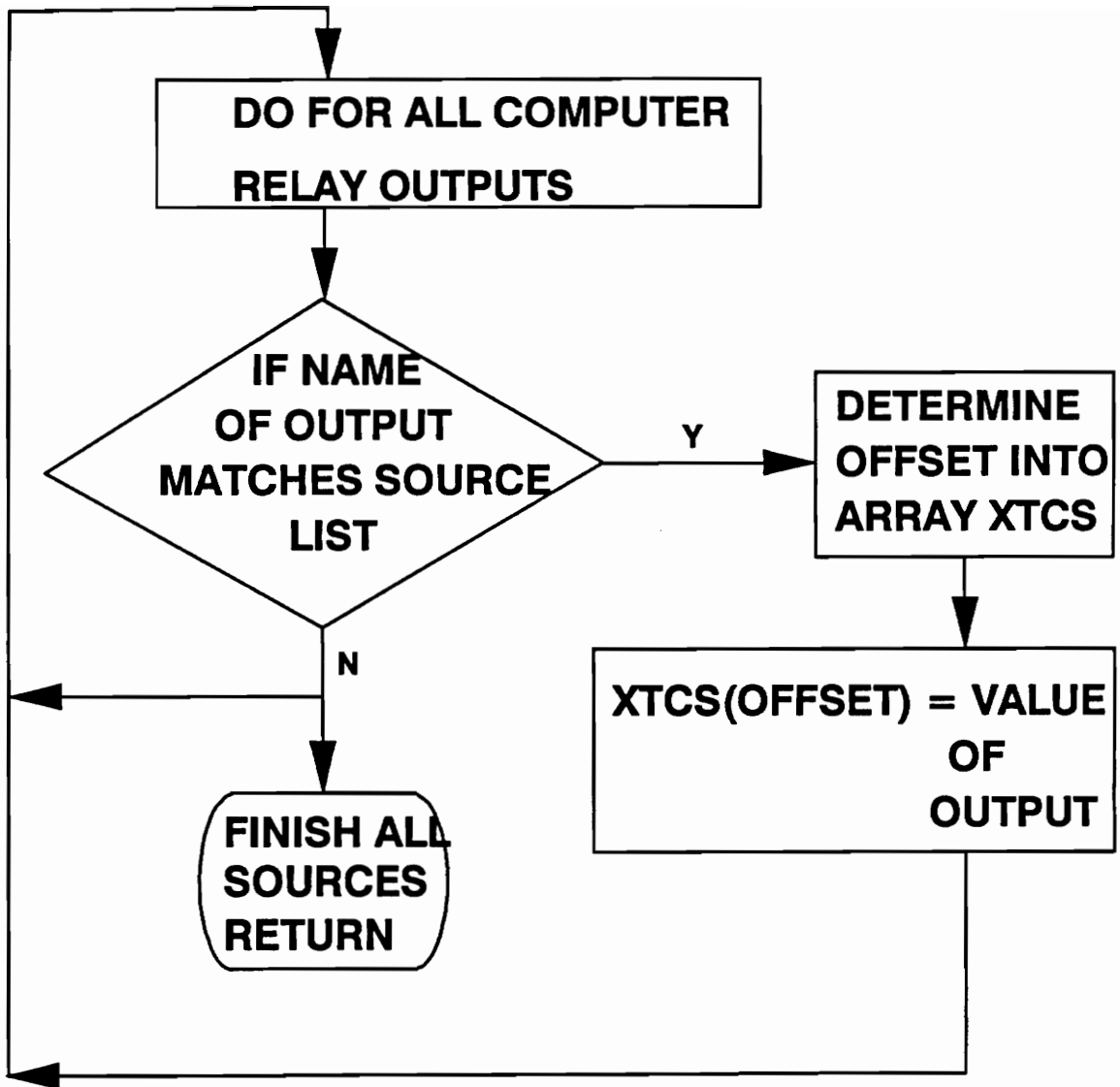
Figure 38.   Flow chart of Subroutine OUTPUT

In subroutine OUTPUT, the name of the output whose value has to be moved into TACS is in array CROTPT. This same name must be defined as a TACS Type 94 source in EMTP data case. The name of the output in CROTPT is compared to the name of the source in TEXVEC. The addresses of the sources are stored in array ILNTAB. If there is a match, then a valid source is encountered. The value of the source to be moved to TACS is in array CRVLOT. The exact location within array XTCS is determined by adding KXTCS + NUK + I (I is the number of the source -- maximum value is KONSCE). At this location within array XTCS, the value in CRVLOT is assigned to it. This procedure is repeated for all sources in array CROTPT whose values have to be passed into TACS.

4.7 EXAMPLE DATA CASE IMPLEMENTED

Ref. [46.] develops a distance-measurement algorithm for digital computer relaying. The goal of this research was to develop a simple algorithm which works efficiently in a low-cost processor. The algorithm is described and then its implementation in TACS is explained; the algorithm is also implemented using subroutine COMPREL.

4.7.1 Algorithm of the Schweitzer distance relay

At the relaying point, the voltage and current waveforms can be described by the following equations :-

$$v(t) \;=\; V \sin(\omega t + \phi) \tag{4.1}$$

$$i(t) \;=\; I \sin(\omega t + \phi - \theta) , \tag{4.2}$$

where V, I, ϕ, and θ are constants which change to new values at $t = 0$, the instant of fault occurrence.

Consider two finite duration impulse response (FIR) filters, SAL(x) and CAL(x), defined as follows :-

$$
\begin{aligned}
SAL(x) &= 1 & 0 \leq x < 1/2 \\
&= -1 & 1/2 \leq x < 1 \\
&= 0 & \text{for all other } x
\end{aligned}
\tag{4.3}
$$

and

$$
\begin{aligned}
CAL(x) &= 1 & 0 \leq x < 1/2 \text{ or } 3/4 \leq x < 1 \\
&= -1 & 1/4 \leq x < 3/4 \\
&= 0 & \text{for all other } x ,
\end{aligned}
\tag{4.4}
$$

$$\text{where } x = \frac{\omega t}{2\pi} .$$

Let $x(t) = X \sin(\omega t + \phi)$ be sampled N times per cycle at times $t = k\Delta t$, where $\Delta t = \frac{2\pi}{N\omega}$. If the samples are denoted by x_k, then

$$
\begin{aligned}
x_k &= X \sin(\omega k \Delta t + \phi) \\
&= X \sin(\frac{2\pi k}{N} + \phi).
\end{aligned}
$$

(4.5)

If N is a multiple of four, the results of time-discrete convolution of the input samples x_k with the SAL and CAL finite-duration impulse responses are:

$$
S_x = AX \cos(\phi + \frac{\pi}{N})
$$

(4.6)

$$
C_x = AX \sin(\phi + \frac{\pi}{N})
$$

(4.7)

$$
\text{where } A = \frac{2}{\sin(\frac{\pi}{N})}.
$$

These are calculated from the samples x_k using

$$
S_x = \sum_{k=1}^{N/2} [x_k - x_{k+\frac{N}{2}}]
$$

(4.8)

and

$$
C_x = \sum_{k=1}^{N/4} [x_k - \{x_{k+\frac{N}{4}} + x_{k+\frac{N}{2}}\} + x_{k+\frac{3N}{4}}].
$$

(4.9)

The N-th sample is the most recent, and the N samples preceding the time of calculation are used in the calculation of S_x and C_x. The filter outputs S_V, C_V, S_I, and C_I, are found using equations (4.8) and (4.9) above.

If S_V and C_I have opposite signs, and if

$$\frac{|S_V|}{|C_I|} < Z_{protected},\tag{4.10}$$

then trip. If C_V and S_I have the same signs, and if

$$\frac{|C_V|}{|S_I|} < Z_{protected},\tag{4.11}$$

then trip.

Two successive trip signals must be calculated by the relay to produce a final trip output. This feature increases the security of the relay.

4.7.2 Implementation of the Schweitzer algorithm

This algorithm was implemented first in the Fortran subset which is available in TACS. This implementation was not an easy task, in the absence of arrays and DO loop capability. Some of the main features of the implementation are explained now. TIMEX is a built-in TACS source which contains the simulation time in seconds. FREQHZ is another built-in source which contains the system frequency in Hz. Using the FORTRAN subset in TACS and the values of the

two built-in sources, the maximum integer number of periods the simulation has reached is calculated. The time corresponding to the maximum integer number of periods is subtracted from TIMEX, to give a value of time -- REMIDT. The value of REMIDT is employed to generate four sampling signals (for a four sample relay). The first sampling signal is generated if REMIDT lies between (0.0 and 0.00023 secs). The second sampling signal is generated if REMIDT lies between (0.00417 and 0.004398), which corresponds to a five degree interval from 90°. The interval of 5° is chosen to accommodate different time steps up to 5° on a 60 Hz basis. The third and fourth sampling signals are similarly generated corresponding to phase angles 180° and 270°. The voltage signal is sampled using the TACS Device number 62, the Sample and Track device. Each of these samples is held for one cycle, till the next sampling signal is generated.

The current sampling signals are similarly generated, but with a phase shift to account for the angle of the line impedance. Thus the values of the voltage and current samples are available to compute the filter outputs according to Eqns. (4.8) and (4.9). Eqns. (4.10) and (4.11) are used to compute the trip signal. The trip signal is delayed by 4.2 ms to have it available to check whether two consecutive trips are issued before issuing a final trip. It is clear that a more complex algorithm, requiring matrix algebra, could not be implemented with the present Fortran capability in TACS.

The same algorithm was implemented in subroutine COMPREL. The current and voltage samples were stored in arrays. A DO loop was used to compute the

filter outputs. Subroutine COMPREL was compiled and linked to main EMTP, along with subroutines SOURCES and OUTPUT. The same data case was run. Identical results for the trip time were obtained. However, the data case with subroutine COMPREL took longer to run than the regular EMTP data case. This result is surprising, and warrants a detailed investigation. The addition of new subroutines to create a new EMTP.EXE is one source of the additional time. Thus, running a regular EMTP data case (one that does not need the Fortran capability) on the new EMTP.EXE takes a longer than it does on the regular EMTP.EXE.

4.8 CONCLUSIONS

It has been shown that total Fortran capability can be implemented in EMTP. Thus, complex algorithms can be interfaced with EMTP, and this capability by itself augments EMTP. But, more importantly, studies which could not be conducted previously can be conducted now. For example, the dynamics of the interaction of the protection system on the network and vice-versa can now be studied, with a consequent improvement of the reliability of the system. A series of sequential events can be simulated, which was not possible previously even in the most complex of Transient Network Analyzers.

Chapter V

5.0 LINE AND TRANSFORMER RELAY MODELS

5.1 INTRODUCTION

Relays are important protection devices, and there exist a large number of relays specifically designed for tasks such as distance protection, transformer protection, generator protection, etc. In this chapter, a distance relay (SLY12C) and a transformer differential relay (BDD15B) are modeled. The user can define the relay settings. These two relays were chosen, among others, by tabulating the responses of a questionnaire sent by Dr. A.G. Phadke to various utilities, manufacturers, and consultants. Thus, the choice of these relays reflects an industry consensus on the most desirable relays for modeling within the EMTP.

The testing of these relays was done at AEP. A relay data acquisition was built at Virginia Tech. This unit consists of a microprocessor (MC68020) and a 16 channel A/D converter. The voltages of up to 16 different points within the relay can be sampled at 2.88 kHz. The analog voltages are converted to digital values by a 12 bit A/D converter. The digital values are stored in circular tables in the RAM of the data acquisition unit. A communications program transfers the data to floppy disks for analysis.

5.2 SLY RELAY MODELING

5.2.1 Introduction

The SLY relay is a static mho phase distance relay manufactured by General Electric Company of USA. The type SLY designation covers a family of static mho phase distance relays intended for the protection of transmission lines. The specific SLY relay chosen by AEP for testing was the SLY12C. The SLY12C is specifically designed to provide high-speed multi-phase fault protection in step distance and/or directional comparison blocking schemes. Details of the SLY and SLY12C are given in Refs. [47.] and [48.].

In this section, a brief description of the relay and its important components is given. Some derivations of the transactor transfer functions are given. The relay

model is developed, and its implementation in TACS is explained. The implementation in EMTP through the module method is also explained. Validation of the model is done by testing the relay model with the AEP test data.

5.2.1 Relay Operating Principles

The mho characteristics for the SLY relays are shown in Figure 39 on page 121. All measurements are made on a phase-to-phase basis. $(V_a - V_b)$ is compared to $(I_a - I_b)$ in order to obtain the same relay reach for a phase-to-phase fault, a three-phase fault, and a double phase-to-ground fault. The principle used to derive the electrical characteristics is illustrated in Figure 40 on page 122, using a mho unit as an example. The axes are "IR" and "IX". The IZ quantity is a voltage proportional to the line current obtained by passing the line current through an air gap transformer, also called a transactor. The setting of this quantity establishes the "Base Reach" of the relay. The V quantity is the line voltage at the relay location, equal to $I\vec{Z}_F$ when $\vec{Z}_F$ is the line impedance to the fault. The quantity $(I\vec{Z} - \vec{V})$ is the phasor difference between these two quantities. Note that the three characteristics are drawn for the same value of $I\vec{Z}$ (Base reach tap). The greater the value of $\vec{V}$, the more remote the fault. The angle B between $\vec{V}$ and $(I\vec{Z} - \vec{V})$ is less than 90° for a fault internal to the relay characteristic, equal to 90° on the balance point, and greater than 90° for an external fault for which the relay should not operate. The quantities $\vec{V}$ and $(I\vec{Z} - \vec{V})$ are the relay
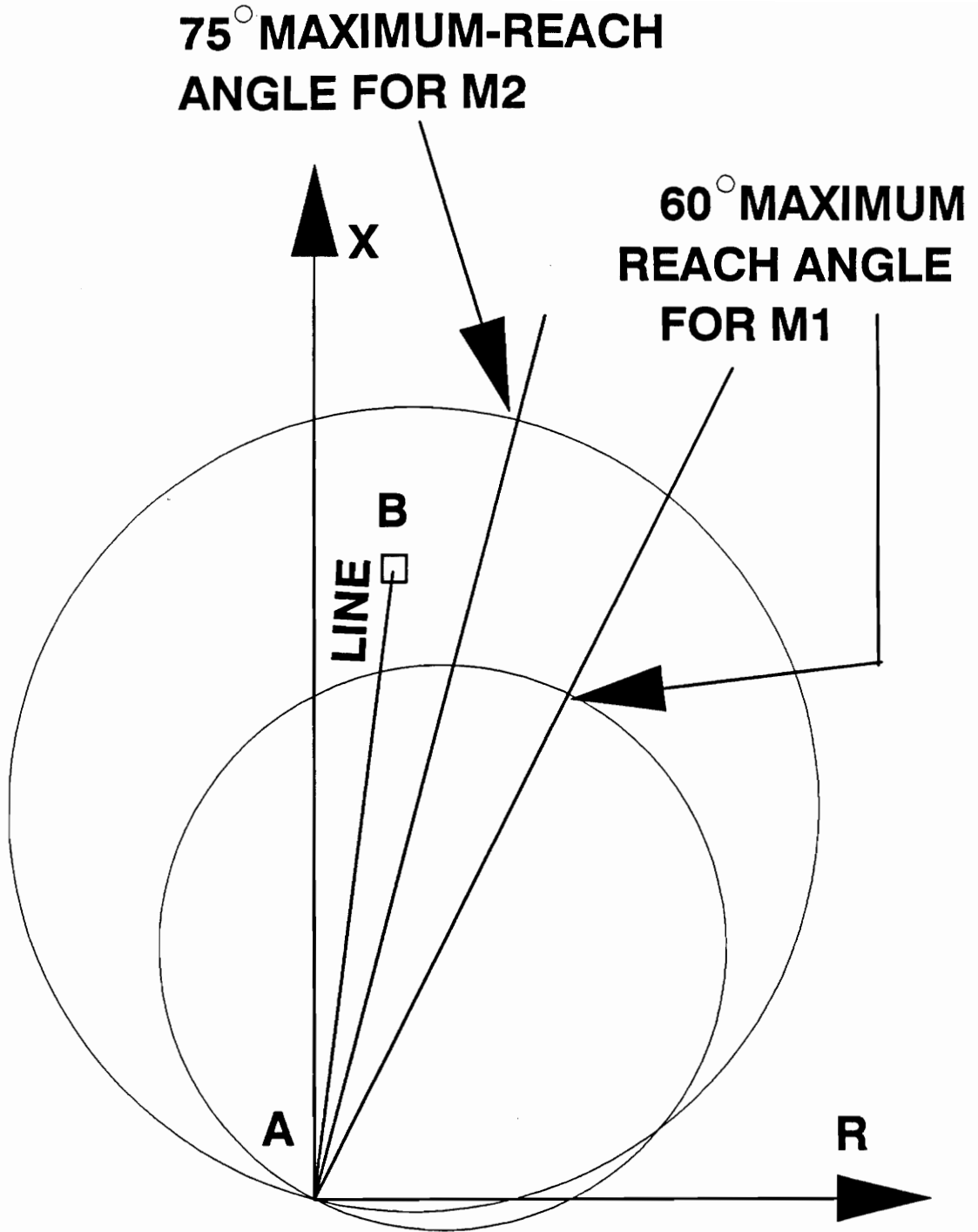
Figure 39. Typical characteristics for zones of SLY Relay.

Θ = LINE ANGLE

Φ = ANGLE OF MAXIMUM REACH
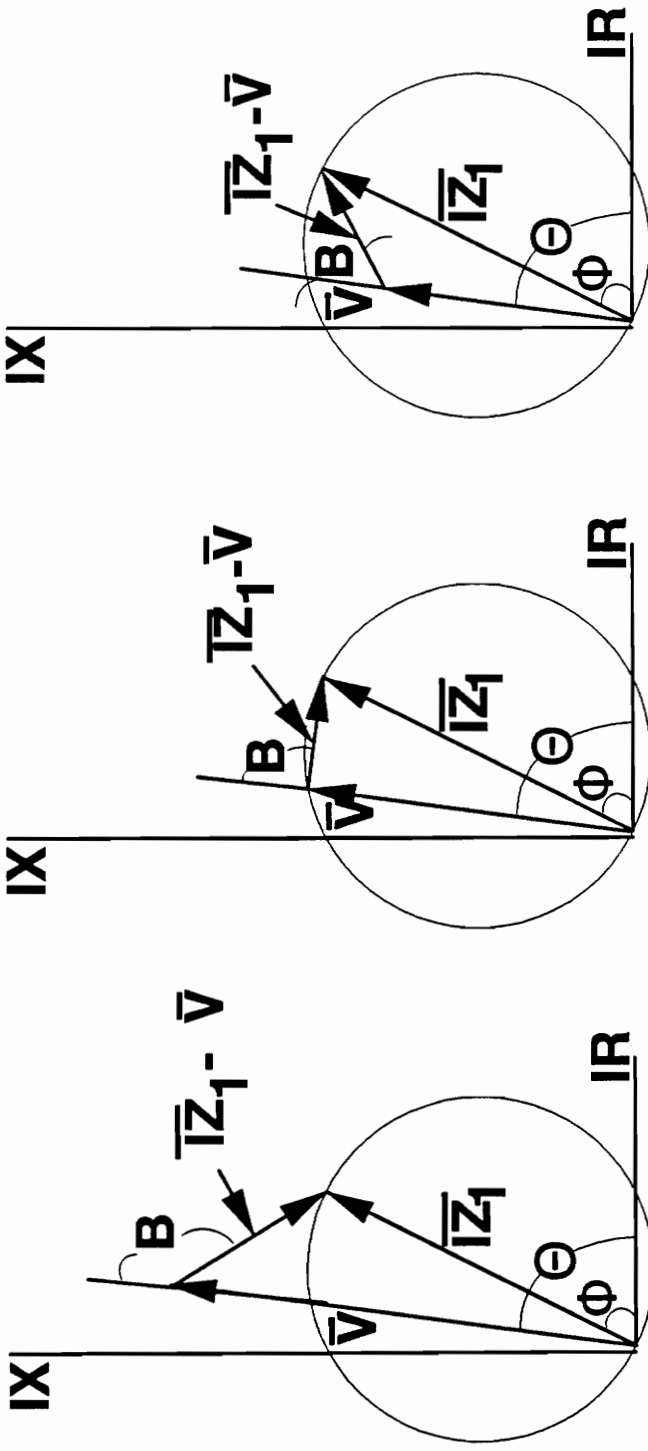
(a)

EXTERNAL FAULT
B>90°

(b)

BALANCE POINT
B=90°

(c)

INTERNAL FAULT
B<90°

Figure 40. Mho characteristics by Phase-angle measurement

input quantities and are converted into blocks of voltage, and then the coincidence (having the same polarity) is measured. Blocks which are 90° apart are coincident for 4.15 ms (for a 60 Hz frequency). Blocks which are less than 90° apart are coincident for more than 4.15 ms. The mho function consists of a discriminator circuit to determine the coincidence of the two input quantities $\vec{V}$ and $(\vec{IZ} - \vec{V})$, followed by a 4/9 millisecond time measurement.

5.2.1.1 I_M Current Monitoring Function:

The current monitoring functions (I_M) operate from each of the phase currents I_A, I_B, and I_C. I_{M1} is set high when the current I_A is above 1.0 A (rms). The I_{M1} and I_{M2} functions supervise the M1 function, and both I_{M1} and I_{M2} have to be present to obtain a trip output of the M1 phase 1-2 function. The I_{M2} and I_{M3} supervise the M1 phase 2-3 function and both I_{M3} and I_{M1} have to be present to obtain an output of M1 phase 3-1.

5.2.1.2 $I_{3\phi}$ Supervisory 3-Phase Overcurrent Function:

The three-phase overcurrent function operates by means of delta currents I_A-I_B, I_B-I_C, and I_C-I_A. The signals obtained from the transactors are proportional to I_A-I_B, I_B-I_C, and I_C-I_A, and are combined in an "OR" circuit, also referred to as an "Auction Circuit." Outputs obtained from the "Auction Circuit" are supplied to the $I_{3\phi}$ level detector. Because of the parallel configuration of the "Auction Circuit," the level detector will detect the signal with the highest magnitude.

The output of the $I_{3\phi}$ fault detector will be used to supervise the mho distance output.

5.2.2 Functional Description of Components

5.2.2.1 Transactor: The transactor serves to transform the input current with a dc offset to an output voltage which is proportional to the input current but without any dc offset. The transfer impedance of the transformer, i.e. the ratio between secondary open circuit voltage and primary current, serves the purpose of relay replica impedance. The air gap serves to linearize the core behavior. The leakage inductance is small and can be neglected. A resistive burden is imposed on the secondary to impart the requisite phase angle to the replica impedance. The actual circuit and its electrical equivalent are shown in Figure 41 on page 125 and in Figure 42 on page 126, respectively. The transfer impedance is

$$Z = \frac{V}{I}$$
$$= \frac{j\omega MR}{R + j\omega M} .$$

(5.2.0)

By changing the value of R, different impedance magnitudes and angles are obtained. R should have a resistance comparatively lower than that of the relay, such that variation of relay impedance does not hamper the replica impedance property. (Ref. [49.])

AIR GAPPED CORE
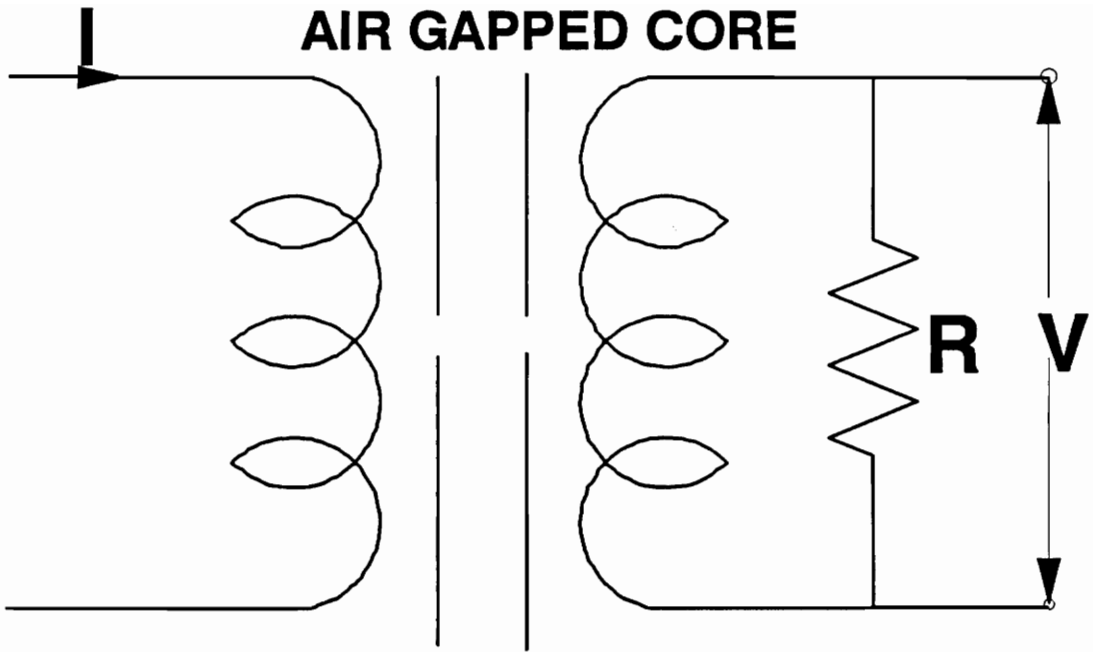
Figure 41. Transactor
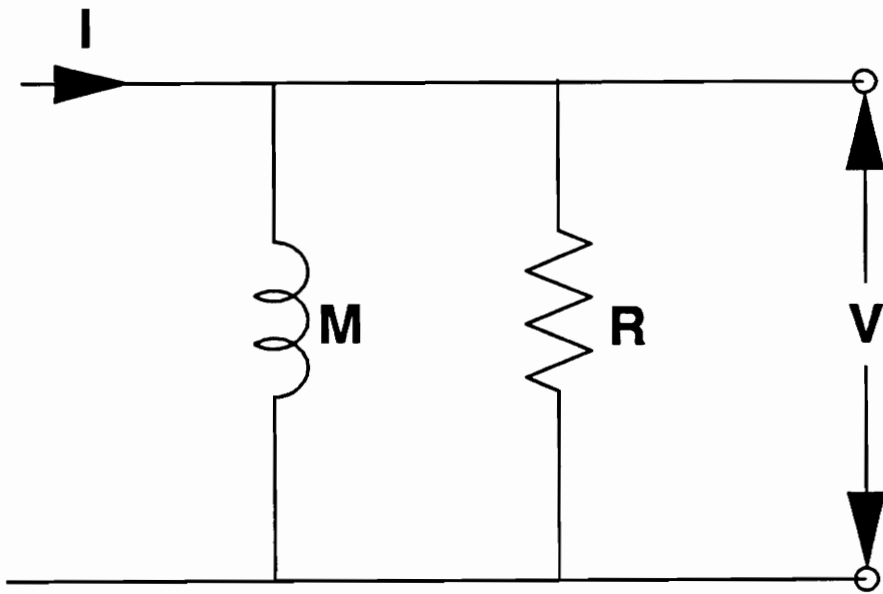
Figure 42.   Transactor equivalent circuit

5.2.2.2 Auction Circuit

The auction circuit is shown in Figure 43 on page 128. The primary currents in each of the transformers are I_A-I_B, I_B-I_C, and I_C-I_A. The secondaries of the three transformers are center-tapped, with capacitors across the outputs. The diodes ensure that only the maximum voltage appears across the output resistor.

5.2.2.3 Angle Measurement - Operating Time:

The M1 and M2 functions use a block-block measuring scheme, in which both input quantities $(\vec{IZ} - \vec{V})$ and $\vec{V}$ are converted to blocks of voltage, and the duration of their coincidence (having the same polarity) is measured. Blocks which are 90° apart are coincident for 4.15 ms. Thus, the mho functions consist of a circuit to detect coincidence of the two input blocks, followed by a 4.15 ms time measurement. In the mho functions, positive half-cycle coincidence is checked separately from negative half-cycle coincidence.

The exact operating time for a given fault varies considerably with the angle of incidence of the fault. The maximum operating time is 12 ms, and the minimum operating time is 4 ms, based on 60 Hz steady state conditions.
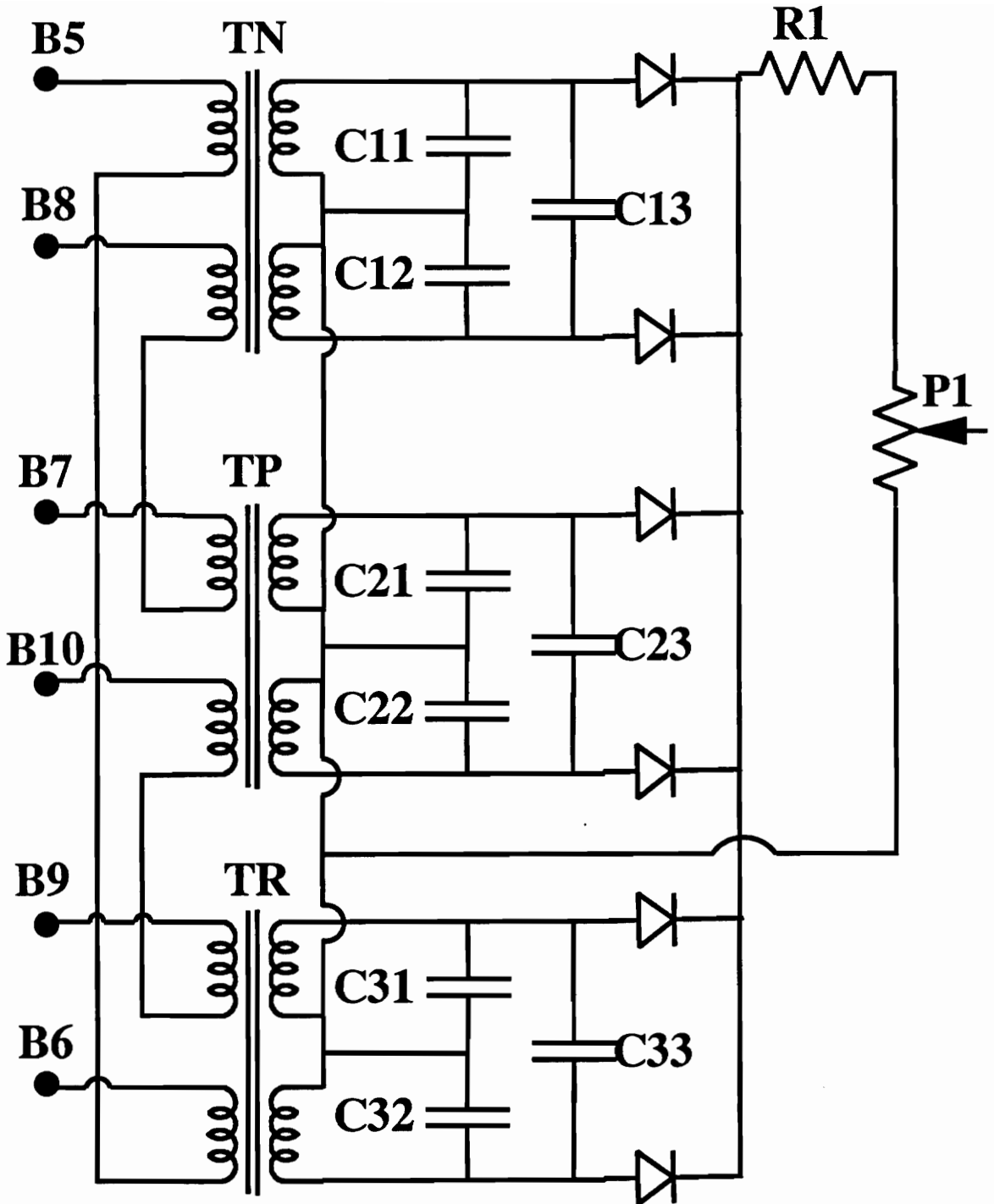
Figure 43. Auction circuit

5.2.3 Modeling of Functions in EMTP

5.2.3.1 Transactor: As mentioned in Section (5.2.2.1) earlier, the transactor can be represented by a transfer function. The transfer function magnitude must give the correct magnitude of $Z_{setting}$ of the line. The transfer function angle gives the desired angle setting of the line.

$$\text{The transfer function is } = \frac{s}{1 + sT}. \tag{5.2.1}$$

For a sinusoidal input, the transfer function can be written as

$$= \frac{j\omega e^{(j\omega t)}}{1 + j\omega T e^{(j\omega t)}} \tag{5.2.2}$$

$$= \frac{\omega \angle 90°}{\sqrt{1 + (j\omega T)^2} \ \angle arctan(\omega T)}. \tag{5.2.3}$$

Now, for f = 60 Hz and with the M1 transactor set for an 80° phase shift

$$\Rightarrow \quad arctan(\omega T) = 10°$$

$$\Rightarrow \quad T = \frac{\tan(10)}{(2. \times \pi \times 60.)}.$$

To get a net gain equal to 1.0

$$\Rightarrow \quad \text{transfer function gain} = \frac{\sqrt{(1. + \omega^2 \times T^2)}}{\omega}.$$

If the required $Z_{setting}$ is 3.0 ohms, then the transfer function gain is multiplied by the $Z_{setting}$, 3.0 ohms. In TACS, there is the capability to represent s blocks and transfer functions. This is used to implement transactors for M1, M1 reverse, and M2 functions. This method simplifies modeling transactors, and reduces the computational burden, without affecting its basic characteristics.

5.2.3.2 Auction Circuit: The 3ϕ Auction Circuit is simulated by a TACS device type 63 -- the instantaneous minimum/maximum function. In this study, we use the instantaneous maximum function. The inputs to the first instantaneous maximum function are $(I_A\text{-}I_B)$, $(I_B\text{-}I_C)$, and $(I_C\text{-}I_A)$. The inputs to the second instantaneous maximum function are $-(I_A\text{-}I_B)$, $-(I_B\text{-}I_C)$, and $-(I_C\text{-}I_A)$. The outputs of the first and second instantaneous functions are inputs to a third instantaneous maximum function. The output of this third instantaneous maximum function is the maximum instantaneous current. If this instantaneous maximum current is greater than the I_{pickup}, then a trip is allowed.

5.2.3.3 Angle Measurement Operating Method

The SLY functional diagram for the M1 function for A-B phases is given in Figure 44 on page 131. The voltage signal $(V_a - V_b)$ is first multiplied by the tap setting multiplier. The current signal $(I_a - I_b)$ is passed through the transactor transfer function for the forward reach setting. The output from the tap setting
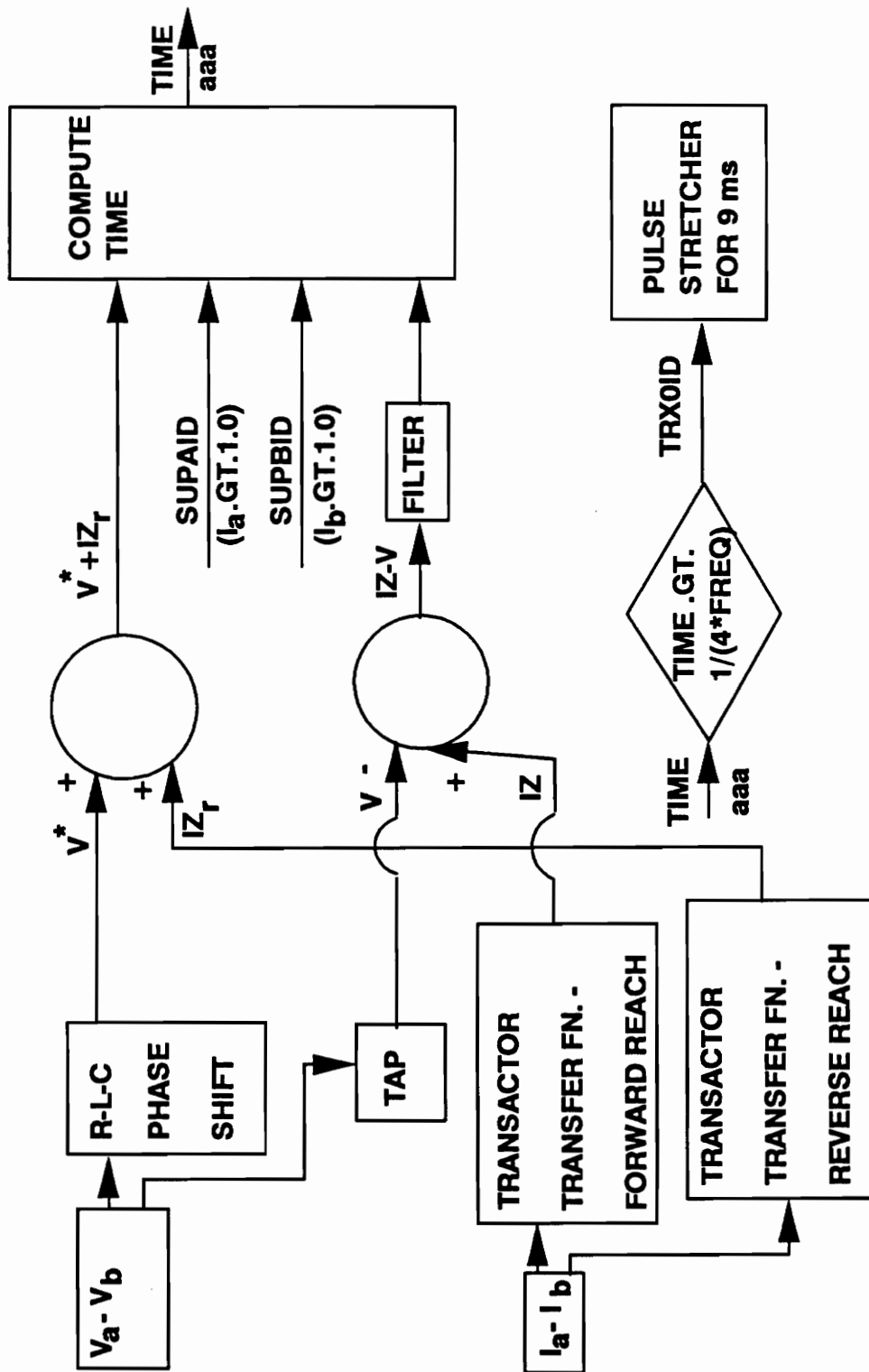
Figure 44. SLY Functional diagram for M1 phase A-B

131

multiplier (V) is subtracted from the output of the transfer function (IZ). The $(\vec{IZ} - \vec{V})$ signal is filtered by parallel tuned L-C filters in the network. Thus, $(\vec{IZ} - \vec{V})$ TACS signal voltage is transferred by a Type 60 source to the network, filtered, and then transferred back to TACS using the Type 90 voltage source. The filter output is the operating input for the time computation block in TACS.

The voltage signal (V_a) is passed through a R-L-C variable phase shifting network. This allows us to set the relay for different angles of maximum reach (from $60° - 75°$) and also provides memory action for a zero voltage close-up fault. The signal V_a is then transferred to TACS using a Type 90 voltage source, where V_b is subtracted from it. The current signal $(I_a - I_b)$ is passed through the transactor transfer function for the reverse reach setting. The output of the R-L-C network (V^*) is added to the transactor output IZ_r, and this sum is the polarizing input to the time computation block.

The current I_a is measured by an rms meter, TACS device number 66. The current I_b is also similarly measured. If the values of I_a and I_b are greater than 1.0 A (rms), then the corresponding signals SUPAID and SUPBID are set high. These signals are required to be set high before the time computation is allowed to proceed. Thus, a measure of security is built into the relay.

All the four inputs $(\vec{IZ} - \vec{V})$, $(\vec{V^*} + \vec{IZ_r})$, SUPAID, and SUPBID are necessary for the time computation to proceed. The time for which the four blocks are coincident is measured. If the measured time is greater than (1./(4.*FREQHZ))

then a trip signal is issued. The trip signal is then stretched for 9 ms. Details of the time computation and pulse stretching are given in Figure 45 on page 134.

The signal CMX2ID is the $SIGN(\vec{IZ} - \vec{V})$, and the signal CMX3ID is the $SIGN(\vec{V} + \vec{IZ_r})$. The four signals CMX2ID, CMX3ID, SUPAID, and SUPBID are ANDed together to form the input IF signal TIX1ID for a TACS device Type 60 Input-IF Component. If TIX1ID is greater than 0, then the signal TIX2ID is PLUS1 (1.). If TIX1ID is less than or equal to 0, then the signal TIX2ID is 0. TIX2ID is the input to the Accumulator TACS device Type 65, the reset signal of which is NTX1ID. As long as the trip signal is high, the accumulator is enabled and is counting. The time (TIX4ID) is computed by multiplying the accumulator output by the time step magnitude (DELTAT). Once TIX1ID goes low, NTX1ID goes high and the accumulator is reset to zero. The accumulator is now ready to count for the next occurrence of a high TIX1ID.

If TIX4ID is greater than $(1./(4.*FREQHZ))$ then the rising edge of the trip signal TRX0ID is generated. The falling edge of the trip signal has to be stretched by a period of 9 ms. This period will provide an overlap for the trip signal produced by measurements on the negative half cycle. The falling edge of the trip signal is generated by ANDing the signals TRX1ID and NTX1ID. The signal BEGXID is stretched by using a positive feedback loop which takes OTX1ID as one input and OTX2ID as the feedback input. After a delay of 9 ms, the signal OTX4ID is added to the z block with a negative sign. This causes a zero in the output OTX3ID and hence TRX2ID.
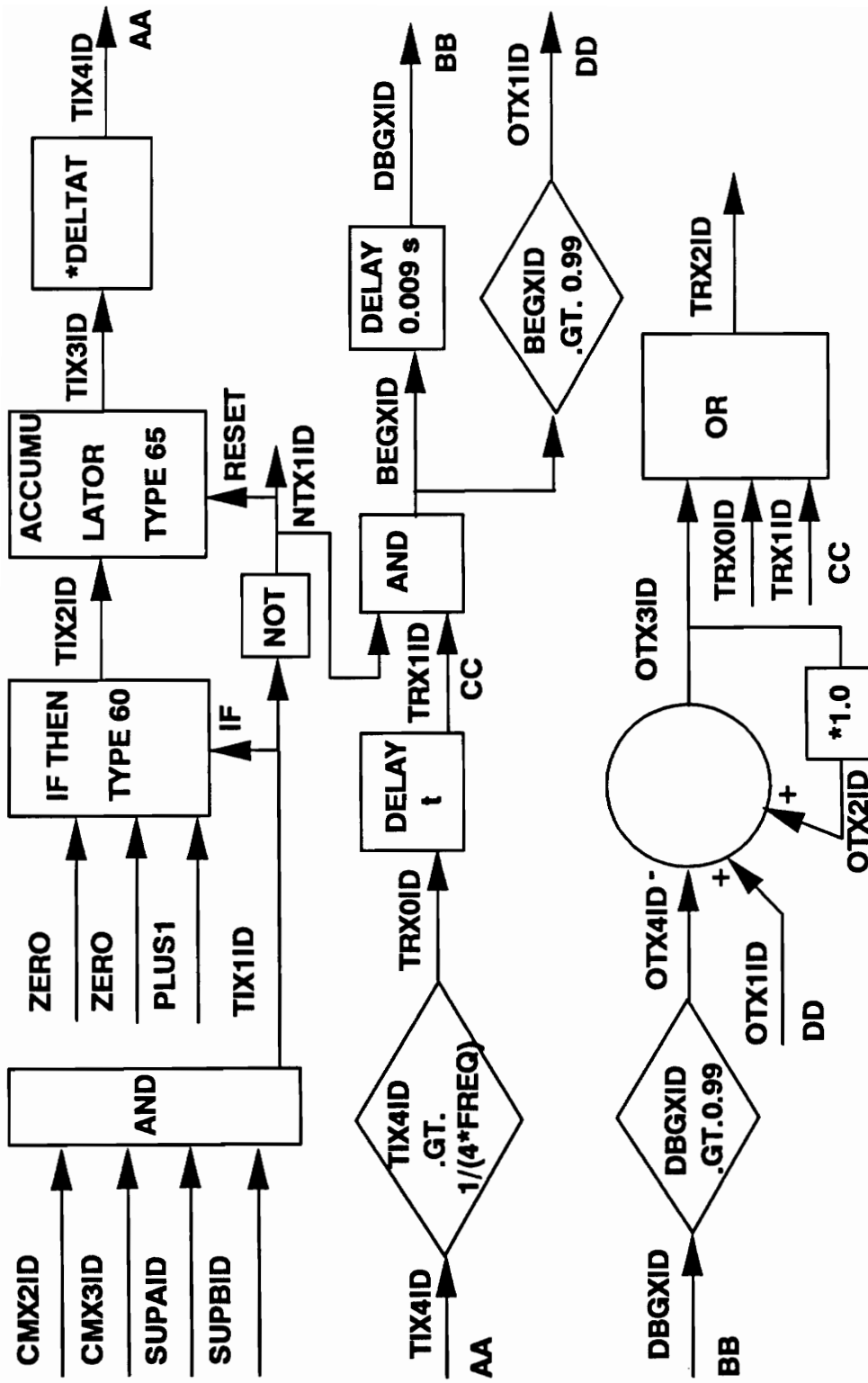
Figure 45. SLY positive cycle trip generation and pulse stretching

134

A similar "circuit" is used for the negative half cycle. The trip output in the negative half cycle analogous to TRX2ID is TRX5ID. Thus, the trip output of the M1 function for phases A-B TRX6ID is created by ORing the signals TRX2ID and TRX5ID. In a similar manner, the trip outputs of the M1 function for phases B-C and C-A are TRY6ID and TRZ6ID, respectively.

The M2 function has a fixed angle of maximum reach of 75°. Thus no phase shifting circuits are required. The functional diagram for the M2 phase A-B function is given in Figure 46 on page 136. The important feature of this figure is the magnitude and sign of the polarizing input $-(\vec{IZ_0} - V^*(1-2))$. Another feature of the M2 function is the provision for forward offset of the relay reach. The forward offset has to be less than the total relay reach. Thus, we can generate the so called "figure eight" characteristics, which prevent the relay from misoperating under heavy load conditions. The trip signal generation and pulse stretching are similar to the description above.

The trip signals are combined as shown in Figure 47 on page 137. The signals correspond to Fig. 8 on Page 16 of Ref. [48.].

5.2.4 Validation of the SLY EMTP Model

Using the circuit of Figure 48 on page 138, the mho characteristic of the relay is plotted. The SLY relay is set for a reach of 2.0 Ω, at an angle of maximum reach
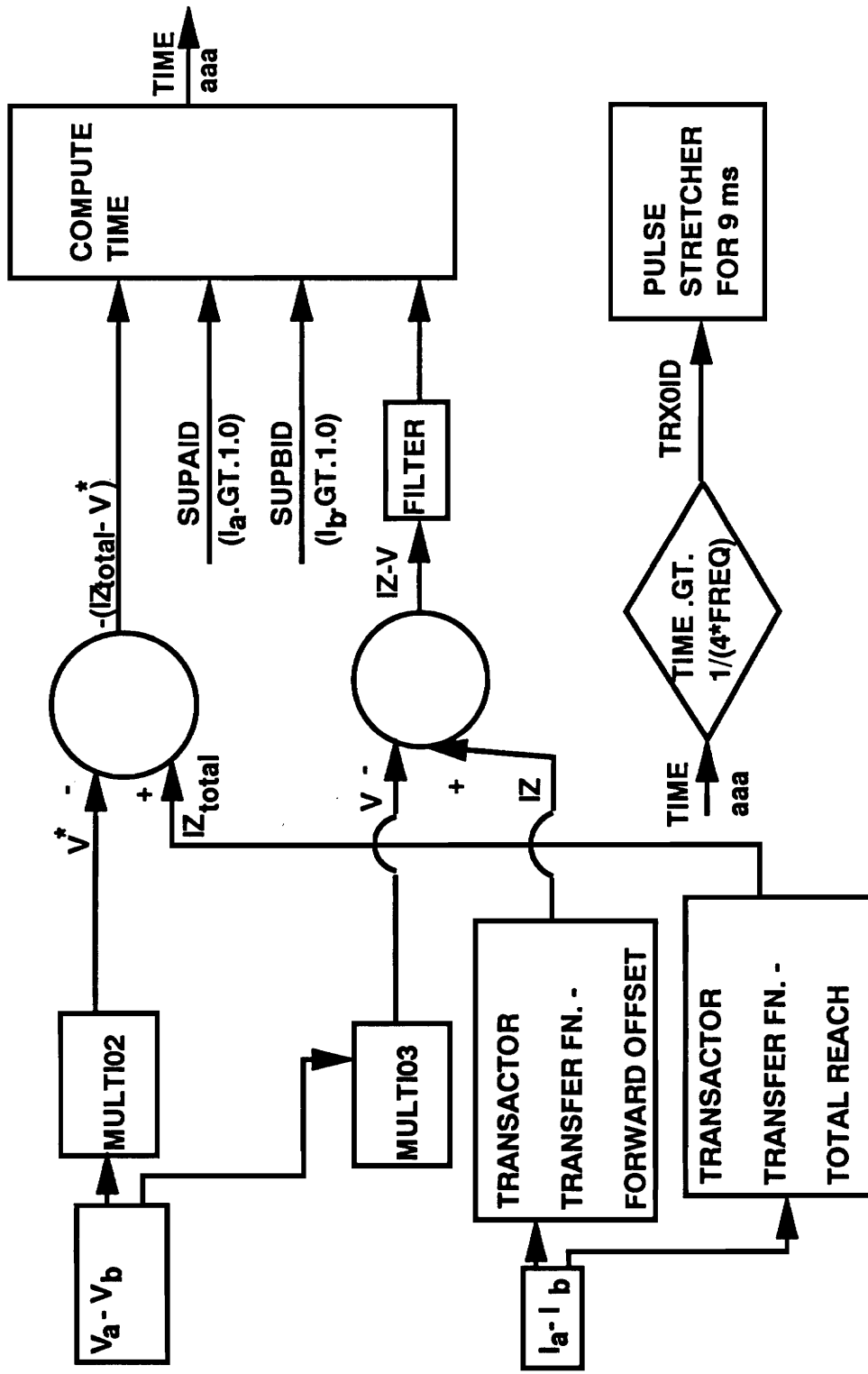
Figure 46. SLY Functional diagram for M2 phase A-B
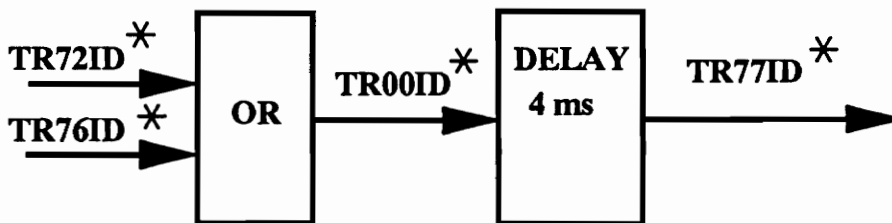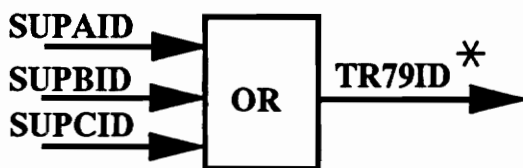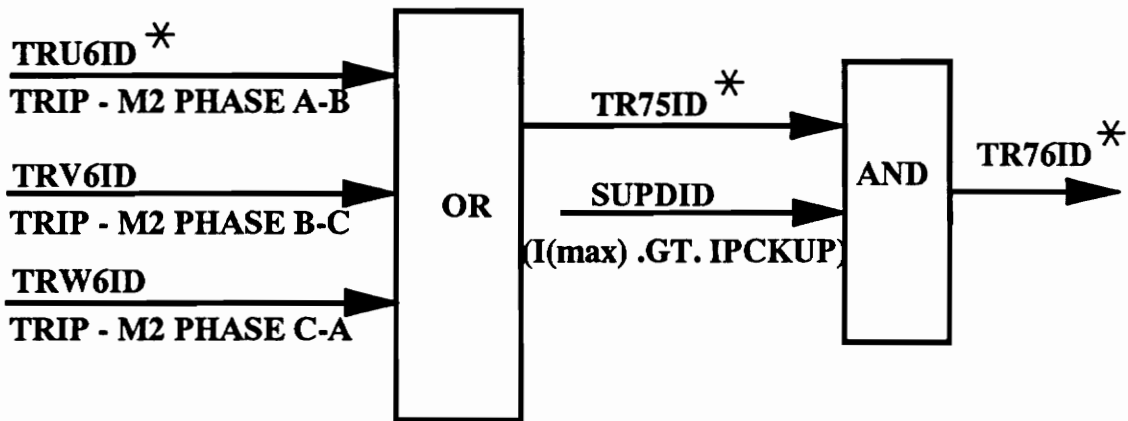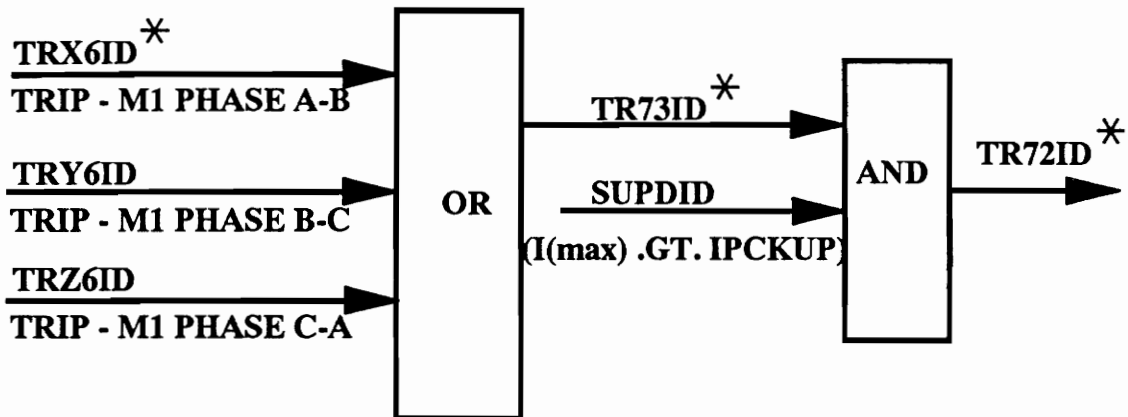
Figure 47.   Final trip outputs of SLY relay
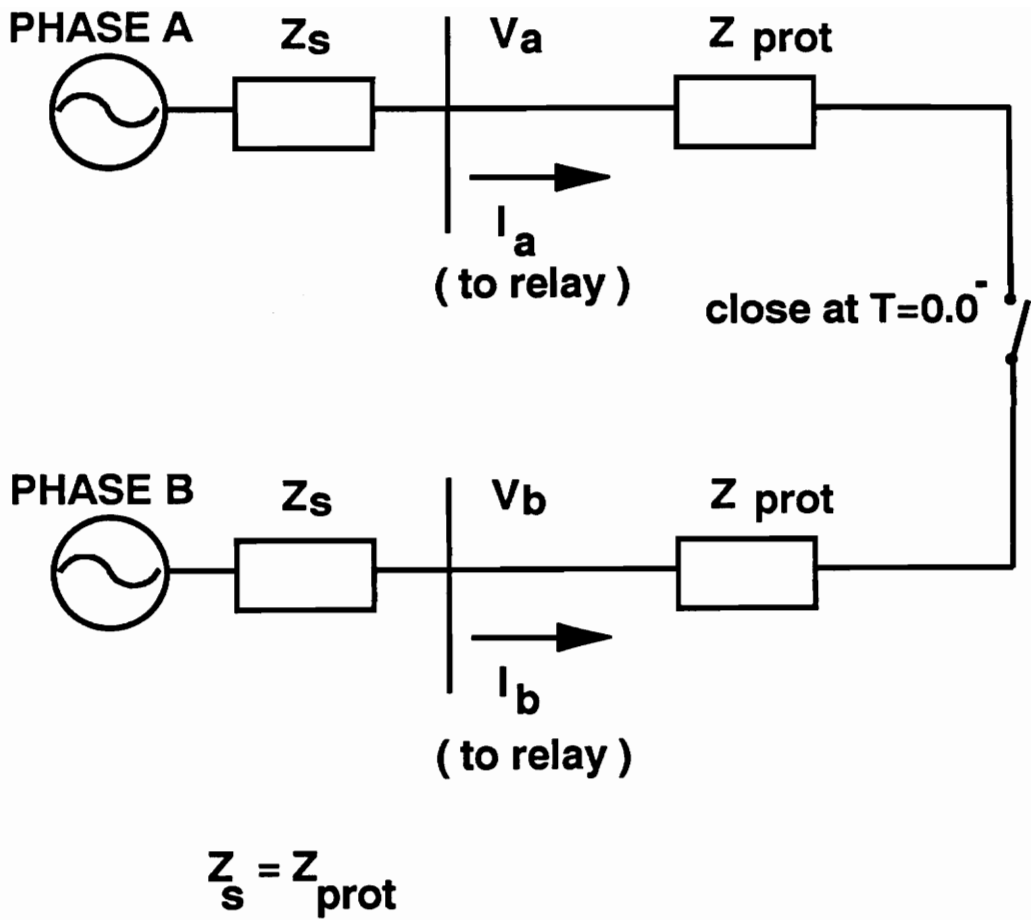
Figure 48. Validation circuit of SLY Relay.
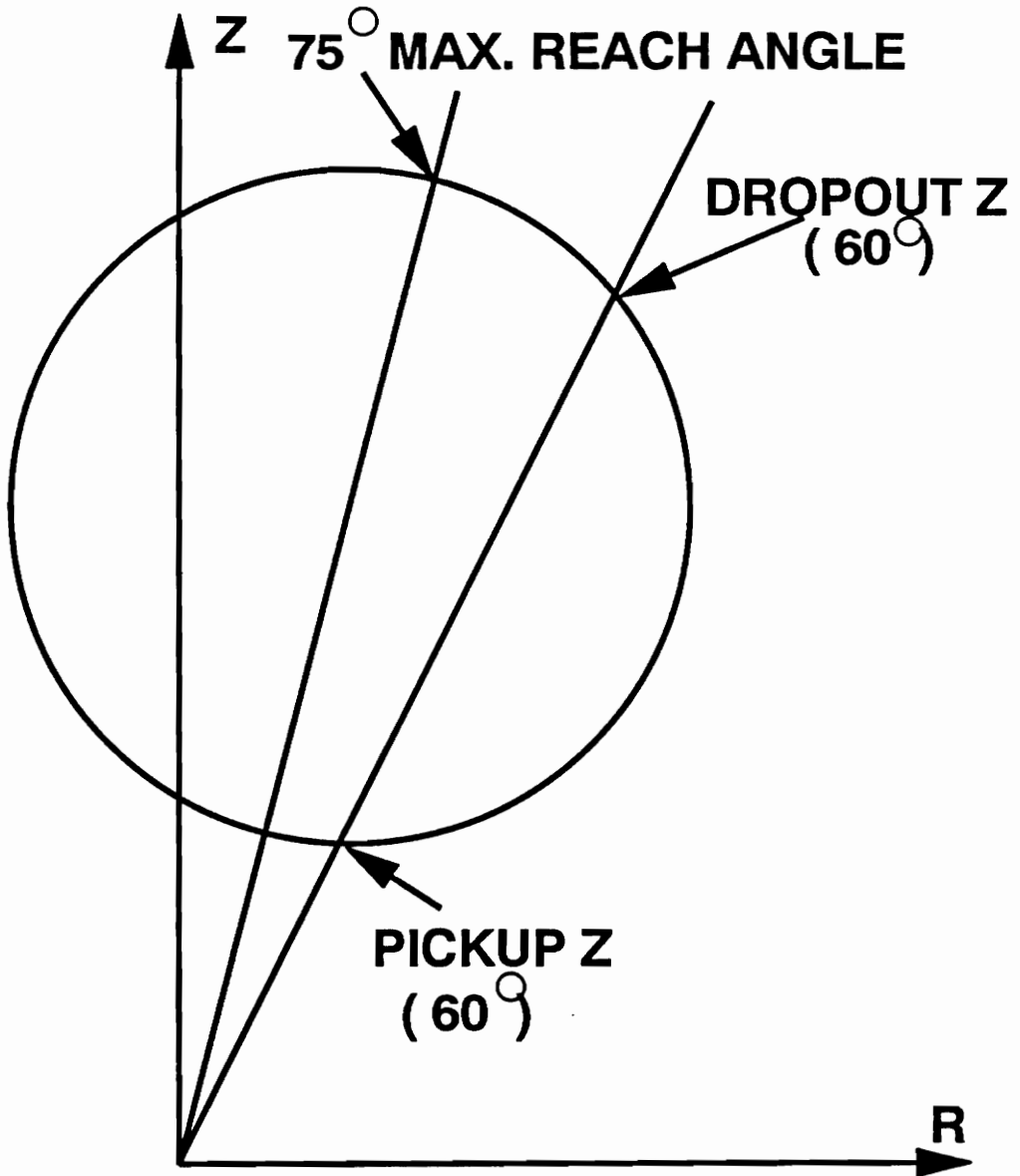
Figure 49. M2 Function Characteristic of SLY Relay

of 60°, with a voltage restraint tap set at 100%. The procedure for the plotting of the mho characteristic at a particular angle is as follows:-

At an angle of 85°, the value of

$$Z_{prot} = 2.0 \cos(60° - 85°) \angle 85°$$
$$= 1.812 \angle 85°. \tag{5.2.4}$$

This value of Z_{prot} was used in the circuit of Figure 48 on page 138. The relay tripped for a fault in the circuit. The value of Z_{prot} was slowly increased (in 1% steps), till no trip was observed. The factor by which Z_{prot} had to be increased to get no trip was 1.07.

This procedure was repeated for line impedances at different angles of 65°, 45°, 25°, 15°, 0°. The factor by which the relay overreached ranged from 1.06 to 1.11. The maximum overreach assumes the form of an ON - OFF trip pulse, and not of a continuous trip signal.

The voltage restraint tap was set at 50%. This increased the relay reach by a factor of two. A test similar to the one described above was conducted. The factor of the overreach for various line impedances ranged from 1.06 to 1.07.

To test the M2 function forward offset MHO characteristic, the following settings were used:-

$$Z_{\text{total reach}} = 3.0 \angle 75°$$

$$Z_{\text{forward offset}} = 1.0 \angle 75°$$

Voltage setting taps = 100% (for both Z settings).

The operating characteristic was first plotted as shown in Figure 49 on page 139. At a particular line angle, the pickup and dropout values for the protected line impedance were marked. These values were taken as the base case with a factor equal to 1.0. The pickup impedance had to be multiplied by a factor to achieve a relay trip. The pickup impedance had to be increased by a factor of 1.03 - 1.07 for various line impedance angles. The dropout impedance had to be multiplied by a factor to achieve a relay dropout. The dropout impedance had to be increased by a factor of 1.03 for various line impedance angles.

The transactor transfer function gains are multiplied by a factor of 0.9 times its theoretical computed gain. This compensates for the tendency of the relay to overreach, which gives the relay a measure of security, to avoid tripping for a fault at the end of the line.

AEP had conducted frequency response and tripping time tests on the relay. The test circuit is shown in Figure 50 on page 142. A similar circuit modelling the simulator was set up in an EMTP data case. The voltage signals are taken from the simulator and reduced before being input to the relay. The relay input voltage reduction factor was found by examining the voltage magnitudes from the AEP test and from the EMTP data case. The ratio of the peak voltage of the AEP case

PHASE A   Zs   Va   Z prot

I a
(to relay)

close at varying times

PHASE B   Zs   Vb   Z prot

I b
(to relay)
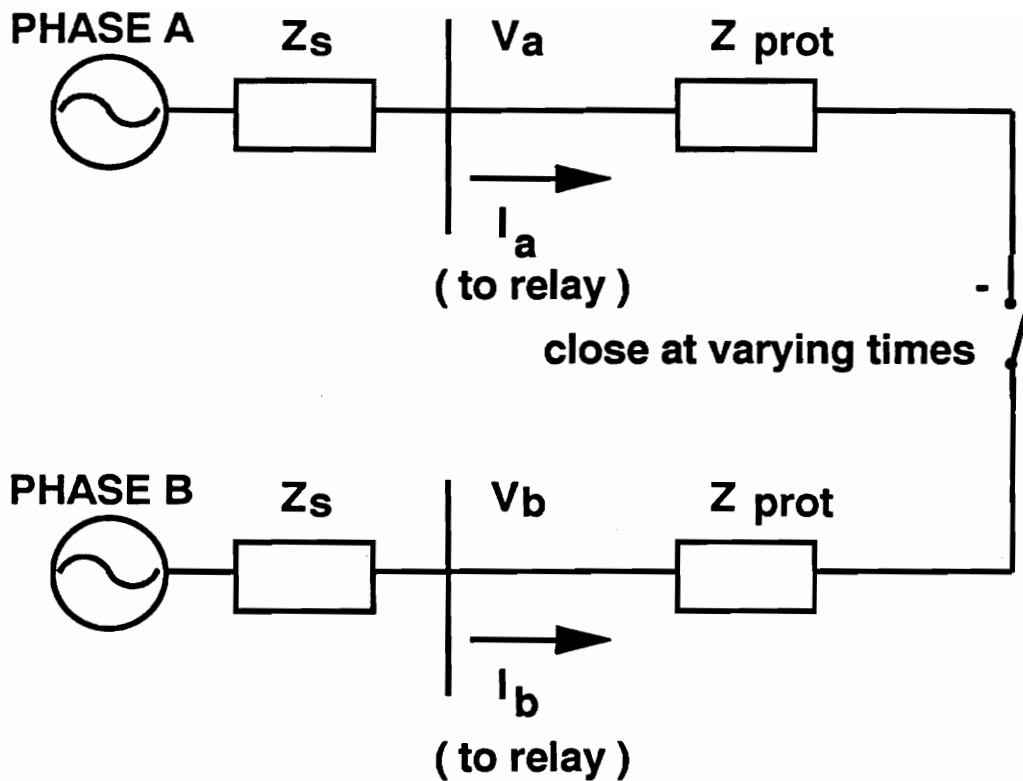
$$Z_s = 0.925 + j20.43 \quad \text{OHMS}$$

$$Z \ (\text{per 12.5 miles}) = 0.13 + j2.87 \ \text{OHMS} \quad (\text{for } Z_{prot})$$

$$\left| V_a \right| = \left| V_b \right| = 60 \ \text{Volts (rms)}$$

Figure 50.   AEP Test Circuit for SLY Relay

to the peak voltage of the EMTP data case gives the voltage reduction factor. The current signal was taken from the simulator and amplified before being fed to the relay. This amplification was necessary because of the low current carrying ability of the simulator at AEP. The current amplification factor was difficult to determine, because of the variable dc offset in the current waveforms. A factor of 3.5 was chosen, which was the best estimate to cover the varying amounts of dc offset. These varying amounts of dc offset were created to test for the relay operating time.

The values of the time to trip in the AEP test and in the SLY EMTP Model are given in Table 2 on page 144.

The faults are created at different points along the length of the line. The percentage of the length of the line at which the fault is applied is given. The faults were created at different points on the current wave to give varying DC offsets. "DC25" refers to a dc offset of 25 percent of the maximum dc offset (the magnitude of the dc offset was adjusted approximately). "NDC" refers to no dc offset and "EOL" refers to End Of Line.

The results are in good agreement. The SLY Model is faster than the actual relay. One reason is that the exact current is not being supplied to the SLY Model, because of approximating the current amplification factor and the X/R ratio of the circuit. Another reason is that the model is idealized; there are no delays of the circuit or logic elements. With this, the SLY EMTP Model is validated.

Table 2. Comparison of AEP test data and SLY model trip times

Test case	AEP test data (time in ms)	SLY model time (time in ms)
NDC29PERCNTSLY.VPI	10.7	8.75
DC25_29PERCNTSLY.VPI	11.3	9.3
NDC57PERCNTSLY.VPI	11.7	9.25
DC25_57PERCNTSLY.VPI	10.3	9.7
DC50_57PERCNTSLY.VPI	12.0	10.1
NDC77PERCNTSLY.VPI	12.3	9.8
DC25_77PERCNTSLY.VPI	12.0	10.4
DC50_77PERCNTSLY.VPI	11.0	10.8
DC75_77PERCNTSLY.VPI	13.7	11.6
NDCEOLSLY.VPI	No Trip	No Trip
DC25_EOLSLY.VPI	No Trip	No Trip
DC50_EOLSLY.VPI	No Trip	No Trip
DC75_EOLSLY.VPI	No Trip	No Trip
DC100_EOLSLY.VPI	No Trip	No Trip

5.2.5 Implementation of the SLY Model in EMTP

The relay has been modelled by creating a module called SLY12C.INC, using the AUX part of EMTP. This module is a basic structure of the relay. The details needed by this module include the node names of the current transformer secondaries, node names of the voltage transformer secondaries, the gains on the transactors, the multipliers for the voltage tap settings, the magnitude of the variable inductor, and a unique identifier for the SLY relay. To run an EMTP data case, the instrument transformer secondary names and the relay settings must be given. The subroutine RELAYS processes the input data case, computes

the magnitudes of the quantities required by the module, and inserts the module SLY12C.INC into the data case. This module is processed by subroutine DATAIN and is included in the data case. The relay outputs are the trip outputs identified by the the two character unique identifier of the relay.

The module SLY12C.INC has been created from the file SLY12C.DAT which contains all the model structure. The module needs the following data:

- three pairs of current transformer secondary names
- three voltage transformer secondary names
- a two character unique identifier for the relay
- three multipliers for the voltage tap settings of the relay
- three gains for the transactors
- a value for the pickup current to be compared with the $I_{3\phi}$ maximum current
- a value for the inductor to give a variable phase shift for the angle of maximum reach.

The module SLY12C.INC is created by running AUX on SLY12C.DAT. An important change has to be made to subroutine SUBR40.FOR of AUX. The parameters MAXARG and MAXCHA must be changed from 99 and 200 to 1000 and 4000, respectively. The new version of SUBR40 must be compiled and linked to AUX to create a new executable version of AUX. This was required because of the complexity and the large number of arguments required by this relay. It is not necessary for the user to compile, link, and create a new executa-

ble version of AUX, which will be required if the file SLY12C.INC is lost and the user wishes to generate SLY12C.INC from SLY12C.DAT again.

To run an EMTP data case, the user inputs data as shown in Figure 51 on page 147. The subroutine RELAYS processes the data as shown in Figure 52 on page 148. The relay settings given in the data case are used to compute the following values :-

- gain for the M1 forward reach transactor
- gain for the M1 reverse reach transactor
- gain for the M2 total reach transactor
- gain for the M2 forward offset reach transactor
- multiplier for the restraint tap setting for the forward ohmic reach of the M1 function
- multiplier for the restraint tap setting for the total ohmic reach of the M2 function
- multiplier for the restraint tap setting for the forward offset ohmic reach for the M2 function
- the value of the inductance (in mH) to give the desired phase shift to match the angle of maximum reach

Subroutine RELAYS then inserts the module SLY12C.INC, together with the node names, the identifier, and the computed values, in the data case. The SLY12C.INC file is read in together with the vectors KARD, KARG, KBEG,

SLY12C DATA FORMAT CARD

C SLY12C

C CTTRA1 CTTRA2 CTTRB1 CTTRB2 CTTRC1 CTTRC2...

...VOLTRA VOLTRB VOLTRC SLYIDN

C OHMFM1 OHMRM1 OHMTM2 OHMOM2 RSTRM1...

...RSTRM2 RSFOM2 ANGMRE IPCKUP

FORMAT

ALL CT & VT NODES	A6
SLYIDN	A2
OHMFM1.....IPCKUP	F5.1

OHMFM1 - Forward reach of M1

OHMRM1 - Reverse reach of M1

OHMTM2 - Total reach of M2

OHMOM2 - Forward Offset reach of M2

RSTRM1 - Restraint tap on M1

RSTRM2 - Restraint tap on total M2

RSFOM2 - Restraint tap on For. Off. of M2

ANGMRE - Angle of Maximum Reach

IPCKUP - Pickup current (compare to I max)

Figure 51.   EMTP Input data for SLY Relay

FLOW CHART OF SUBR RELAYS FOR SLY12C
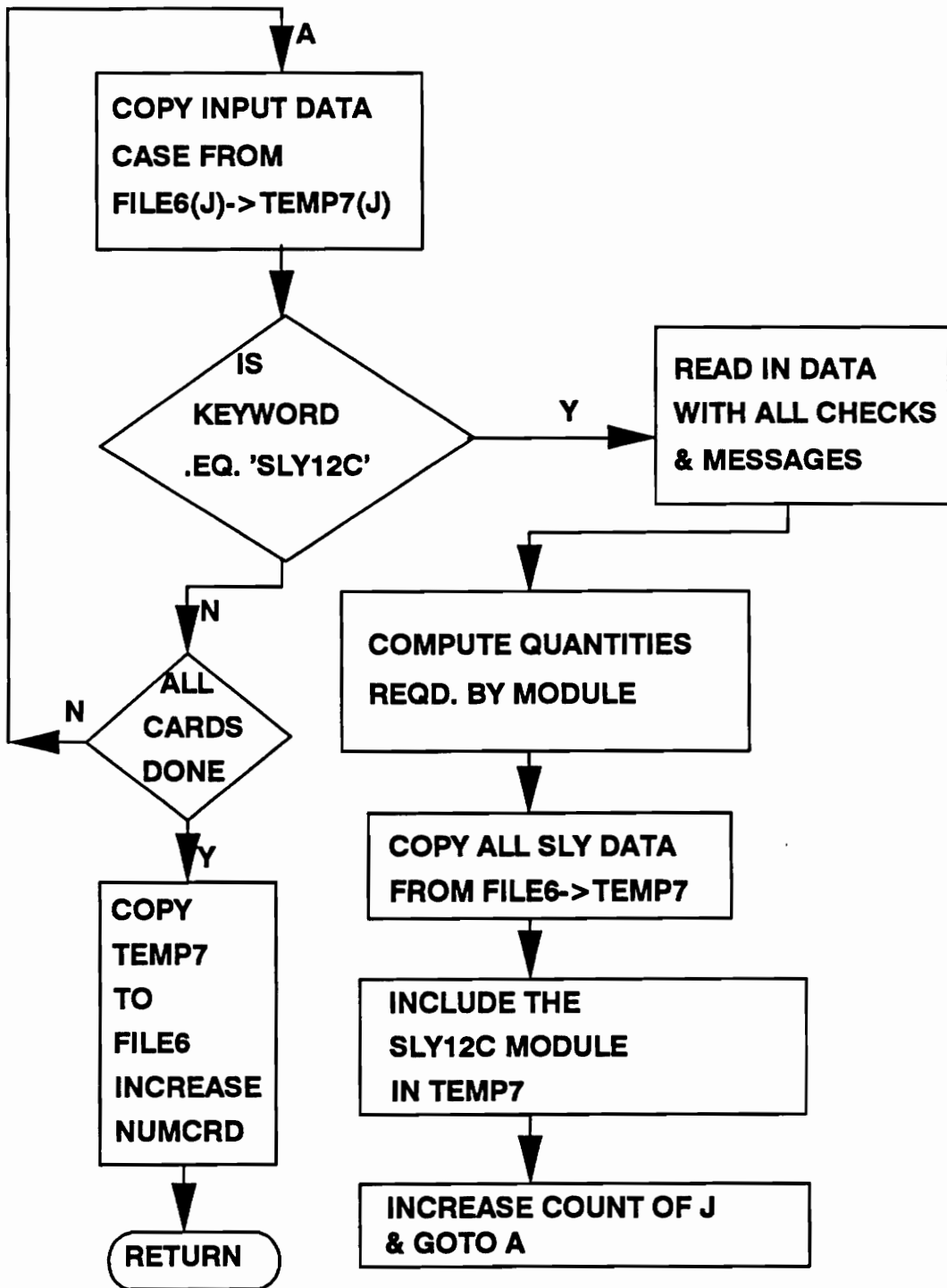
Figure 52.   Subroutine RELAYS flowchart for SLY Relay

KEND, and KTEX by the subroutine DATAIN. The five vectors direct the substitution of the arguments of the module in the data case. Subroutine DATAIN then sorts the EMTP data case according to the order of the cards, i.e., /TACS, /BRANCH, /SWITCH, and then /SOURCE.

The large number of substitutions required by the the module SLY12C.INC causes problems in the execution of the EMTP data case, which necessitates changing the dimension in subroutine DATAIN of LIMSUB and LIMARG from 500 and 999 to 1500 and 3000, respectively. The new version of DATAIN has to be compiled and linked to EMTP.OLB to create a new version of EMTP. With this new version of EMTP, the data case runs without any errors and produces the expected results.

5.3 BDD RELAY MODELING

5.3.1 Introduction

The BDD type relays are differential type relays designed specifically for transformer protection, and the relays are provided with the features of percentage and harmonic restraint and use a polarized unit with an auxiliary relay as the operating element. Percentage restraint permits discrimination between internal and external faults at high fault currents. Harmonic restraint enables the relay to

distinguish, by the difference in waveform, between the differential current caused by the internal fault, and that of transformer magnetizing inrush. The BDD15B, the specific BDD relay chosen by AEP for testing, serves to protect two winding transformers and has two through current restraint circuits and one differential current circuit. Details of the BDD15B relay are given in Ref. [50.].

In this section, a description of the relay and its important components is given. The relay model and the models for the polarized and the instantaneous unit are explained. The BDD15B relay module and the implementation in EMTP are detailed. Validation of the model is done by testing the relay model with the AEP test data.

5.3.2 BDD Relay description

The BDD Relay diagram is shown in Figure 53 on page 151, and is also shown in Fig. 10 of Ref. [50.]. The through current transformer which supplies the restraint winding has two primary windings, one for each live current transformer circuit. Winding No. 1 terminates at stud 6 and winding No. 2 terminates at stud 4. A differential current transformer which mainly supplies the operate winding has one primary lead brought out to stud 5. The primary circuit of the through current transformer and the differential current transformer is completed through a special tap block arrangement. Two horizontal rows of tap positions are provided, one row for each through current transformer winding. A tap on the dif-
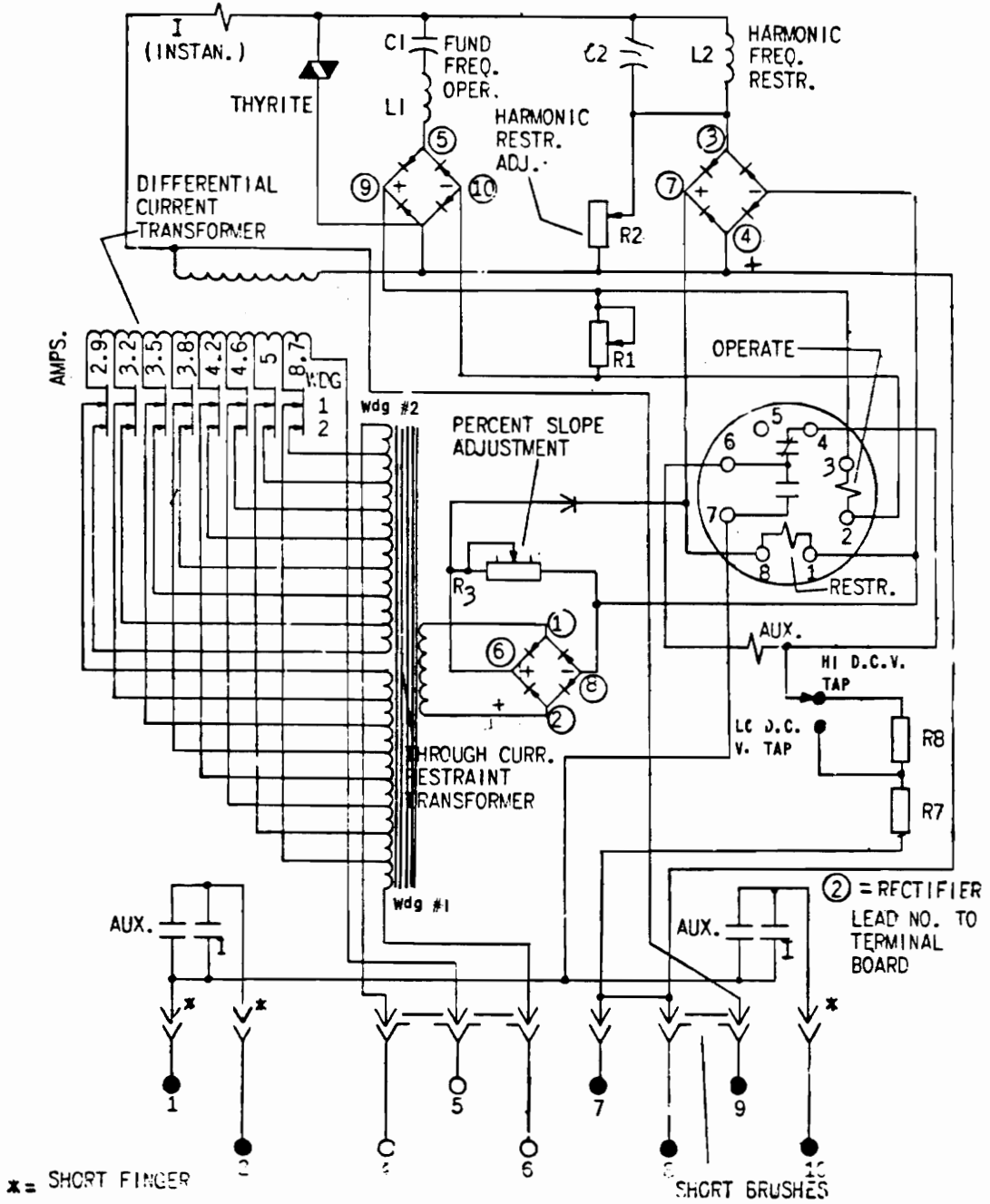
Figure 10 (0165A7513-2) Internal Connections Diagram For The 12BDD15B11A And Up Relays

Figure 53.   BDD relay diagram

32

5.0 LINE AND TRANSFORMER RELAY MODELS   151

ferential current transformer is connected to a corresponding tap of the through current restraint windings by inserting tap plugs in the tap blocks. The taps permit matching of unequal line current transformer secondary currents. The tap connections are so arranged that in matching the secondary currents, when a tap plug is moved from one position to another in a horizontal row, corresponding taps on both the differential current transformer winding and one of the through current transformer windings are simultaneously selected so that the percent through current restraint remains constant.

5.3.2.1 Through current restraint circuit:

The secondary of the through current restraint transformer is connected to the input terminals of a full wave bridge rectifier. The rectifier output is connected to a tapped resistor R3 through the percent slope tap at the front of the relay, which allows the adjustment of 15, 25, or 40 % slope. The resistor R3 is connected in parallel with the restraint winding of the polarized unit through a diode.

5.3.2.2 Differential current circuit:

The secondary output of the differential current transformer supplies the instantaneous unit directly, and both the operating coil and the restraining coil of the polarized unit through rectifiers. The current of the operating coil of the polarized unit is first passed through a series L-C tuned circuit, then it is rectified through a full wave bridge rectifier. The series L-C tuned circuit offers a low impedance to 60 Hz currents and a high impedance

to other frequencies. On the dc side of the rectifier, resistor R1 is connected in parallel with the operating coil of the polarized unit. Resistor R1 is used to control the magnitude of the operating coil current. The current to the restraint coil of the polarized unit is first passed through a parallel tuned L-C circuit; then it is rectified by a full wave bridge rectifier and paralleled with the output of the through current restraint transformer. The parallel tuned L-C circuit offers high impedance to 60 Hz currents, while allowing currents of higher frequencies to pass with relatively lower impedances. Resistor R2 is in parallel with the harmonic restraint rectifier on the ac side and can be adjusted to give the desired amount of harmonic restraint.

5.3.2.3 Overcurrent unit: The instantaneous unit is a hinged armature relay with a self contained target indicator. On extremely heavy internal fault currents, this unit picks up and completes the trip circuit.

5.3.2.4 Main operating unit: The main operating unit is a sensitive polarized unit with components as shown in Figure 53 on page 151. The unit has one operating coil and one restraining coil. Relay operation occurs when the square of the ampere-turns of the operating coil is greater than the square of the ampere-turns of the restraining coil.

5.3.3 Relay Modeling

5.3.3.1 Modeling of restraint ct and differential ct

The models of the through current restraint transformer and the differential current transformer are given in Figure 54. CTSCB1 and CTSCB2 are the secondary terminals of the two line current transformers on either side of the protected power transformer. The through current restraint transformer and the differential current transformer are designed to be operated at constant primary ampere-turns, ensuring a constant accuracy class of the CT's at all the ampere taps. Thus, different ampere taps on the line current transformer will require different number of turns on the primary of both transformers. Because the number of turns on the winding DFC2ID to DFC1ID must be positive, the number of turns from DFC1ID to GROUND must be less than the number of turns from DFC2ID to GROUND. To satisfy the constant ampere-turns requirement, this implies that DFC1ID, and hence CTSCB1, must have higher ampere tap rating. (For a constant ampere-turn CT, a higher ampere tap rating implies a lower number of turns.) CTSCB2 has the equal or lower ampere tap rating. If CTSCB2 has the equal or lower ampere tap rating, then a higher number of turns are required between DFC2ID to GROUND, than between DFC1ID to GROUND, which allows for a positive number of turns between DFC2ID to DCFC1ID. If CTSCB2 has the same ampere rating as CTSCB1, then the number of turns between DFC2ID and DFC1ID is chosen as 0.1, which

CTSCB1

TRS1ID

THROUGH CURRENT
TRANSFORMER
(1980 TURNS)

CTSCB2

TRS2ID

DFS1ID

DFC2ID

DIFFERENTIAL CURRENT
TRANSFORMER
(900 TURNS)

DFC1ID

DFS2ID
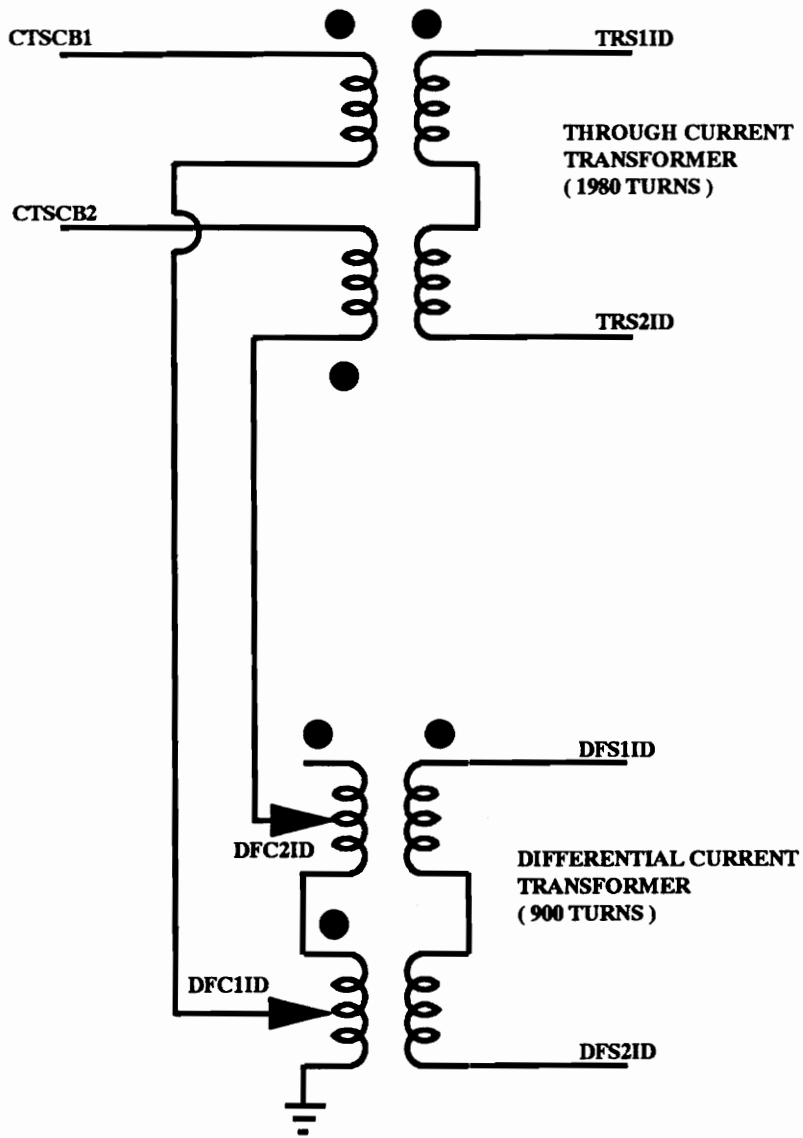
Figure 54.   Through ct and differential ct connections

leads to a maximum of 1.2% error ($0.1 \times 100./8.$) in the differential current transformer secondary current. (8 is the minimum number of turns on the primary of the differential current transformer)

The dots on the through current restraint transformer are chosen so that on an external fault the secondary through current restraint transformer is proportional to the sum of the line current transformer currents. During an internal fault, the secondary through current restraint transformer is proportional to the difference of the line current transformer currents.

The through current restraint transformer and the differential current transformer are modeled without their magnetization impedances because the magnetization curve of the transformers is not available. Thus, the transformers are idealized in the BDD relay. This idealization should not cause any problem in most cases; however, under extremely large fault currents, when saturation of BDD CT's occurs before the line CT's, then the BDD model could be inaccurate. No such case is available to us to simulate and determine the difference in operation between the actual BDD relay and the BDD model. Yet, it is anticipated that there may not be a large difference, because of the operation of the instantaneous relay.

5.3.3.2 Modeling of rectifiers

Anode

Cathode

TYPE 11 SWITCH

MODELING A DIODE
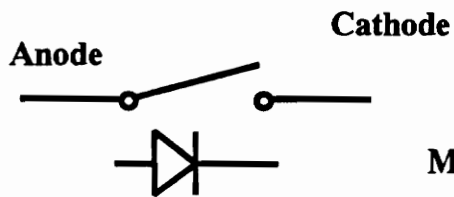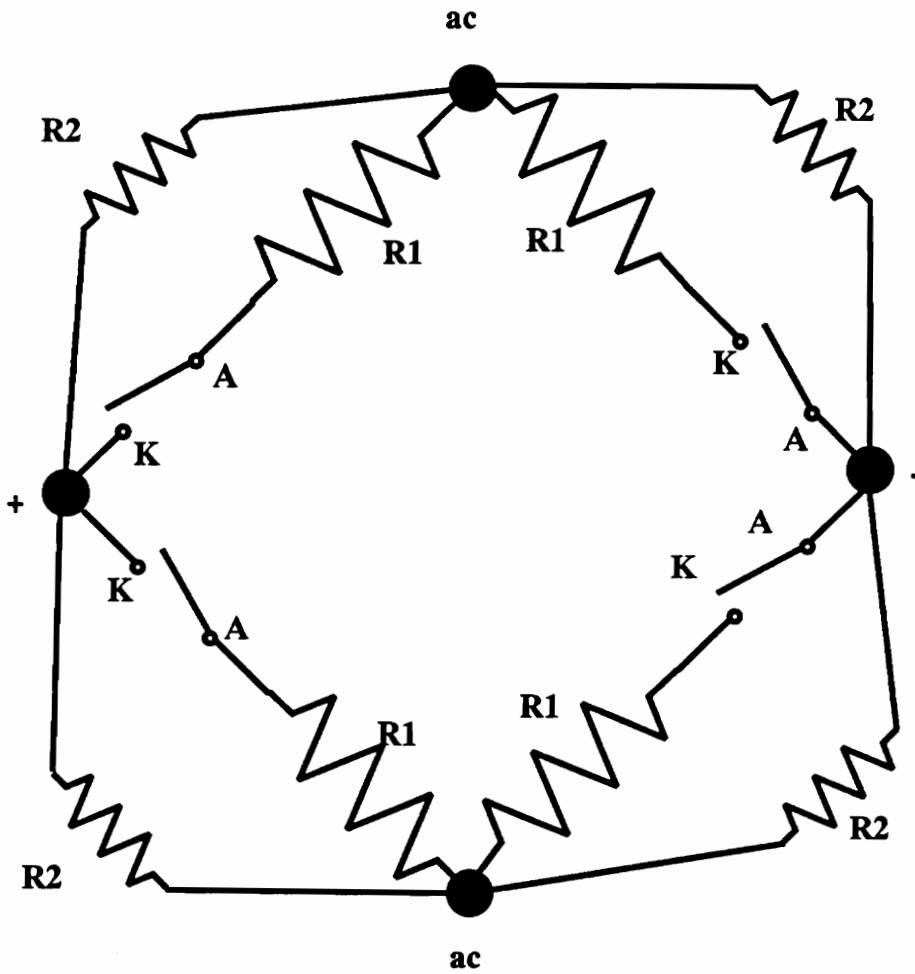
R1 - Forward resistance of diode

(0.1 OHMS)

R2 - 100,000 OHMS

Figure 55.   Full wave rectifier model

The full wave rectifiers are modeled as shown in Figure 55 on page 157. The diode is modeled as a Type 11 switch, with an ignition voltage of 0.0 V and a holding current of 0.0 A. Thus, the diode is on at the instant the anode voltage is higher than the cathode voltage. The 100K resistor across the arms of the bridge is necessary to avoid the floating subnetwork message of EMTP, and the subsequent errors in simulation that ensue after this message. The 0.1 ohm resistor is the forward resistance of the diode and is necessary to avoid a loop of switches, which is a fatal EMTP error.

5.3.3.3 Modeling of main relay and auxiliary relay operation

The main operating unit is shown in Figure 56 on page 159. After this polarized unit operates, the auxiliary relay is energized and the trip circuit contacts are closed. The time of operation of the BDD relay is the sum of time of operation of the main and auxiliary relay. The operation of the polarized unit is given by the following equation :-

$$F_{operate} = (N_1 \times I_{operate})^2 - (N_2 \times I_{restraint})^2 - 120.0 \,, \qquad (5.3.1)$$

where,

$N_1 =$ Number of turns in operating coil $= 880$ turns,

$N_2 =$ Number of turns in restraining coil $= 2400$ turns,

$$IOPER \longrightarrow \boxed{(NOPER)^2 * \\ IOPER} \xrightarrow{FOPER} \bigoplus \xrightarrow{FOR1ID} $$

FOR1ID

AA

$$IRES \longrightarrow \boxed{(NRES)^2 * \\ IRES} \xrightarrow{+} \bigoplus \xrightarrow{FRES}$$

$$\boxed{K} \xrightarrow{+}$$

FOR1ID

AA $\longrightarrow \boxed{LIMITER} \xrightarrow{FOR2ID} \boxed{\dfrac{1.}{ms^2 + bs + c}} \xrightarrow{MOV1ID}$

Type 52 Level
Triggered Switch

FIXED
THRESHOLD

PLUS1 ⟶ ▭ ⟶ TRX1ID

HOLDING CIRCUIT

Type 13 Switch controlled
by TRX1ID

DCR1ID   DCR2ID   0.1   DCR4ID

1000.

0.1

220. V

Type 13 Switch controlled   500.
by TRX2ID   DCR3ID

(TRX2ID = DCR4ID .GT. 100. V)
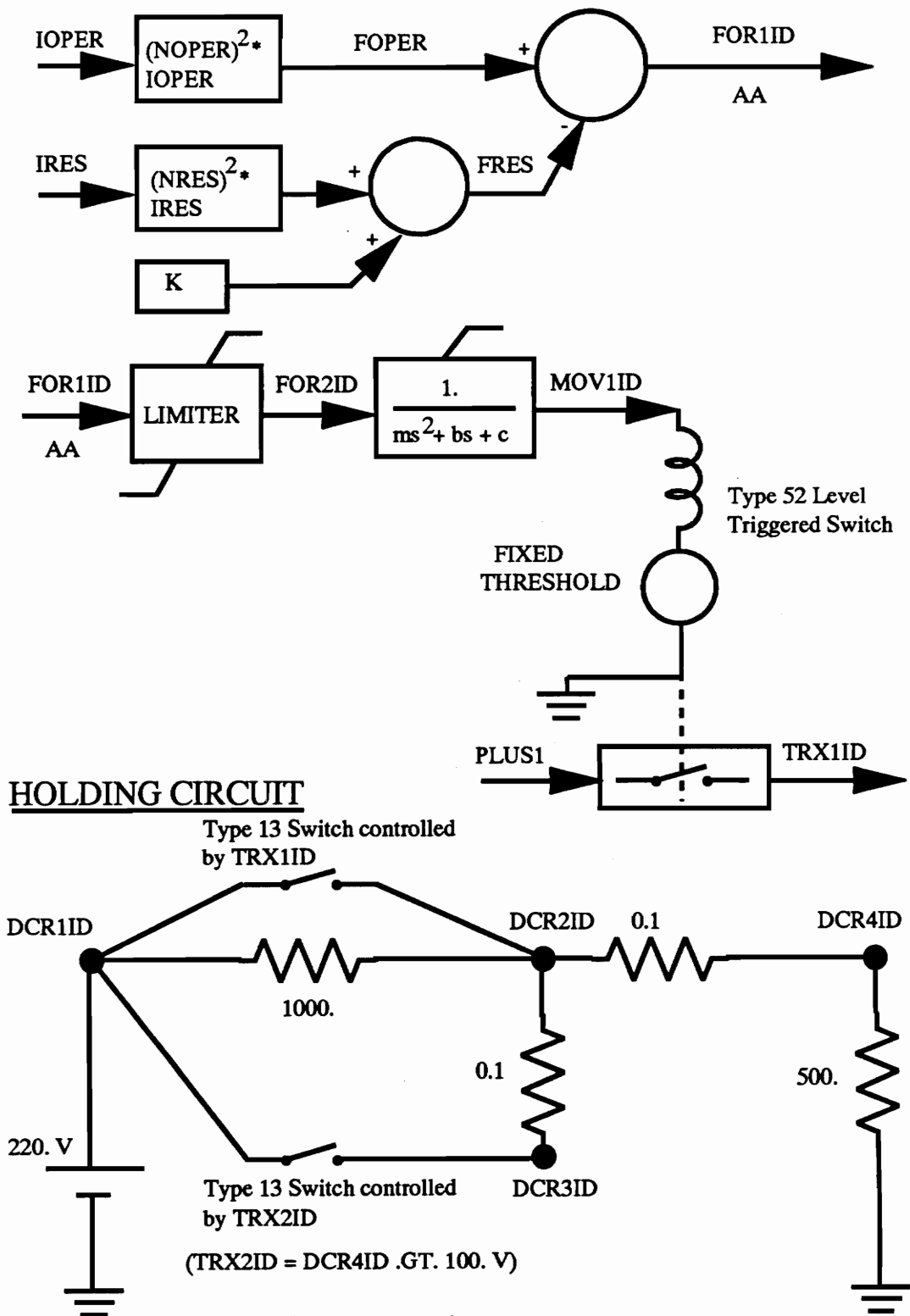
Figure 56. Main relay and auxiliary relay modeling

$$I_{operate} = \text{current in the operating coil,}$$

$$I_{restraint} = \text{current in restraining coil.}$$

The relay equation can be written as :-

$$F_{operate} = m\ddot{x} + b\dot{x} + cx ,\qquad (5.3.2)$$

where,

x is the distance traversed by the moving contact;

m is the mass of the contact;

b is the coefficient of friction;

c is the spring constant.

The differential equation can be modeled as a second-order transfer function in TACS, after taking the Laplace transform of Eq. No. (5.3.2). Thus, the distance traversed by the moving contact is given by the following second-order transfer function :-

$$x = \frac{F_{operate}}{ms^2 + bs + c} .\qquad (5.3.3)$$

When the distance traversed by the armature is more than the contact separation, the relay operates. Because of saturation, the relay has a definite minimum time of operation and implies the use of a maximum limit on the operating force. To

simulate the reset action of the relay, a negative minimum limit on the operating force is allowed.

The relay modeling is shown in detail in Figure 56 on page 159. The holding circuit to simulate the action of the auxiliary relay is also shown in Figure 56 on page 159.

The determination of the constants m, b, c, and of limits on the force is done by matching the operating time given by the time-current curve in Fig. 5 of Ref. [50.] and from details of the main relay sent by GE. The choice is validated by comparing the AEP test results in Section 5.4.3.

5.3.3.4 Modeling of the instantaneous relay

The secondary current of the differential current transformer is transferred to TACS as a Type 91 source. The rms current is measured by connecting the TACS device 66, the rms meter. The time-current curve is given in Fig. 5 of Ref. [50.]. The modeling of the relay is shown in Figure 57 on page 162 and is similar to the main relay and auxiliary relay model, except that there is no polarization. The static restraint is determined by the pickup current being eight times the relay differential current. Because of the constant primary ampere-turns (equal to 70.0) design of the differential current transformer,

$$\Rightarrow \text{constant secondary current} = \frac{70}{900}$$
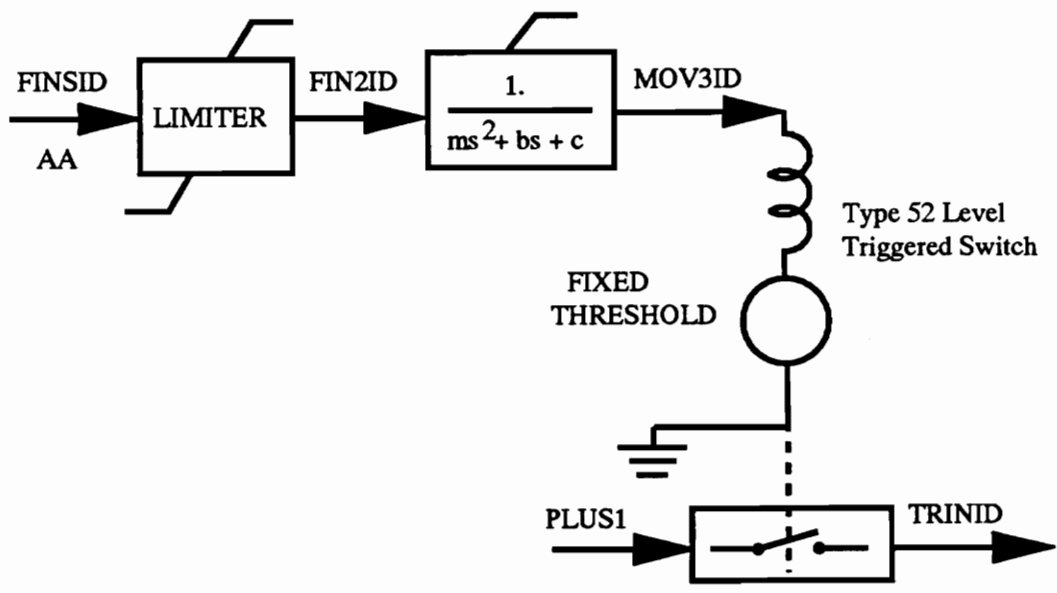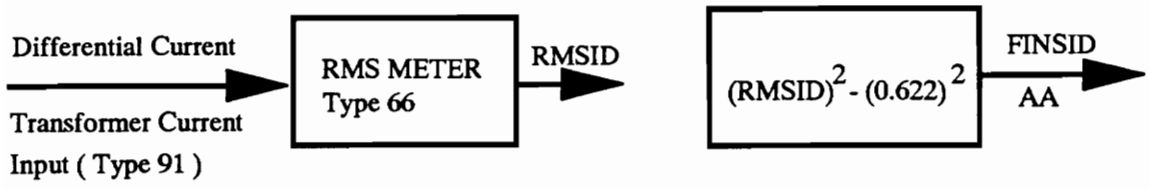
Figure 57.   Instantaneous relay modeling

(900 turns are on the secondary of the differential current transformer).

The pickup current of the instantaneous unit is,

$$I_{pickup} = \frac{70 \times 8}{900}$$
$$= 0.622$$

Hence, the

$$F_{operate} = (I_{rms})^2 - (0.622)^2 .$$

The relay equation can be written as in Eq. (5.3.2)

$$F_{operate} = m\ddot{x} + b\dot{x} + cx ,$$

where,

x is the distance traversed by the moving contact;

m is the mass of the contact;

b is the coefficient of friction;

c is the spring constant.

The differential equation can be solved by taking the Laplace transform of Eqno. (5.3.3) and modeling it as a second-order TACS transfer function. Thus, the distance traversed by the armature is given by the following second-order transfer function:

$$x = \frac{F_{operate}}{ms^2 + bs + c} .$$

When x is larger than the contact separation, the relay trips. This is modeled by the TACS device number 52 -- the Level-Triggered Switch.

The determination of the constants m, b, c, and of the limits on the force is done by matching the time-current curve in Fig. 5 of Ref. [50.]. Large primary currents are required to get the instantaneous unit to pickup. In the AEP test result, this large current was not passed to have the instantaneous unit to pickup, and hence there is no formal validation of this unit. However, on passing large primary currents, the instantaneous relay picks up before the auxiliary relay.

5.3.4 Validation of the BDD15B EMTP model

The circuit in Figure 58 on page 165 is used to validate the BDD15B EMTP model. This circuit simulates the power system simulator that was used at AEP to test the BDD15B relay. By selecting suitable values for R and X and varying the time at which the fault occurs, and adjusting the source voltage, currents that matched the AEP test currents were generated. It was not possible to get identical current waveforms, because of the saturation of the A/D converters in some cases. The current waveforms were varied by changing the magnitude of the voltage source and the time at which the fault occurred.
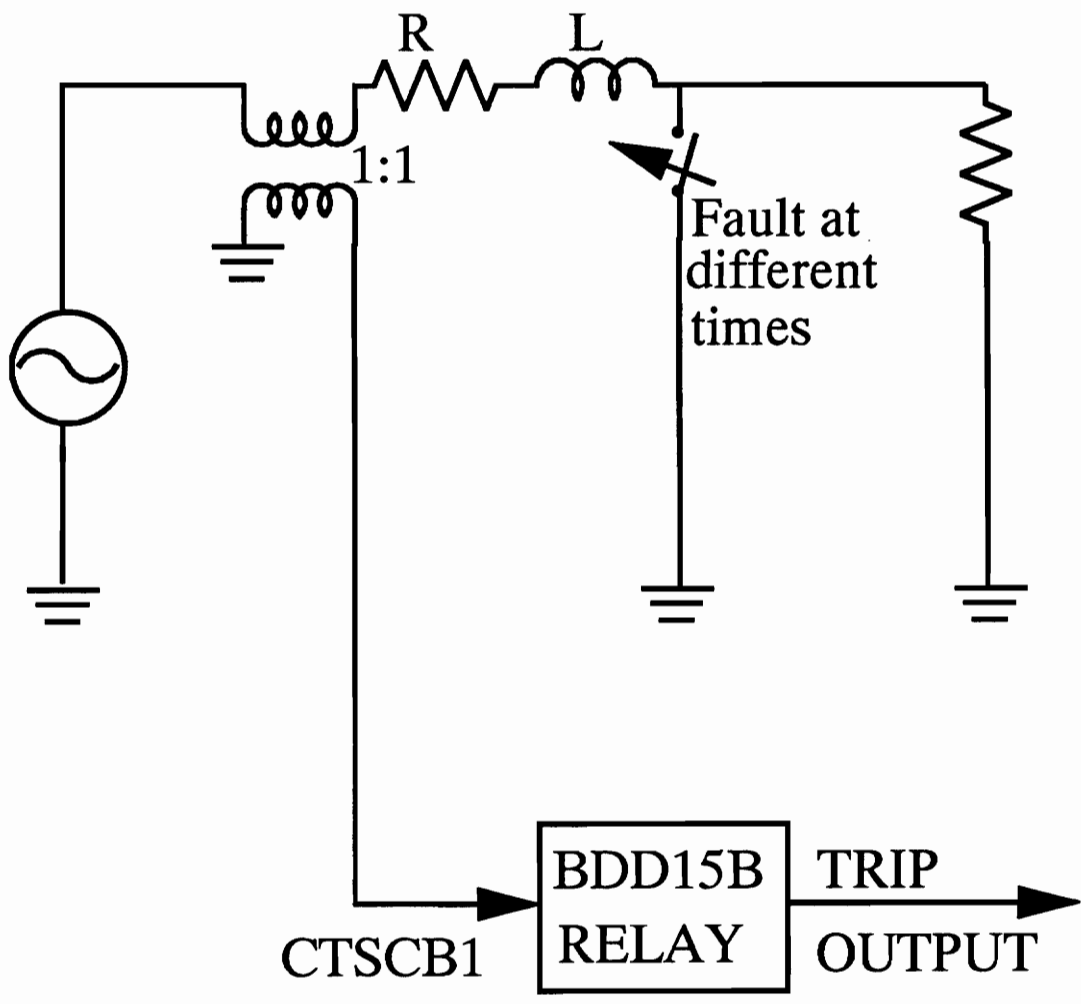
Figure 58. Validation circuit for BDD15B relay

The values of the time to trip in the AEP test and in the BDD15B EMTP Model results are given in Table 3 on page 167. The test cases BDDINRUSH60V and BDDINRUSH72V are simulated by using a 120 Hz source.

The two results are in good agreement. The model's operation time is close to the actual test operation time. Some variation occurs because the relay input currents are not identical in both cases. Determining the exact time to operate in the AEP test is difficult because of contact bounce. The relay model is secure (i.e., it does not operate for external faults and for inrush conditions).

5.3.5 Implementation of the BDD model in EMTP

The BDD15B relay has been modeled by creating a module named BDD15B.INC, using the AUX part of EMTP. This module contains the structure of the relay. It needs the following data as shown in Figure 59 on page 168:

- the node names of the secondaries of the current transformers on either side of the protected transformer

- a two character unique identifier for the relay

- ampere tap on winding 1

Table 3. Comparison of AEP test data and BDD model trip times

Test case	AEP test data (time in ms)	BDD model time (time in ms)
INTFLTFULLWDG70V	55.7	61.0
INTFLTFULLWDG60V	56.03	60.4
INTFLTFULLWDG50V	73.0	70.0
INTFLTFULLWDG40V	No Trip	No Trip
INTFLTFULLWDG30V	No Trip	No Trip
EXTERNFAULT40V	No Trip	No Trip
EXTERNFAULT30V	No Trip	No Trip
INRUSH60V120HZ	No Trip	No Trip
INRUSH60V120HZ	No Trip	No Trip
INTFLTHALFWDG50V	54.3	58.2
INTFLTHALFWDG40V	57.0	71.7

- ampere tap on winding 2

- resistance to control the pickup of the relay [Suggested value = 79.2 ohms, max. value = 150.0 ohms]

- resistance to control the harmonic restraint [Suggested value = 342.0 ohms, max. value = 1000.0 ohms]

- resistance to adjust the percentage slope (for 15%, 25%, and 40% the value is 5.7, 9.3, and 14.7 ohms, respectively)

C BDD15B

C CTSCB1 CTSCB2 BDDIDN

C WD1TAP WD2TAP R1OPCL R2HACL R3SLOP

FORMAT

CTSCB1, CTSCB2   A6

BDDIDN   A2

WD1TAP, WD2TAP, R1OPCL, ...   F6.2
R2HACL, R3SLOP   F6.2

Figure 59.   Data format for BDD15B relay

The subroutine RELAYS processes the input data as shown in Figure 60 on page 170. The relay settings given in the data case are used to compute the following values:

- number of turns in the primary of winding 1 of the through current restraint transformer

- number of turns in the primary of winding 2 of the through current restraint transformer

- number of turns in the primary of winding 1 of the differential current transformer

- number of turns in the primary between winding 1 and winding 2 of the differential current transformer

Subroutine RELAYS then inserts the module BDD15B.INC in the data case, along with the node names, the identifier and required numerical values of quantities needed by the module. This data is then processed by the Subroutine DATAIN, which takes the values of the variables and substitutes them in the required place in the BDD15B module. The data case is then sorted to group all elements in the required order, e.g., TACS, branches, switches, followed by sources. The outputs of the BDD relay are the following:

FLOW CHART OF SUBR RELAYS FOR BDD15B
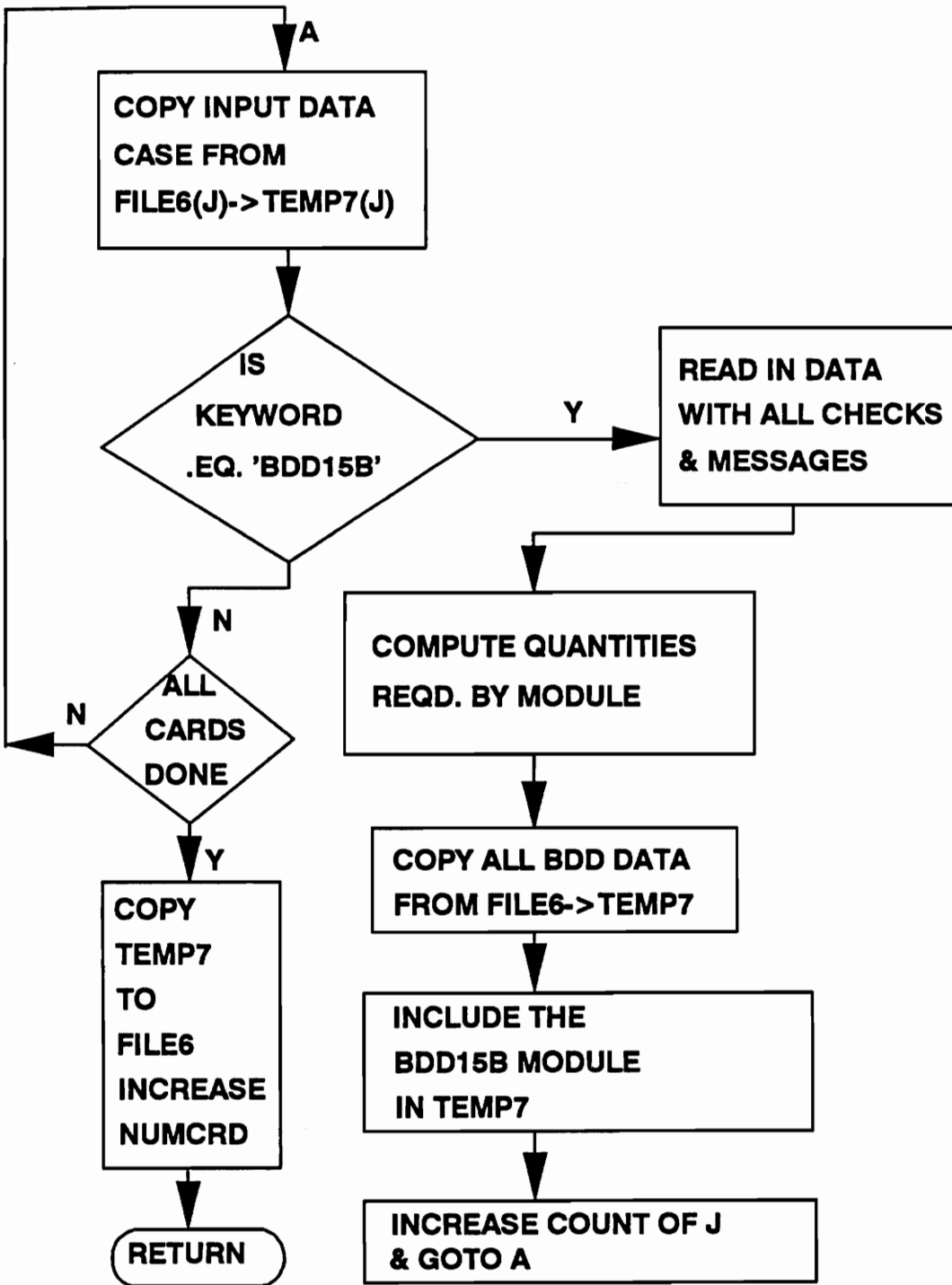
Figure 60.   Flow chart of Subroutine RELAYS for BDD15B relay

- trip output of main operating unit and auxiliary relay

- trip output of instantaneous relay

- trip output which is the result of 'OR'ing of the previous two trip signals

Chapter VI

6.0 PROTECTION SYSTEM

IMPLEMENTATION IN EMTP

6.1 INTRODUCTION

To implement the models in a data case, a new executable version of the EMTP must be created. Changes must be made to the subroutine DATAIN. The subroutines INSTFR and RELAYS must be compiled and linked along the DATAIN.OBJ file to create a new executable version of EMTP. The changes made to EMTP and the procedure to create a new executable version of EMTP are explained in detail in Ref. [51.]. To employ the models developed in this dissertation, the reader is referred to Ref. [52.] for a comprehensive explanation and listing of all the user options. An applications manual (Ref. [53.]) has also been

written, which includes example data cases and graphical outputs employing all the models developed in this dissertation. In this chapter, one data case is simulated which demonstrates the essential features, including the capability of relay decisions affecting changes in the configuration of the power system.

6.2 EXAMPLE DATA CASE

In this example data case, a $3 - \phi$ 500 kV power system EMTP model, together with a protection system was implemented. The power system consisting of two sources with their respective source impedances and two parallel untransposed transmission lines with mutual coupling was modeled. The data for the transmission lines was taken from Ref. [54.]. The transmission line is divided into two parts, and each part has the shunt capacitances and the phase-to-phase capacitances lumped at each end. The protection system consists of three CTs, three CVTs (one for each phase), and an SLY12C relay model. The trip output of the SLY12C controls a TACS-controlled switch Type 13. The single line diagram and a more detailed connection diagram are given in Figure 61 on page 174 and in Figure 62 on page 175.

The appropriate relay settings are calculated for this case based on the Ref. [48.]. A line-to-line fault between phases A and B is created at T = 0.01667 secs. The SLY relay picks up after 18 ms and issues a trip signal to the

PARALLEL LINES WITH MUTUAL COUPLING
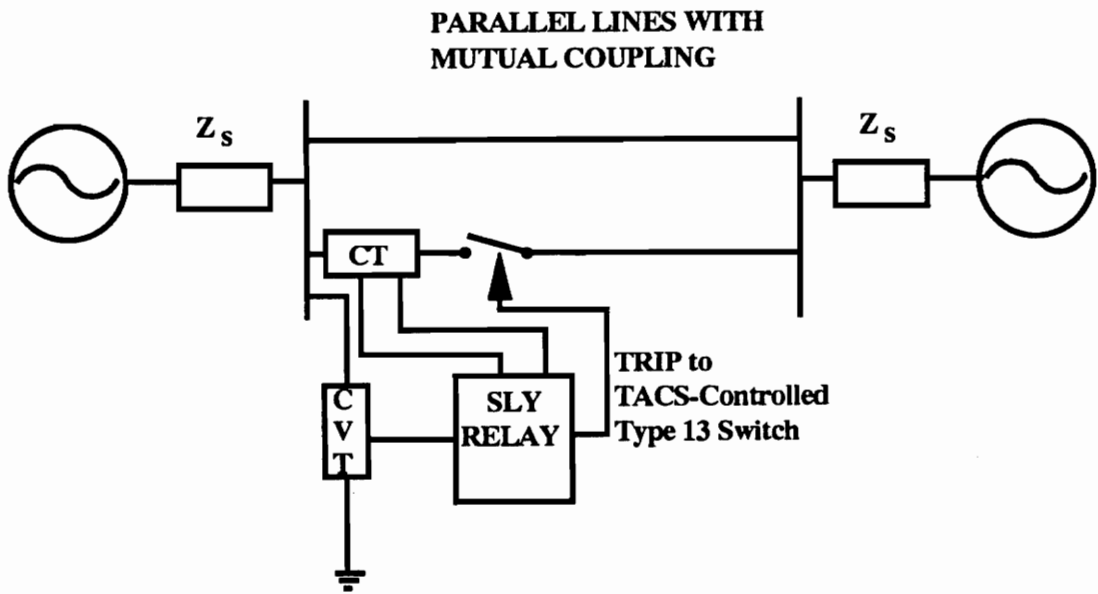
Figure 61. Single line diagram of the test system
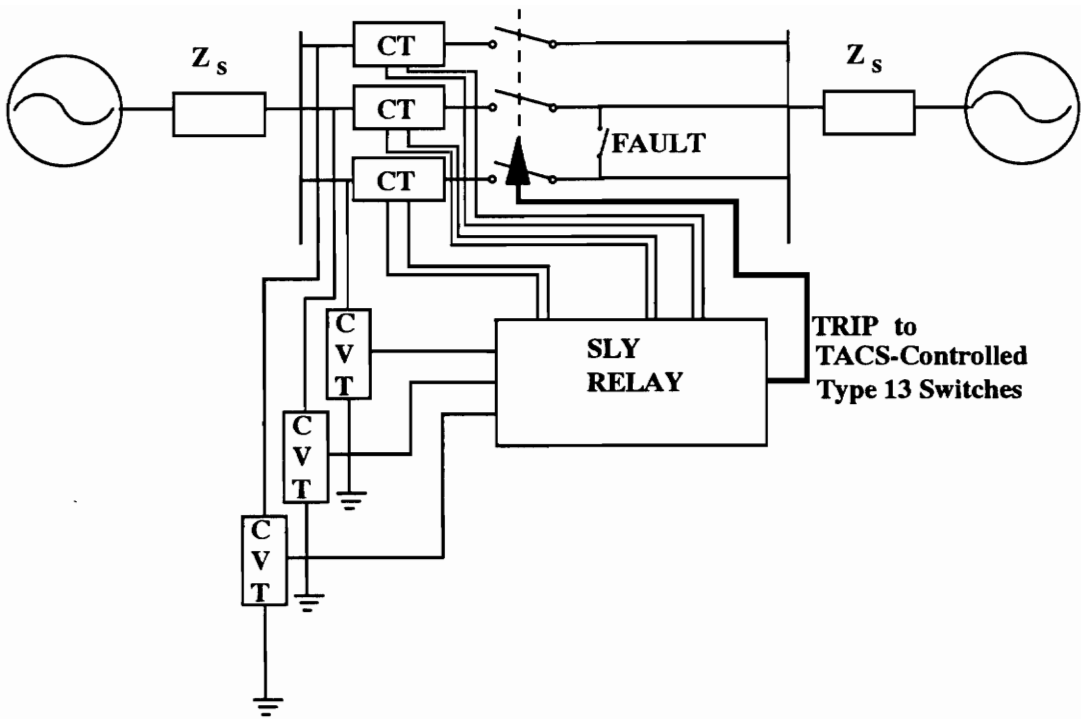
Figure 62. Detailed connection diagram of the SLY12C Relay
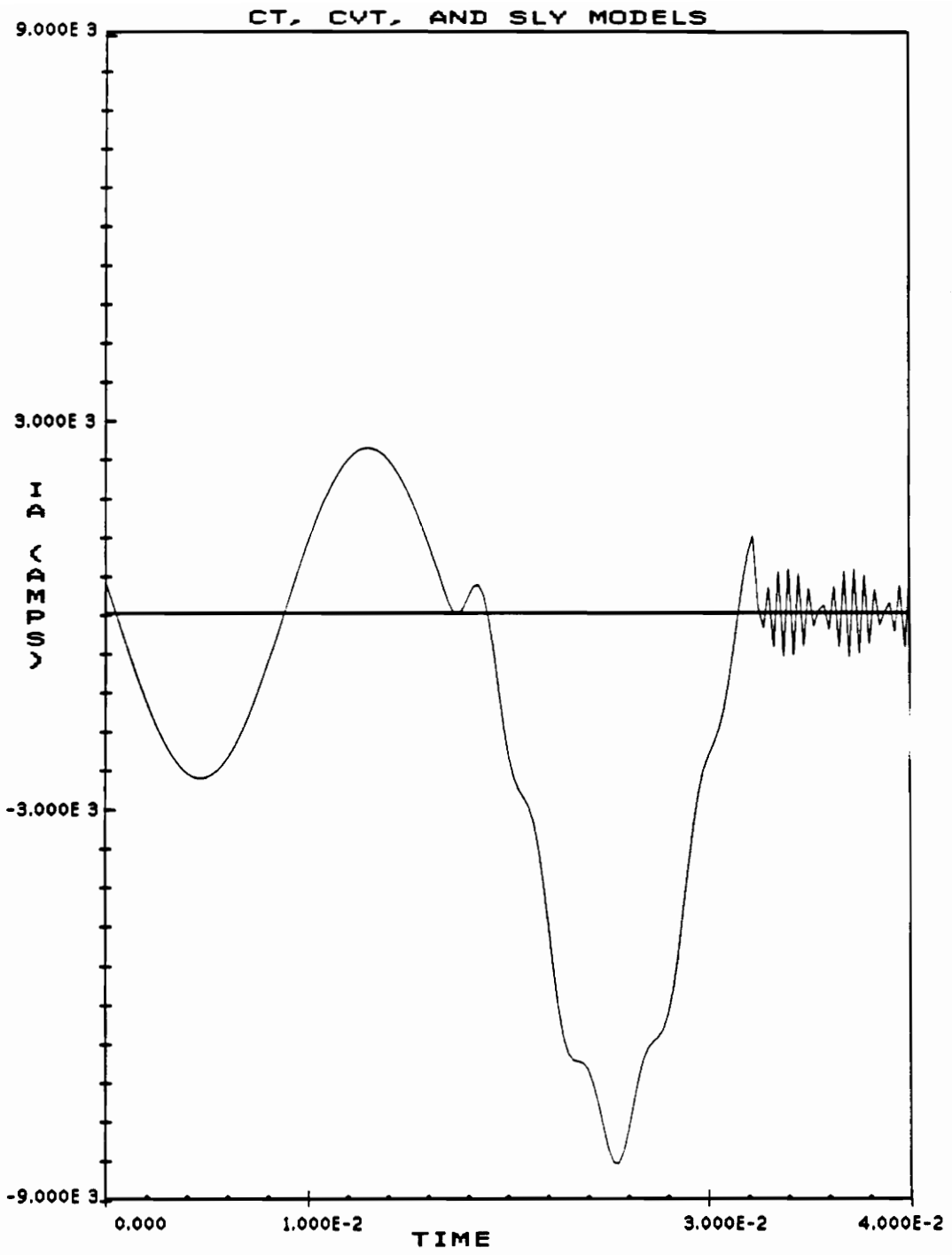
Figure 63. Phase A fault current
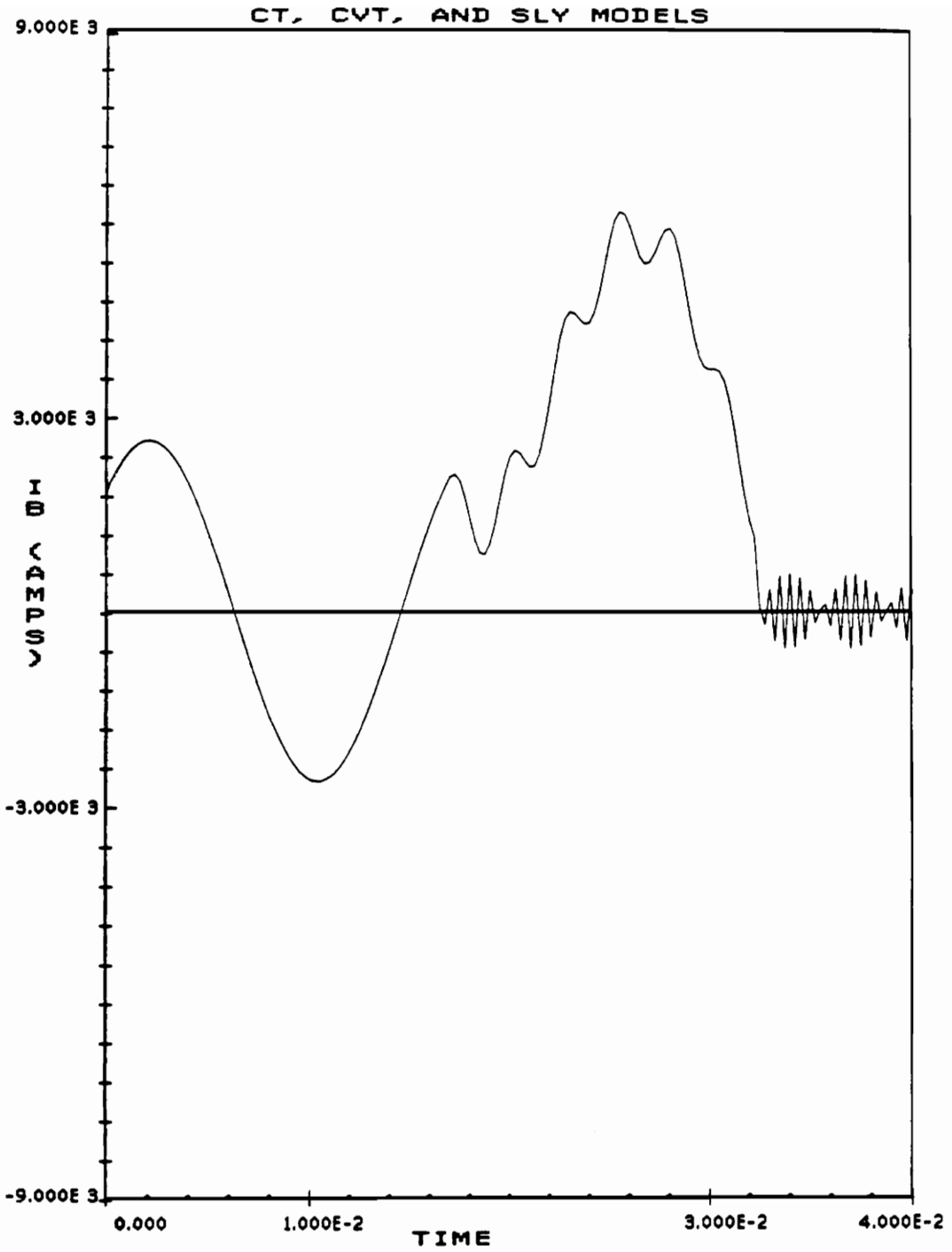
Figure 64. Phase B fault current
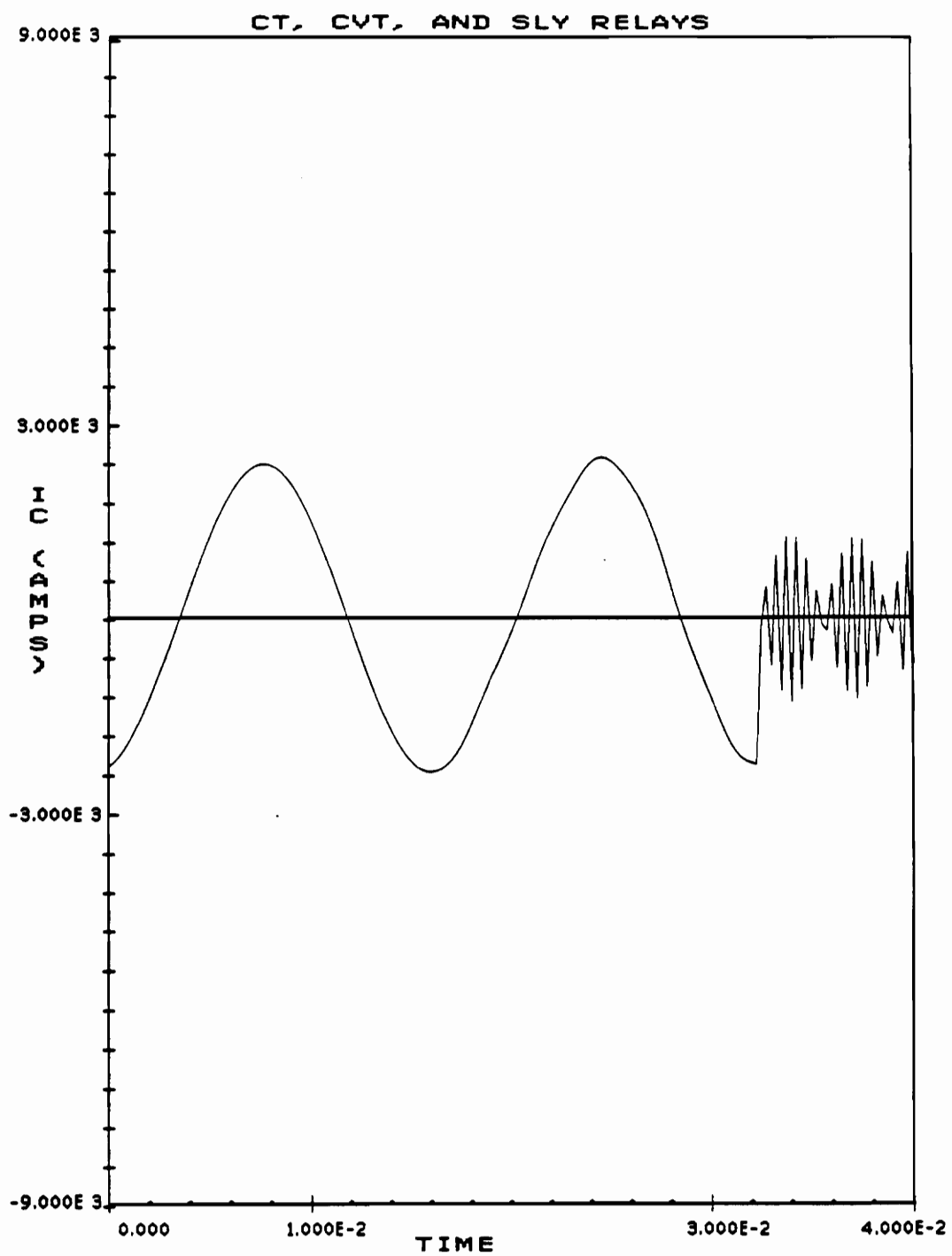
Figure 65.   Phase C current (unfaulted phase)
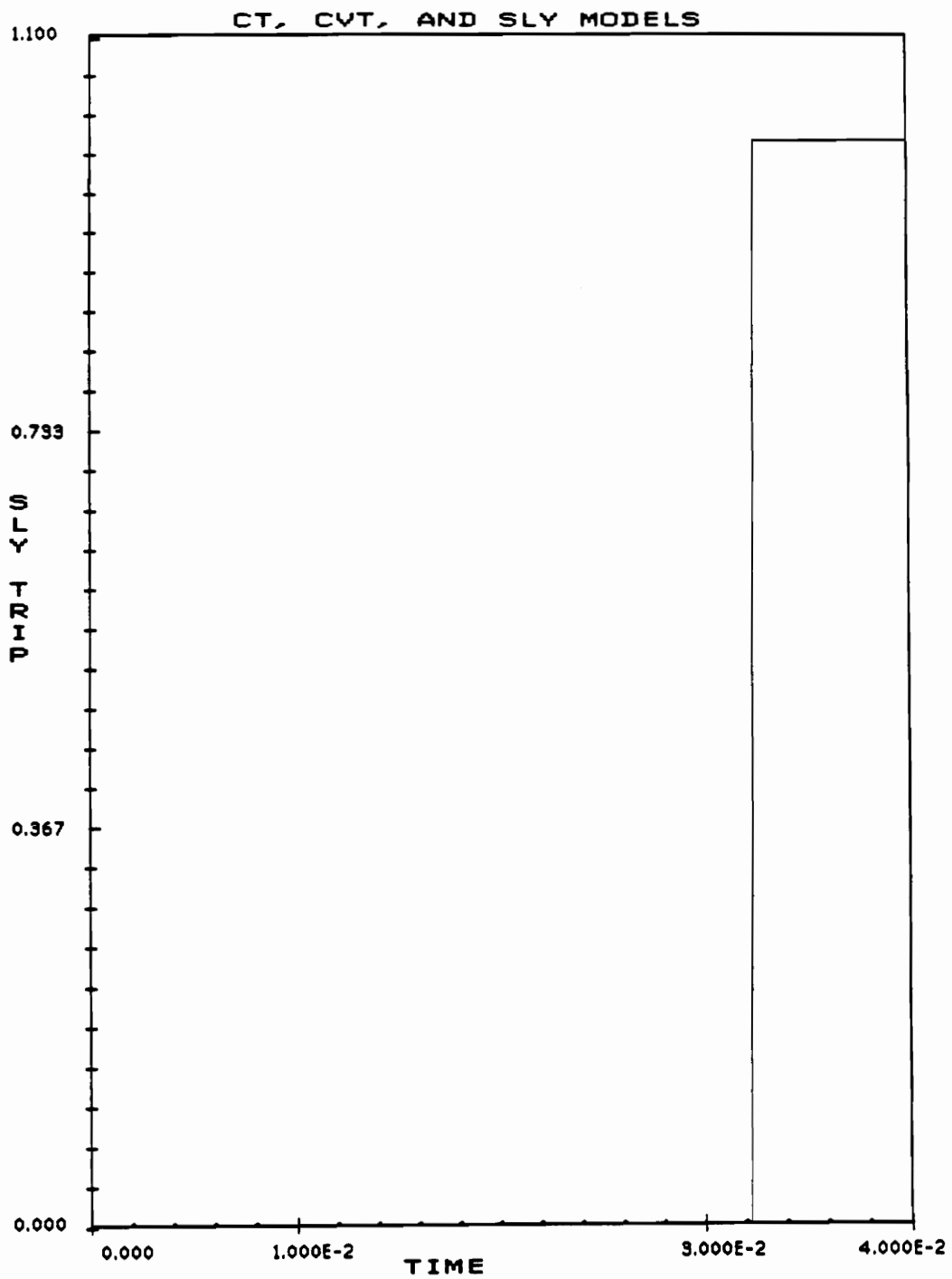
Figure 66. SLY trip signal

TACS-controlled switch Type 13 to clear the fault. The phase A, B, and C currents are plotted in Figure 63 on page 176, in Figure 64 on page 177, and in Figure 65 on page 178, respectively. The trip signal is graphed in Figure 66 on page 179. The oscillations in the current waveform are the result of the sudden reduction in the current through an inductor and the excitation of the capacitances and the inductances in the circuit.

Thus, a power system model and a protection system model are simulated simultaneously (except for the one time step delay between TACS and the network). The dynamic interactions of the two systems can be studied in detail.

Chapter VII

7.0 CONCLUSIONS

7.1 CONTRIBUTIONS OF THIS DISSERTATION

The following is a summary of the main contributions of this dissertation :--

1. The development, validation, and incorporation of a current transformer model in EMTP Version 2.0, which represents the nonlinear behavior, hysteresis, and remanent flux.

2. The development, validation, and incorporation of a capacitor voltage transformer model, which is valid for most protection studies, except overvoltages above two per unit.

3. The capability to integrate a user-defined Fortran algorithm within EMTP. This dynamic feature enables the decisions of the computer relay Fortran algorithm (to use a specific example) to open and reclose network switches.

4. The development, validation, and incorporation of the SLY12C relay model. The SLY12C is a $3 - \phi$ static mho phase distance relay designed for the protection of transmission lines. This complex relay has been modeled using transfer functions, instantaneous maximum functions, rms meters, and many other TACS and EMTP components.

5. The development, validation, and incorporation of the BDD15B relay model in EMTP Version 2.0. This relay is a $1 - \phi$ transformer differential relay, with percentage and harmonic restraint features.

6. With the incorporation of the above features, the main elements of a protection system have been added to EMTP. This enables the simulations of the dynamic interactions between a power system and a protection system.

7.2 RECOMMENDATIONS FOR FUTURE WORK

The following are some recommendations for future work in this area :--

1. Prediction of the remanent flux in a transformer. In Ref. [3.] the non-

repeatability of the magnitude of the switching surge voltage was traced to the remanent flux in the transformer. The lack of the ability to predict the remanent flux in a transformer is a serious disadvantage of digital simulation, particularly in the case of current transformers. The code for the Type 96 pseudononlinear hysteretic inductor component in the EMTP has to be modified to achieve this ability. Also, only one material's (ARMCO M4 Cold rolled grain oriented silicon steel) hysteresis curve is modeled in the Type 96 element. This hysteresis curve also does not account for air gaps in the core. Ref. [36.] elaborates on the reduction in remanent flux of a current transformer core with an air-gap. Thus, it is important to predict the remanent flux and include a hysteresis curve model with an air gap.

2. It may be necessary to develop a capacitor voltage transformer model with the protective gaps across different components to make it applicable for overvoltage studies. This task is not difficult per se but the lack of data prevents its accomplishment.

3. It is reported that a new EMTP transformer model is being developed, which includes the frequency dependent behavior of the core and the windings. This new EMTP transformer model can be incorporated in the CT and the CVT models. There is also a need to create new CT and CVT models to represent the next generation of broad bandwidth instrument transformers which will be needed for the next generation of protective relays.

4. A library of Fortran computer relay models can be established. Some of the relays suggested for modeling are :--

a. Ref. [55.] and Ref. [56.] contain the algorithm for the Symmetrical Component Discrete Fourier Transform relay and the field experience gained in the implementation of this relay, respectively. Thus, this relay is a good candidate for implementation.

b. In Ref. [57.] and Ref. [58.], distance relays based on the Kalman Filter theory have been proposed, which can be implemented.

c. An out-of-step relay model can be included in the library.

d. In Ref. [59.], the algorithm for a microprocessor based overcurrent relay is given. This model can be incorporated with some of the features of adaptive relaying, as described in [23.] and [60.].

5. The nonlinear magnetization characteristics of the SLY and BDD relays can be included.

a. The non-linear magnetization characteristics of the nine transactors involved in the measurement of the M1, M1 reverse, and M2 functions can also be included. However, it is important to note that the transactors contain air-gaps to linearize the core behavior.

b. The non-linear magnetization characteristics of the BDD relay's current transformers can be included. The nonlinear magnetization characteristics will affect the relay operating time only if extremely large currents (approximately 20 times rated) flow in the transformer protection current transformer secondary. But, the BDD relay has an instantaneous unit which picks up if the current transformer secondary current is greater than eight times the rated current. Thus, the nonlinear magnetization characteristics are not very important.

6. Modeling a power system for a protection study involves a reduction of the system model with a Thevenin equivalent. The extent of the truncation allowed is a subject of further research. However, in the interim, a model power system which has at least four generators and four buses can be made available to all users. The model power system can include models for transmission lines with mutual coupling and frequency dependent parameters. Allowance should be made to include different Source Impedance Ratios (SIR). The primary nodes of the CT models should be defined, which will enable the easy connection of the CT model. TACS-controlled switches of Type 13 must also be embedded in the model system. This system model will enable the inclusion of protection system components with different parameters, such as different CT ratios, different CT magnetization characteristics, different magnitudes of CT remanent flux, and different settings of relays. This power system model can be used to simulate various schemes, such as the directional comparison and the phase comparison protection schemes.

7. To prove the security and the dependability of a protection scheme or a relay, a few thousand fault tests and simulations are carried out. (See discussion by J.T. Tengdin in Ref. [61.] and the subsequent reply by the authors.) A technique called "numerical logic replacement" has been introduced in Ref. [10.], which gives an indication of how close a relay is to issuing a trip signal, or, if a relay does issue a trip signal, of the margin by which the threshold to trip is crossed. In the case of the SLY relay, the magnitude of the timer count's difference from 4.15 ms (a quarter cycle on a 60 Hz basis) is an accurate measure of the nearness to trip, if the difference is negative. If the timer count's difference from 4.15 ms is positive, then this positive quantity is a measure of by how much the threshold to issue a trip is exceeded. This "numerical logic replacement" technique contains the potential to reduce the number of simulations. Since the relay models are implemented using modules, it is relatively easy to make changes in the modules, without changing the EMTP source code, compiling the affected subroutine, or creating a new executable version of the EMTP.

Bibliography

1. Electromagnetic Transients Program (EMTP) Revised Rule Book Version 2.0, Volume 1, EPRI EL-6421-L.

2. Murari Mohan Saha and Roland Pfistner, "The State of the Art of Numerical Relaying," Invited Paper, 10'th Power Systems Computation Conference, Graz, Austria, August 19-24, 1990.

3. M. Hirakami and W. Neugebauer, "Transient Network Analyzer Operation with Digital Computer Control and Analysis," IEEE Transactions on Power Apparatus and Systems, Vol. PAS-100, No. 4, April 1981, pp. 1597-1607.

4. A. Wright and C.C. Charalambous, "Modelling of power-system protective equipment on analogue computers," Proc. IEE, Vol. 119, No. 6, June 1972, pp. 689-699.

5. W.D. Humpage, K.P. Wong, M.H. Al-Dabbagh, and E.S. Mukhtar, "Dynamic simulation of high-speed protection," Proc. IEE, Vol. 121, No. 6, June 1974, pp. 474-479.

6. A. Wright and D.J. Rhodes, "Protective-equipment analysis using a digital computer," Proc. IEE, Vol. 121, No. 9, September 1974, pp. 1001-1006.

7. P.F. Lionetto, G. Santagostino, I. Heller, and M. Souillard, "Transient Network Analyzer and High-Speed Static Relays: An Interesting Application to Assess Transient Relay Performance," IEE Conference Publication, Developments in Power-System Protection, 1980, pp. 245-249.

8. P. Bornard, P. Erhard, and M. Pavard, ""Morgat": A Digital Simulator foe EHV Relaying Scheme Tests," Proceedings of the Eighth Power Systems Computation Conference, Helsinki, 19-24 August, 1984, pp. 1147-1154.

9. A. Williams and R.H.J. Warren, "Method of using data from computer simulations to test protection equipment," IEE Proceedings, Vol. 131, Pt. C, No. 7, November 1984, pp. 349-356.

10. Bretton W. Garrett, "Digital Simulation of Power System Protection Under Transient Conditions," Ph.D. Thesis, The University of British Columbia, 1987.

11. Gunnar Nimmersjö, Odd Werner-Erichsen, Birger Hillström, and George D. Rockefeller, "A Digitally-Controlled, Real-Time, Analog Power-System Simulator for Closed-Loop Protective Relaying Testing," IEEE Transactions on Power Delivery, Vol. 3, No. 1, January 1988, pp. 138-152.

12. Hermann W. Dommel, Electromagnetic Transients Program Reference Manual (EMTP Theory Book), The University of British Columbia, August 1986.

13. Electromagnetic Transients Program (EMTP) Source Code Documentation, EPRI EL-4652P

14. Hermann W. Dommel and W. Scott Meyer, "Computation of Electromagnetic Transients," Proceedings of the IEEE, Vol. 62, No. 7, July 1974, pp. 983-993.

15. W.F. Tinney and J.W. Walker, "Direct Solutions of Sparse Network Equations by Optimally Ordered Triangular Factorization," Proceedings of the IEEE, Vol. 55, November 1967, pp. 1801-1809.

16. F. Rowbottom and C.R. Gillies, "A Digital Model of a Current Transformer-Distance Relay Combination," Electrical Engineering Transactions, The Institution of Engineers, Australia, Vol. EE11 - EE12, 1975-1976, pp. 8-14.

17. Transient Response of Current Transformers, IEEE Paper 76CH1 130-4 PWR.

18. M. Chamia, "Transient Behaviour of Instrument Transformers and Associated High-Speed Distance and Directional Comparison Protection," Electra, No. 72, October 1980, pp. 115-139.

19. G.G. Richards and O.T. Tan, "Fault location for transmission lines with current-transformer saturation," IEE PROC., Vol. 130, Pt. C, No. 1, January 1983, pp. 22-27.

20. G.A. Gertsch, "Capacitive Voltage Transformers and their Operation in Conjunction with System Protection Relays," CIGRE 1960, Report No. 318.

21. M.A. Hughes, "Distance relay performance as affected by capacitor voltage transformers," Proc. IEE, Vol. 121, No. 12, December 1974, pp. 1557-1566.

22. Transient Response of Coupling Capacitor Voltage Transformers IEEE Committee Report," Working Group of the Relay Input Sources Subcommittee, IEEE Transactions on Power Apparatus and Systems, Vol. PAS-100, No.12, Dec. 1981, pp. 4811-4814.

23. Arun G. Phadke and James S. Thorp, Computer Relaying for Power Systems, Taunton, England: Research Studies Press Ltd., 1988.

24. L. Mouton, A. Stalewski, and P. Bullo, "Non conventional Current and Voltage Transformers," Electra, No. 59, July 1978, pp. 91-122.

25. A. Papp and H. Harms, "Magnetooptical current transformer. 1: Principles," Applied Optics, Vol. 19, No. 22, 15 November 1980, pp. 3729-3734.

26. H. Aulich, W. Beck, N. Douklias, H. Harms, A. Papp, and H. Schneider, "Magnetooptical current transformer. 2: Components," Applied Optics, Vol. 19, No. 22, 15 November 1980, pp. 3735-3740.

27. H. Harms and A. Papp, "Magnetooptical current transformer. 3: Measurements," Applied Optics, Vol. 19, No. 22, 15 November 1980, pp. 3741-3745.

28. T.W. Cease, "Field Testing of a Magneto Optic Current Transducer," Blacksburg Conference on Computer Relaying, Oct. 6-7, 1987, II-6.

29. Allan Greenwood, Electrical Transients in Power Systems, New York: John Wiley & Sons, Inc., 1991.

30. J.G. Frame, N. Mohan, and T-H. Liu, "Hysteresis modeling in an electromagnetic transients program," IEEE Trans. on Power Apparatus and Systems, Vol. PAS-101, Sept. 1982, pp. 3403-3412.

31. A. Wright, Current Transformers - Their Transient and Steady State Performance, London: Chapman and Hall, 1968.

32. B.D. Jenkins, Introduction to Instrument Transformers, Cleveland, Ohio: Chemical Rubber Co. Press, 1967.

33. R. Garrett, W.C. Kotheimer, and S.E. Zocholl, "Computer Simulation of Current Transformers and Relays for Performance Analysis," Blacksburg Conference on Computer Relaying, Oct. 6-7, 1987, II-7.

34. H.T. Seeley, "The Effect of Current-Transformer Residual Magnetism on Balanced-Current or Differential Relays," AIEE Transactions, Vol. 62, April 1943, pp. 164-169.

35. N.E. Korponay, "Nongapped Cores, Antiremanence gapped Cores or Linear Cores for Current Transformers," IEEE Transactions on Power Apparatus and Systems, Vol. PAS-97, No. 2, March/April 1978, pp. 569-573.

36. "Gapped Core Current Transformer Characteristics and Performance," An IEEE Power System Relay Committee Report, IEEE Transactions on Power Delivery, Vol. 5, No. 4, November 1990, pp. 1732-1737.

37. "Description High Capacitance Coupling Capacitor Potential Device Type CD31B, Rev. 13, LBI-6351U," Telecommunication Products Department, General Electric Company, Lynchburg, VA.

38. Andrew Sweetana, "Transient Response Characteristics of Capacitive Potential Devices," IEEE Transactions on Power Apparatus and Systems, Vol. PAS-89, Nov-Dec. 1970, pp. 1989-1997.

39. American Electric Power Test Data on GE CD31 CVT. (Unpublished)

40. M. Kamar, "Modelisation des Transformateurs de Tension Capacitifs," Thesis, Universite de Liege, Belgium, 1981-1982.

41. K.P. Wong and W.D. Humpage, "Capacitor-Voltage-Transformer Modelling and Response Evaluations," The Institution of Engineers, Australia, Vol. 14, No. 2, 1978, pp. 48-52.

42. Andrew S. Tanenbaum, Structured Computer Organization, Prentice Hall Inc., Englewood Cliffs, NJ, 1967.

43. R.L. Glass, "An Elementary Discussion of Compiler/Interpreter Writing," Computing Surveys, Vol. 1, No. 1, March 1969.

44. Gary Kenney, "System Integration Series: Operating Systems," Electronic Design, November 10, 1983.

45. Robert H. Lasseter and Jiarong Zhou, Draft: TACS Code Documentation, May 29, 1990.

46. E.O. Schweitzer and A.J. Flechsig, "An efficient directional distance algorithm for digital computer relaying," IEEE PES Summer Meeting, Mexico City, Mexico, July 17-22, 1977.

47. "Static Phase Distance Relays, Type SLY," GEK-26487B, Power Systems Management Department, General Electric, Philadelphia, PA.

48. "Static Phase Distance Relays, Type SLY12C," GEK-27948, Insert Booklet-GEK-26487, Power Systems Management Department, General Electric, Philadelphia, PA.

49. S.P. Patra, S.K. Basu, S. Choudhri, Power System Protection, Oxford & IBH Publishing Co., Calcutta, 1983.

50. "Transformer Differential Relay with Percentage and Harmonic Restraint," GEH-2057 E, Power Systems Management Department, General Electric, Philadelphia, PA.

51. Arvind K.S. Chaudhary, K-S. Tam, and A.G. Phadke, <u>Protection System Representation Programmers Manual,</u> Document Number 175 T 331 C #3, Virginia Polytechnic Institute and State University, August 1991.

52. Arvind K.S. Chaudhary, K-S. Tam, and A.G. Phadke, <u>Protection System Representation Users Manual,</u> Document Number 175 T 331 C #1, Virginia Polytechnic Institute and State University, August 1991.

53. Arvind K.S. Chaudhary, K-S. Tam, and A.G. Phadke, <u>Protection System Representation Applications Manual,</u> Document Number 175 T 331 C #2, Virginia Polytechnic Institute and State University, September 1991.

54. <u>Transmission Line Reference Book, 345kV and Above</u> /Second Edition, EPRI, EL-2500, 1982, Table 3.3.16, p. 127.

55. A.G. Phadke, T. Hlibka, and M. Ibrahim, "Fundamental Basis for Distance Relaying with Symmetrical Components," IEEE Transactions on Power Apparatus and Systems, Vol. PAS-96, No. 2, March/April 1971, pp. 742-750.

56. A.G. Phadke, T. Hlibka, M.G. Adamiak, M. Ibrahim, and J.S. Thorp, "A Microcomputer Based Ultra-High Speed Distance Relay: Field Tests," IEEE Transactions on Power Apparatus and Systems, Vol. PAS-100, No. 4, April 1981, pp. 2026-2036.

57. A.A. Girgis and R.G. Brown, "Application of Kalman Filtering in Computer Relaying," IEEE Transactions on Power Apparatus and Systems, Vol. PAS-100, No. 7, July 1991, pp. 3387-3397.

58. M.S. Sachdev, H.C. Wood, and N.G. Johnson, "Kalman Filtering Applied to Power System Measurements for Relaying," IEEE Transactions on Power Apparatus and Systems, Vol. PAS-104, No. 12, December 1985, pp. 3565-3573.

59. Gabriel Benmouyal, "Design of a Digital Multi-Curve Time-Overcurrent Relay," IEEE Transactions on Power Delivery, Vol. 5, No. 4, November 1990, pp. 1725-1731.

60. A.G. Phadke, J.S. Thorp, and S.H. Horowitz, "Study of Adaptive Transmission System Protection and Control," Final Report Prepared for Oak Ridge National Laboratory by Virginia Polytechnic Institute and State University, 1988.

61. M. Chamia and S. Liberman, "Ultra High Speed Relay for EHV/UHV Transmission Lines - Development, Design and Application," IEEE Transactions on Power Apparatus and Systems, Vol. PAS-97, No. 6, Nov/Dec. 1978, pp. 2104-2116.

62. R.K. Aggarwal and A.T. Johns, "Digital Simulation Techniques for Testing Line Protection Relays during 3-Phase Autoreclosure," IEE Conference Publication, Developments in Power-System Protection, 1980, pp. 250-254.

63. Electromagnetic Transients Program (EMTP) Volume 4: Workbook IV (TACS), EPRI EL-4651

Appendix A

CT MODEL DATA EXPLANATION

The data format of the ct model is shown in Figure 17 on page 57. Many numerical quantities are read in as characters, because of the format E6.2 used together with F6.2 to read EMTP branch and transformer data. The format E6.2 is used to represent very large and very small numbers, such as 210000. and .000008, which can be represented as .21 + 06 and .80-05. It is not possible to represent these numbers in the F6.2 format. Using the format E6.2, a number can be read, but it is not possible to write a number using the E6.2 format, because the format **Ew.d** requires that $w \geq (d + 7)$, to allow space for the sign of the number, a leading zero, a decimal point, and E with the exponent and its sign, while writing the number. Thus, large numbers, e.g. 120000.0, represented as .12 + 06 in the E6.2 format, cannot be written in the ct module, which is done in the Subroutine INSTFR. Subroutine INSTFR reads the input data, and computes quantities required by the ct module, and writes this data with the appro-

priate module in an internal file. The format E6.2 must be used to write the number because the field width is six for branch and transformer data. The validity of the numbers is checked at a later stage within the EMTP.

An example of an EMTP data case employing the CT model is given in Figure 18 on page 58. An explanation of the various terms is now given.

CARD # 1   KEYWORD

CTMODEL   this card is required to include the appropriate CT module in the
(3-9)   data case

CARD # 2   CT NODE NAMES

IDEFLG   = 00, or [user inputs values of ct parameters] (I2)

(3-4)   = 01 [to use the default value of the ct model] XOPT =0 &
            COPT = 0 (I2)

CTPRI1   = ct primary terminal node name (A6)
(5-10)

CTPRI2   = ct primary terminal node name (A6)
(11-16)

CTOUT1   = ct output (secondary) terminal node name (A6)
(17-22)

CTOUT2   = ct output (secondary) terminal node name [usually grounded
(23-28)   - enter ########] (A6)

CTRIDN   = a three character, unique identifier of a particular ct (A3)
(29-31)

CARD # 3   CT TRANSFORMER PARAMETERS

RNPRIM = number of primary turns of ct (A6)

(3-8)

RNSEC = number of secondary turns of ct (A6)

(9-14)

PRIRES = resistance of primary winding of ct (ohms) (A6)

(15-20)

PRILEK = leakage inductance of primary winding of ct (in mH) (A6)

(21-26)

SECRES = secondary winding resistance of ct (A6)

(27-32)

SECLEK = leakage inductance of secondary winding of ct (in mH) (A6)

(33-38)

CARD # 4   CT BURDEN AND LEAD PARAMETERS

IBURFG = 00 OR [user connects the burden externally] (I2)

(3-4) = 01 [the burden is connected by the program, i.e., the values of BURRES, BURIND, BURCAP are connected across CTOUT1 and CTOUT2] (I2)

BURRES = resistance of the ct burden (A6)

(5-10)

BURIND = inductance of the ct burden (in mH if XOPT =0) (A6)

(11-16)

BURCAP = capacitance of the ct burden (in uf if COPT =0) (A6)

(17-22)

ILEDFG = 00 OR [No lead impedance required] (I2)

(23-24) = 01 [lead impedance to be connected] (I2)

RLDRES
(25-30)
= resistance of lead, if required, in ohms (A6)

RLDIND
(31-36)
= inductance of lead, if required, in mH (if XOPT =0) - (A6)

RLDCAP
(37-42)
= capacitance of lead, if required, in μF (if COPT =0) - (A6)

CARD # 5   CT MAGNETIZATION PARAMETERS

IHYSFG
(3-4)
= 00 OR [user supplies V(rms) - I(rms) curve] (I2)

= 01 [user supplies ψ(peak)-i(peak) - 22 points required] (I2)

REMFLX
(5-10)
= remanent flux in the core (in Wbt) - (A6)

FREQ
(11-18)
= frequency of the power system (E8.0)

RISAT
(19-26)
= the current at the saturation point on the V(rms)-I(rms) curve
(E8.0)

VSAT
(27-34)
= voltage at the saturation point on the V(rms)-I(rms) curve
(E8.0)

CARD # 6 onwards (variable length) - CT MAGNETIZATION CURVE

RIRMS
(3-18)
the I(rms) or the I(peak), depending on IHYSFG - (E16.0)

VRMS
(19-34)
the V(rms) or the ψ(peak), depending on IHYSFG - (E16.0)

CARD # 7   THE TERMINATION CARD

9999.
the number 9999. signals the end of the variable length V(rms)-

(3-18)   I(rms) curve. If the user inputs the ψ(peak)-i(peak) curve, then 22 points are required to define the curve, after which the number 9999. should be entered.

Appendix B

CVT MODEL DATA EXPLANATION

The data format of the cvt model is shown in Figure 31 on page 84. Many numerical quantities are read in as characters. An explanation similar to the explanation given in Appendix A is applicable in the case of CVTs. An example of an EMTP input data case employing the CVT model is given in Figure 32 on page 86. An explanation of the various terms is now given.

CARD # 1   KEYWORD

CVTMODEL this card is required to include the appropriate CVT module in the

(3-10)   data case

CARD # 2   CVT NODE NAMES

IDEFLG   = 00, or [user inputs values of cvt parameters] (I2)

(3-4)   = 01 [to use the default values of the cvt model] XOPT =0 &
                COPT = 0 (I2)

CVTPR1   = cvt primary terminal node name (A6)

(5-10)

CVTPR2   = cvt primary terminal node name (usually grounded - enter
(11-16)   ######) (A6)

CVTOT1   = cvt output (secondary) terminal node name (A6)
(17-22)

CVTOT2   = cvt output (secondary) terminal node name [usually grounded-
(23-28)   enter ######] (A6)

CVTIDN   = a three character, unique identifier of a particular cvt (A3)
(29-31)

CARD # 3   CAPACITOR DIVIDER VALUES, AND TUNING
INDUCTOR VALUES

CPDIV1   = value of capacitor (C1) of capacitor voltage divider (A6)
(3-8)

CPDIV2   = value of capacitor (C2) of capacitor voltage divider (A6)
(9-14)

SLFIND   = the value of the inductance of the tuning inductor (in mH)
(15-20)   (A6)

RESIND   = the value of the resistance of the tuning inductor (in ohms)
(21-26)   (A6)

CAPIND   = the value of the capacitance of the tuning inductor (in μF if
(27-32)   COPT = 0) (A6)

CARD # 4   CVT TRANSFORMER PARAMETERS

RNPRIM   = number of primary turns of cvt (A6)
(3-8)

RNSEC
(9-14)
= number of secondary turns of cvt (A6)

PRIRES
(15-20)
= resistance of primary winding of cvt (ohms) (A6)

PRILEK
(21-26)
= leakage inductance of primary winding of cvt (in mH) (A6)

SECRES
(27-32)
= secondary winding resistance of cvt (A6)

SECLEK
(33-38)
= leakage inductance of secondary winding of cvt (in mH if XOPT = 0) (A6)

CARD # 5   CVT BURDEN AND LEAD PARAMETERS

IBURFG
(3-4)
= 00 OR [user connects the burden externally] (I2)

= 01 [the burden is connected by the program i.e., the values of BURRES, BURIND, BURCAP are connected across CVTOT1 and CVTOT2] (I2)

BURRES
(5-10)
= resistance of the cvt burden (A6)

BURIND
(11-16)
= inductance of the cvt burden (in mH if XOPT = 0) (A6)

BURCAP
(17-22)
= capacitance of the cvt burden (in uf if COPT = 0) (A6)

ILEDFG
(23-24)
= 00 OR [No lead impedance required] (I2)

= 01 [the lead impedance is connected by the program i.e., the values of RLDRES, RLDIND, and RLDCAP are connected internally] (I2)

RLDRES   = resistance of lead, if required, in ohms (A6)

(25-30)

RLDIND   = inductance of lead, if required, in mH (if XOPT =0) - (A6)

(31-36)

RLDCAP   = capacitance of lead, if required, in μF (if COPT =0) - (A6)

(37-42)

CARD # 6   CVT MAGNETIZATION PARAMETERS

IHYSFG   = 00 OR [user supplies V(rms) - I(rms) curve] (I2)

(3-4)   = 01 OR [user supplies ψ(peak)-i(peak) - 22 points required] (I2)

           = 02 [No Hysteresis curve required in the modelling] (I2)

REMFLX   = remanent flux in the core (in Wbt) - (A6)

(5-10)

FREQ   = frequency of the power system (E8.0)

(11-18)

RISAT   = the current at the saturation point on the V(rms)-I(rms) curve

(19-26)   (E8.0)

VSAT   = voltage at the saturation point on the V(rms)-I(rms) curve

(27-34)   (E8.0)

CARD # 7 onwards (variable length) - CVT MAGNETIZATION CURVE

RIRMS   the I(rms) or the I(peak), depending on IHYSFG - (E16.0)

(3-18)

VRMS   the V(rms) or the ψ(peak), depending on IHYSFG - (E16.0)

(19-34)

CARD # 8   THE TERMINATION CARD

9999.

(3-18)

the number 9999. signals the end of the variable length V(rms)-I(rms) curve. If the user inputs the ψ(peak)-i(peak) curve, then 22 points are required to define the curve, and then the number 9999. should be entered.

Vita

Arvind K.S. Chaudhary was born in Vadhodhara, India on October 4, 1955. He obtained the Bachelor of Science in Physics, Chemistry, and Mathematics from Bangalore University in 1976. The requirements for the Bachelor of Electrical Engineering degree (with distinction) from the Indian Institute of Science, Bangalore, were completed in 1979. He earned the Master's degree in Electrical Engineering from North Carolina State University, Raleigh, in 1985. He has been a graduate student at Virginia Polytechnic Institute and State University since September, 1985. From 1979 - 1983, he was a Design Engineer with Bharat Heavy Electricals Limited, Jhansi, India.